

AD-785 711

INTERMODULATION STUDY. (INTERMODULATION  
PRODUCTS - SATELLITE GROUND ANTENNAS)

J. V. Rootsey, et al

Philco-Ford Corporation

Prepared for:

Army Satellite Communications Agency

24 August 1973

DISTRIBUTED BY:

**NTIS**

National Technical Information Service  
U. S. DEPARTMENT OF COMMERCE  
5285 Port Royal Road, Springfield Va. 22151

REPORT DOCUMENTATION PAGE		READ INSTRUCTIONS BEFORE COMPLETING FORM	
1. REPORT NUMBER	2. GOVT ACCESSION NO.	3. RECIPIENT'S CATALOG NUMBER <b>AD-785711</b>	
4. TITLE (and Subtitle)  <b>Intermodulation Study - Final Test Report Intermodulation Products - Satellite Ground Antennas</b>		5. TYPE OF REPORT & PERIOD COVERED <b>Study and Test Report</b>	
7. AUTHOR(s) <b>ROOTSEY, J. V., GRADISAR, A. A., BORDENAVE, J. R. P.</b>		6. PERFORMING ORG. REPORT NUMBER <b>1 April 72 to 1 April 73</b>	
9. PERFORMING ORGANIZATION NAME AND ADDRESS <b>Philco-Ford Corporation Western Development Laboratories 3939 Fabian Way Palo Alto, California 94303</b>		8. CONTRACT OR GRANT NUMBER(s) <b>DAA B07-72-C-0207</b>	
11. CONTROLLING OFFICE NAME AND ADDRESS <b>US Army Satellite Communications Agency AMCPM-SC-5B Fort Monmouth, New Jersey 07703</b>		10. PROGRAM ELEMENT, PROJECT, TASK AREA & WORK UNIT NUMBERS	
14. MONITORING AGENCY NAME & ADDRESS (if different from Controlling Office)		12. REPORT DATE <b>24 August 1973</b>	
		13. NUMBER OF PAGES <b>157</b>	
		15. SECURITY CLASS. (of this report) <b>UNCLASSIFIED</b>	
		15a. DECLASSIFICATION/DOWNGRADING SCHEDULE	
16. DISTRIBUTION STATEMENT (of this Report) <b>Approved for public release; distribution unlimited.</b>			
17. DISTRIBUTION STATEMENT (of the abstract entered in Block 20, if different from Report)			
18. SUPPLEMENTARY NOTES  <p style="text-align: center;">Reproduced by NATIONAL TECHNICAL INFORMATION SERVICE U S Department of Commerce Springfield VA 22151</p>			
19. KEY WORDS (Continue on reverse side if necessary and identify by block number) <b>Antenna Feed Feed, X-Band Waveguide</b>			
20. ABSTRACT (Continue on reverse side if necessary and identify by block number) A description of tests, observations, problems and results of work performed to reduce the intermodulation products generated in the 5-horn feed of a 60-foot diameter parabolic antenna. The goal was to produce feed components that generated intermodulation products at levels below -140 dBm while subjected to 10 kW CW of total power in any combination of carriers. The receive band was 7.25 to 7.75 GHz; the transmit band was 7.9 to 8.4 GHz.			

(continued)

20. Abstract (continued)

The study was conducted in three phases:

I - The determination of intermodulation levels as a function of total power, proportional power between carrier, waveguide current densities, vacuum, and test configuration,

II - Specific problems encountered in fabricating waveguide devices, specifically flanges, seams, materials, tuning methods, and the degeneration of these factors with time.

III- An effort to obtain specific intermodulation-free components, particularly stable filters and flanges.

i-a

INTERMODULATION STUDY

FINAL TEST REPORT

August 24, 1973

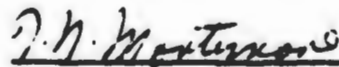
Contributions by:

J. V. Rootsey  
A. A. Gradisar  
J.R.P. Bordenave

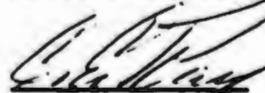
APPROVED:



O. L. McClelland, Supv.  
RF Ground Antenna Section



T. N. Mortimore, Mgr.  
Antenna & Microwave Equipment Dept.



C. E. Ray, Mgr.  
Systems Engineering - HT/MT Program

PHILCO-FORD CORPORATION  
WDL Division  
3939 Fabian Way  
Palo Alto, California

i-k



## TABLE OF CONTENTS

	<u>PAGE</u>
1.0 INTRODUCTION	1
2.0 CONCLUSIONS AND RECOMMENDATIONS	3
3.0 CORRELATION OF THEORY AND EXPERIMENTS	5
4.0 TESTING PROGRAM - PHASE I	8
4.1 LOW POWER SCREEN ROOM TESTS	9
4.1.1 Description of Test Area	9
4.1.2 Screen Room Test Setup	10
4.1.3 Screen Room Test Results	10
4.1.3.1 Closed Waveguide	10
4.1.3.2 Open Waveguide	12
4.1.3.3 Objects Within Waveguide	12
4.1.4 Receive Filter Short Location	14
4.1.5 Transmit Filter Short Location	15
4.2 HIGH POWER WAVEGUIDE TESTS	16
4.2.1 Standing Wave Tests	16
4.2.2 Soft Copper Gasket Design	19
4.2.3 Power Level Effect	20
4.2.4 Travelling Wave Tests	21
4.2.4.1 Smooth Flange Tests	22
4.2.4.2 Coarse Flange Tests	24
4.2.4.3 Matched Discontinuity Tests	26
4.3 HIGH POWER FEED ASSEMBLY TESTS	28
4.3.1 Feed Tests	29
4.3.2 Effect of Single Carrier Variations	33
4.4 LOW POWER VACUUM TESTS	35
4.4.1 Air Gap Tests	36
4.4.2 Higher Order Intermod Levels	37
4.4.3 Closed Waveguide Tests	38
4.5 COLLECTION OF MATCHED LOAD DATA	39

	<u>PAGE</u>
<b>5.0 TESTING PROGRAM - PHASE II</b>	41
<b>5.1 TEST FACILITIES</b>	42
5.1.1 Equipment Block Diagram	43
5.1.2 Retuning the HPA Klystron	44
5.1.3 Transmit Filter	45
5.1.4 Receive Filter	47
<b>5.2 WAVEGUIDE FLANGE EXAMINATION</b>	48
5.2.1 Bolt Loading Curves	48
5.2.2 Standard Flange Appearance	49
5.2.3 Flange Plating Problems	50
5.2.4 Estimated Contact Pressure	51
<b>5.3 FILTER STUDIES</b>	58
5.3.1 Receive Filter Intermods	59
5.3.1.1 Thread Comparison	60
5.3.1.2 Tuning Screw Comparison	60
5.3.2 Filter Tuning Methods Experiments	62
5.3.2.1 Press-fit Tuning	62
5.3.2.2 Solid Collet Tuning	64
5.3.2.3 Dent Tuning	66
5.3.3 Bandstop Filter	68
<b>5.4 FEED ASSEMBLY TESTS</b>	69
5.4.1 Circular Flange Gasket Tests	71
5.4.2 Polarizer Seam Effects	73
5.4.3 Other Polarizer Design Defects	74
5.4.4 Effects of Dipbrazing	75
5.4.5 Temporarily Quieting the HT Feed	76
<b>5.5 OTHER FEED SYSTEM TESTS</b>	77
5.5.1 MSC-46 Feed Tests	77
5.5.2 HT Terminal Tests	80
<b>5.6 DIELECTRIC SEPARATION TESTS</b>	82
<b>5.7 MATERIALS TESTS</b>	84

6.0 TESTING PROGRAM - PHASE III

6.1 SCOPE - PHASE III

6.2 TEST FACILITIES

6.3 FILTER EXPERIMENTATION PROGRAM

6.3.1 Dent-Tuned Bandpass Filters

6.3.2 Untuned Lowpass Filter

6.3.2.1 Solid Copper Lowpass

6.3.2.2 Aluminum Segmented Filter

6.3.2.3 EDM Filter

6.3.3 Pin Tuned Filter

6.3.3.1 The Taper Pin Analysis

6.3.3.2 Taper Pin Experimentation

6.3.3.3 Tuning with Taper Pins

6.4 MATERIALS TEST (cont.)

6.5 ADDITIONAL HIGHER ORDER OBSERVATIONS

7.0 INTERMODULATION PRODUCT FREE WAVEGUIDE FLANGE

7.1 SUMMARY

7.2 ASSUMPTIONS

7.3 DESIGN APPROACH

7.4 DESIGN ANALYSIS

7.4.1 Flange Thickness

7.4.2 Surface Pressure and Flatness

7.4.3 Bolt Loading

7.4.4 Flange Profile

7.4.5 Three-Dimensionally Critical Parameters

7.5 EXPERIMENTAL RESULTS

APPENDIX I

APPENDIX II

## LIST OF FIGURES

<u>Number</u>	<u>Title</u>	<u>Page</u>
4.1-1	RF Sealing Method	9
4.1-2	Screen Room Test Setup	11
4.1-3	Effect of Bolt in Waveguide	13
4.1-4	Short Location - HT/MT Receive Filter	14
4.1-5	Short Location - HT/MT Transmit Filter	15
4.2-1	High Power Standing Wave Setup	16
4.2-2	Waveguide Field Distribution	18
4.2-3	Soft Copper Gaskets	19
4.2-4	Power Level Effects (Standing Wave)	20
4.2-5	High Power Traveling Wave Setup	21
4.2-6	Travelling-Wave Test #1 (High Power)	23
4.2-7	Travelling-Wave Test #2 (High Power)	25
4.2-8	Matched Discontinuities	26
4.2-9	Effects of Mismatched Flange	27
4.3-1	Horn/Feed Test Setup	28
4.3-2	Horn Gaskets (Soft Copper)	29
4.3-3	Feed Test Results	30
4.3-4	Enlarged Photograph of Horn Flanges	32
4.3-5	Carrier Ratio Effects (Standing Wave)	34
4.3-6	Carrier Ratio Effects (Travelling Wave)	34
4.4-1	Vacuum Chamber Setup	35
4.4-2	Vacuum/Gap Effects	36
4.4-3	High Order Intermod Levels	37
4.4-4	Slow Pressure-Drop Effects	38
4.5-1	Collection Matched Load Data	40
5.1-1	DTF Test Facilities	42
5.1-2	Phase II Block Diagram	43
5.1-3	Retuning Effect on HPA Gain	44
5.1-4	Highpass Filter	45
5.1-5	Machined Transmit Filter Response	46
5.1-6	Receive Filter Response	47

<u>Number</u>	<u>Title</u>	<u>Page</u>
5.2-1	Bolt Loading Curves	48
5.2-2	Standard UG 1356/U Flange	49
5.2-3	Plating Defect on MSC-46 Flange	50
5.2-4	Flange Pressure Model	51
5.2-5	Flange Pressure Requirements	52
5.2-6	Comparative Flange Pressures	53
5.2-7	Copper Gasket Compressibility	54
5.2-8	Incremental Compressibility Curves	55
5.2-9	Bolt Torque Required for Yielding	56
5.2-10	Flange Warpage	57
5.3-1	Relative Cavity Intermod Levels	59
5.3-2	Thread Comparison	60
5.3-3	Johannsen Tuning Screw	61
5.3-4	Press Fit Tuning Screw	62
5.3-5	Galling Effects	63
5.3-6	Collet Tuning Experiment	64
5.3-7	Test Cavity	66
5.3-8	Tuning Effect	66
5.3-9	Cavity Tuning Response	67
5.3-10	Bandstop Filter	68
5.3-11	Degradation of the Bandstop Filter	70
5.4-1	Circular Flange Gasket	71
5.4-2	Levels of IM from Circular Flange	72
5.4-3	Disassembled Polarizer	73
5.4-4	Polarizer Design Defects	74
5.4-5	Sample Dipbrazed Horn	75
5.5-1	MSC-46 Feed	77
5.5-2	Levels of IM from Circular Flange	78
5.5-3	Higher Order IM's from MSC-46 Feed	79
5.5-4	IM Level of HT Antenna	80
5.6-1	Dielectric Separation Effects	82
5.7-1	Sample Waveguides	84
5.7-2	Stainless Steel Flange Samples	85

<u>Number</u>	<u>Title</u>	<u>Page</u>
6.2-1	Typical Test Bench	107
6.3-1	Dent Tuned Bandpass	108
6.3-2	Mandrel Residue	109
6.3-3	Result of Dye Penetrant Test	110
6.3-4	Deleted	
6.3-5	Pre-filter Skirt Requirements	113
6.3-6	Copper Lowpass Filter	114
6.3-7	Broached Surface Texture	115
6.3-8	Dipbrazed Lowpass Filter	116
6.3-9	Dipbrazing Seams	117
6.3-10	EDM Sample Filter	118
6.3-11	Taper Pin Geometry	120
6.3-12	Waveguide Taper Pin Models	122
6.3-13	Standard Taper Pin Surface Texture	123
6.3-14	Taper Pin Tuning Model	124
6.5-1	High Power Data (MSC-46)	128
6.5-2	Tuned Filter Levels	128
6.5-3	Slope of 3rd & 5th Orders	128
6.5-4	Effect of power Distribution	128
7.3-1	Waveguide Flange Faces Curved	135
7.3-2	Mating Surface Geometry	136
7.3-3	Rough Surface Elastic Behavior	137
7.3-4	Waviness Surface Load Model	139
7.3-5	Flange Geometry	140
7.4-1	IMP-Free Waveguide Flange	143
7.5-1	Three Models of IMP-Free Flanges	148
7.5-2	IMP-Free Copper Flanges	148
7.5-3	X-Band IMP Measuring Test Setup	149
7.5-4	Function of CU and AL During Salt Fog	149
7.5-5	CU to AL Flange Model from Salt Chamber	150
7.5-6	AL Flange after 418 Hours Salt-Fog	152
7.5-7	CU Flange After 418 Hours Salt-Fog	152

## INTERMODULATION STUDY

### FINAL TEST REPORT

#### 1.0 INTRODUCTION

This report describes the tests, observations, problems and results of the Experimental Intermodulation Study Project. Work performed covers intermodulation level experiments, tests to isolate the non-linear sources, and component fabrication experiments. Included within this program were specific requirements to find a quick temporary method of quieting the Heavy Terminal 5-Horn Feed, and a substantial portion of the program was devoted to this end. The remaining effort concentrated on examining passive waveguide components. The program goal was to produce feed components that generated intermodulation products at levels below -140 dBm while subjected to 10 KW CW of total power in any combination of carriers. The receive band was 7.25 to 7.75 GHz; the transmit band was 7.9 to 8.4 GHz.

In dealing with intermodulation products, this study ignores the high level discharge phenomenon such as experienced with extremely loose flanges or other poor connections reported by Cox\*. The mechanisms observed in this program are those that exist below the Cox sensitivity level, and whose effects are likely to exist in well-designed feeds that are assembled to existing microwave standards. This is not to say, however, that the Cox phenomena was not observed during the program, but that if it were observed the source was isolated and corrected before data was taken or observations made.

Phase I of the experimental program, covering work performed in April-May 1972, is presented in Section 4 of this report. The emphasis during this portion was placed on determining intermodulation levels as a function of total power, proportional power between carriers, waveguide current densities, vacuum,

---

\* Cox, R.D., "Measurement of Waveguide Component and Joint Mixing Products . . .", IEEE Trans., on Comm. Tech., Vol. 18, No. 1, Feb.1970.

and test configuration. Since little information was available to define mechanisms or predict results, tests were made quickly to produce questions that could be answered in subsequent, better controlled tests.

Phase II, covering work performed during July-September 1972, is summarized in Section 5. This effort dealt with specific problems encountered in fabricating waveguide devices and how these relate to intermodulation production. Specific emphasis is given to flanges, tuning methods, seams, materials and degeneration of these factors with time. There is little significant data here as discussions dwell heavily on actual fabrication problems and attempts to correct them.

Phase III is presented in Sections 6 and 7 and covers work performed during the first portion of 1973. The effort is an extension of Phase II in that previous observations were extended to obtain specific intermodulation-free components, particularly stable filters and flanges. The emphasis here was upon the elimination of faulty or potentially troublesome processes and upon the finalization of procedures for immediate feed requirements. Some minor testing was also performed with various materials, and observations taken on higher order (5th, 7th, etc.) products.



and test configuration. Since little information was available to define mechanisms or predict results, tests were made quickly to produce questions that could be answered in subsequent, better controlled tests.

Phase II, covering work performed during July-September 1972, is summarized in Section 5. This effort dealt with specific problems encountered in fabricating waveguide devices and how these relate to intermodulation production. Specific emphasis is given to flanges, tuning methods, seams, materials and degeneration of these factors with time. There is little significant data here as discussions dwell heavily on actual fabrication problems and attempts to correct them.

Phase III is presented in Sections 6 and 7 and covers work performed during the first portion of 1973. The effort is an extension of Phase II in that previous observations were extended to obtain specific intermodulation-free components, particularly stable filters and flanges. The emphasis here was upon the elimination of faulty or potentially troublesome processes and upon the finalization of procedures for immediate feed requirements. Some minor testing was also performed with various materials, and observations taken on higher order (5th, 7th, etc.) products.

## 2.0 CONCLUSIONS AND RECOMMENDATIONS

At the outset of this program definite conclusions were envisioned that would, in an absolute manner, present fundamental laws for allowing or prohibiting a process, a component type, or an assembling procedure. After nearly a year of studying the symptoms, causes and preventions of intermodulation products, it is evident that no such restrictive guidelines are forthcoming. In fact it is becoming increasingly clear that there is no flange junction or bonding process that is unequivocally linear to the requirements of this program, nor is there a corresponding process that is inherently unacceptable. As the reader glances through this report, he will find processes declared acceptable in one phase of the study, only to be discarded in a later phase. Similarly, techniques found unacceptable in early phases are occasionally revived to form the basis of quiet setups later on. Fixed guidelines cannot be established for component design in the light of such apparent contradictions.

What can be concluded from this study, however, is that no matter what method unifies parts and components, if the procedure includes precision manufacturing, tight assembling control, and extreme handling care then it is highly probable that the system will meet the -140 dBm level of quietness for multiple carrier powers totaling 10 KW. It is only when control is relaxed that a system will likely produce significant intermodulation products. The conclusion, therefore, is not a summary of how components can or cannot be built, but what type and level of control must be placed on particular techniques, and which of these techniques are more susceptible to improper fabrication or operational abuse. It is then the responsibility of the reader or his project manager to use appropriate judgment in the selection and control of his design and manufacturing methods.

All aspects of this study can be grouped into five distinct areas:

(1) Material Selection, (2) Flange Configuration, (3) Manufacturing Methods, (4) Bonding Procedures, and (5) Tuning Approaches. Concluding remarks are directed individually toward these areas as follows:

## 2.1 Material Selection

Intermodulation production and suppression appear to be independent of materials or combinations thereof. The program has examined gold, brass, copper, nickel, cadmium, silver, stainless steel, and aluminum, and has produced no correlation between intermodulation level and material type, nor between levels and dissimilar metal junctions. It is also observed that the softer metals are more readily quieted than the harder ones; for instance, gold and annealed copper interfaces frequently become quiet at pressures just beyond finger tight, while stainless flanges (which are of the hardest material) are considerably more susceptible to IMP's. This variation between materials of different hardness appears related to resistance to flattening and reluctance to achieve full area contact between the surfaces. Thus, if the designer selects an inelastic or rigid material he must recognize that all pressure joints must be optically polished and flattened. The softer materials, although inferior from a structural stability point-of-view, allow more latitude in contact area waviness and texture. (Because annealed materials are subject to creep and long-term distortion, allowance must be made in support of framework rigidity.) As a conservative rule-of-thumb it is recommended that surfaces with contact pressures of between 10,000 psi and 12,000 psi be polished to levels indicated in Figure 2-1, depending on material elasticity. Waviness should remain below 10 times the surface finish value. This rule applies to seams within components, as well as flange connections. Lower applied pressures require more highly polished surfaces, while higher pressures permit correspondingly coarser surfaces.

## 2.2 Flange Configuration

The microwave designer can select any of the standard flange types and have a high probability of obtaining an intermodulation-free junction, with or without gaskets, by finishing and assembling to criteria presented in this report. However, typical handling and assembling procedures increase the risk of obtaining observable IMP's initially or soon after site installation for the conventional (MIL) flange designs over the modified design

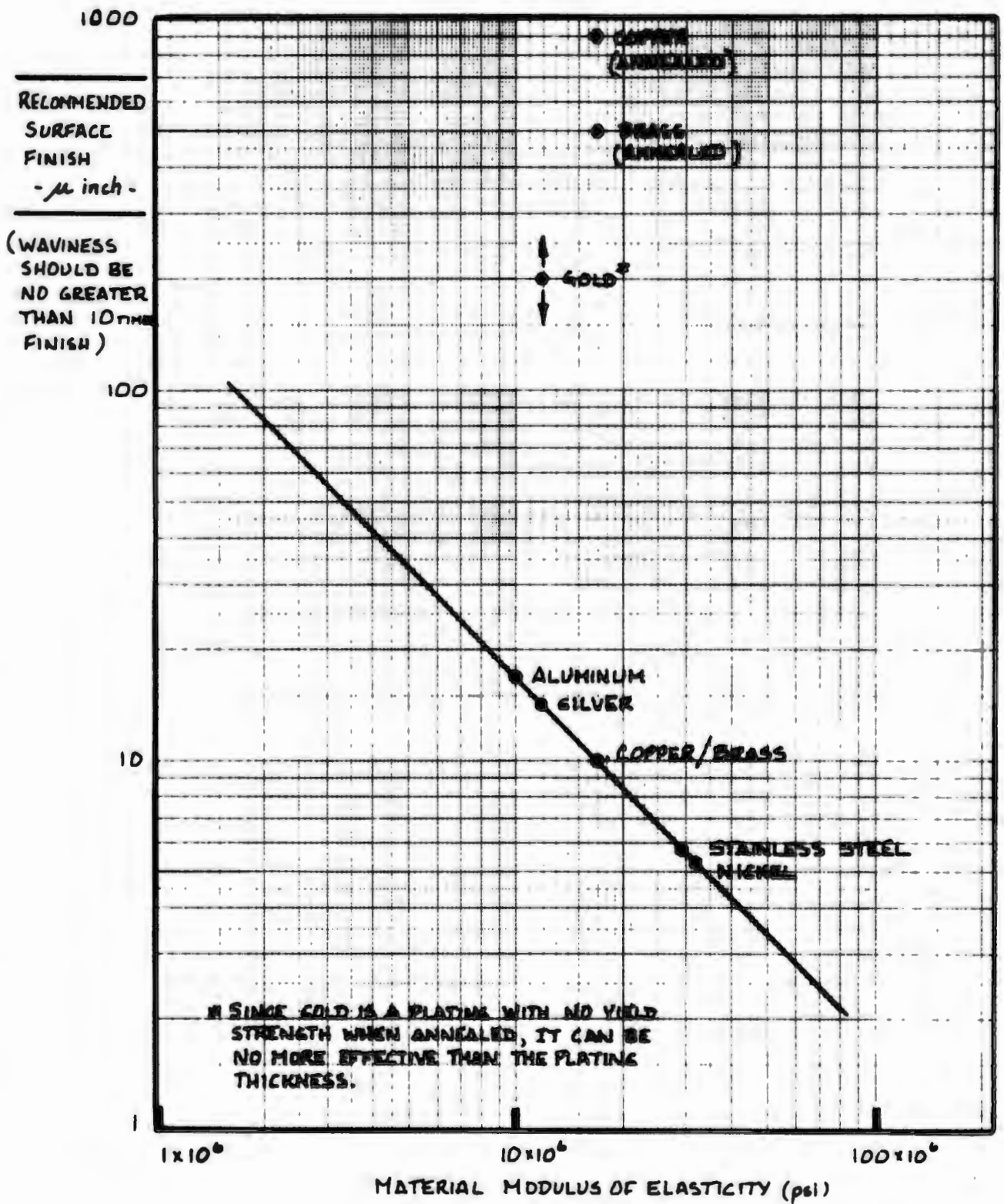


FIGURE 2-1 RULE OF THUMB FOR SURFACE FINISH

described in Section 7. For example, the standard UG 1356/U grooved flange when lapped to a 10 microinch finish or better has repeatedly produced a quiet junction under laboratory conditions. However, when the same flange is subjected to the stresses of a typical feed or waveguide-run installation, its thickness, elasticity and pressure distribution are insufficient to keep consistent contact around the mating surface. Similarly, the unlapped standard flange is easily quieted by an annealed copper gasket that blends into the undulating surface, but this report is reluctant to recommend the wholesale use of the gasket because of possible long term creep that may reduce the contact pressure between surfaces. Nevertheless, if the designer can remove external loading from flanges then the standard or gasketed approaches are acceptable.

It is the conclusion of this report, though, that a more reliable and stable flange junction is obtained if (1) half-hard (or harder) brass, copper or aluminum are used and designed to operate in the elastic region of the material; (2) raised lips nominally 0.1 inch high are added around the waveguide and outer flange edge to provide an elastic cushion for absorbing stress; (3) bolt holes are located so at least one-half of their pressure is applied to the flange wall; (4) the flange thickness is doubled to prevent cupping or similar distortion; (5) the waveguide feeds through the flange to eliminate a butt joint; and (6) copper and brass flanges be bonded with a combination of electroform growth and epoxy or low temperature solder to prevent annealing. These principles are illustrated in Figure 2-2. Of course, the requirements for surface finish established by Figure 2-1 still apply. Flanges meeting all of these requirements consistently meet intermodulation specifications.

Flanges having a septum or dividing strip through the center of the opening (e.g., as for waveguides stacked on top or alongside of each other) are difficult to quiet since the contact pressure along the isolated wall is rarely maintained at a sufficient level for full contact. Such a joint is not recommended because tests show it to be a consistent generator of IMP's. Nevertheless, if divided waveguides cannot be avoided, the flange can be quieted by designing sufficient elasticity, bolt pressure, and optical surface polish into the mating surfaces following the guidelines of Section 7.0.

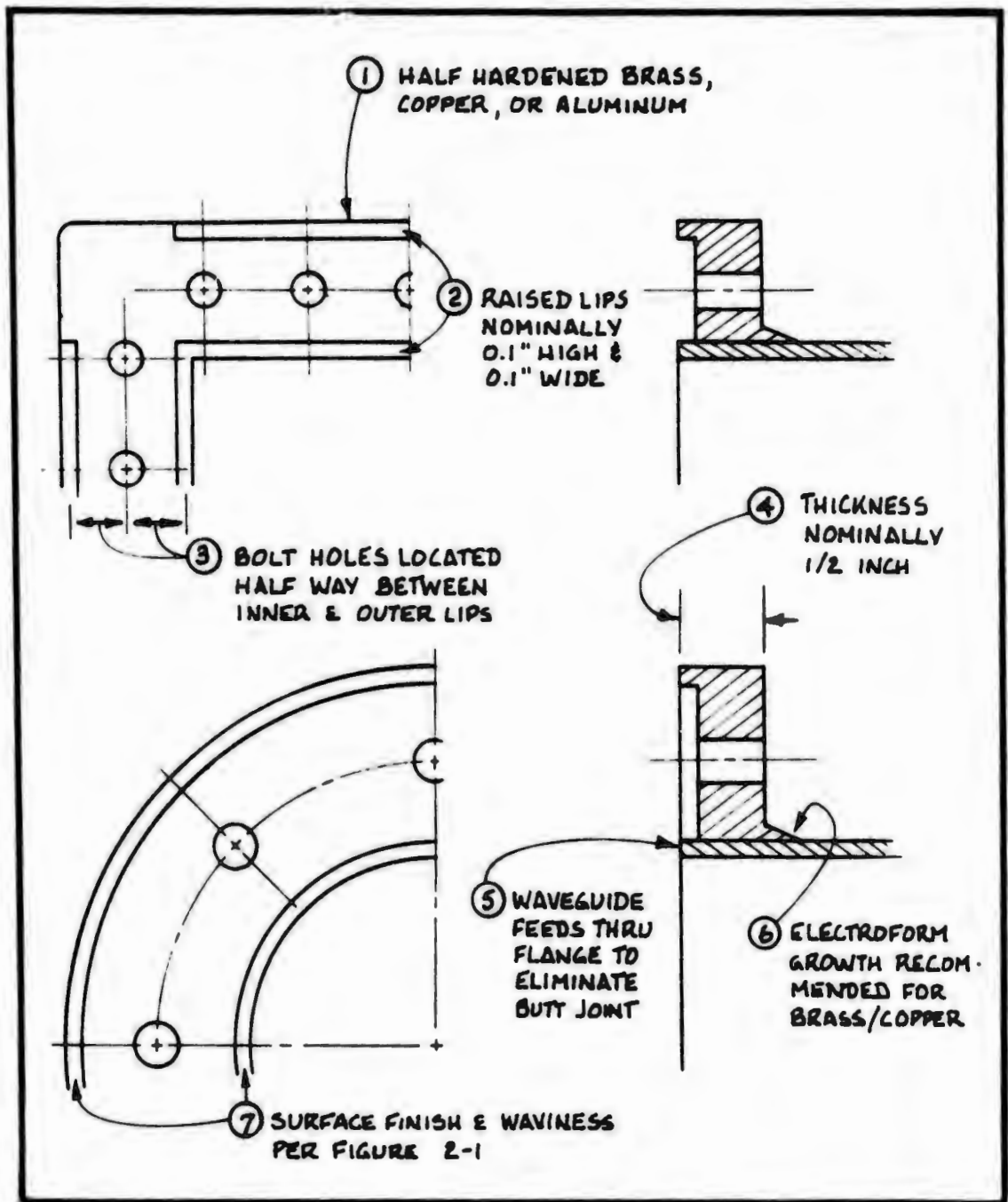


FIGURE 2-2 GENERAL RECOMMENDATIONS FOR  
7.25-8.40 GHz FLANGE DESIGNS



### 2.3 Manufacturing Methods

Items tested under this study cover a significant range of manufacturing processes. Materials have been extruded, machined, cast, electroformed, discharge-machined, broached, ground, and plated; and all methods when properly applied produced a linear device. However, the intermods in many items were directly caused by defects in the manufactured surface rather than at a junction, so the following precautions should be taken with each process.

The most common extrusion is waveguide, which for all tests has remained quiet. But occasionally small particles of copper or other residual imbedded in the interior surfaces has been noted, so as standard practice, the interiors of waveguides tested in this study were inspected before use. All surfaces that were machined, ground, plated or electrical-discharge machined (EDM) were also acceptable, although deburring of corners was necessary on several items. Casting is generally a good process providing visible fractures and blow holes are absent; however, the casted piece must be finished by machining in the vicinity of flanges as the texture produces poor contact and non-linear RF characteristics. Visible pores and any deformity that would impede current flow should be welded and re-finished.

A reliably quiet component is almost always obtained by electroforming over a solid mandrel; however, if inserts are placed in the mandrel and the plating expected to bond to the insert, there is a high risk that the junction will produce intermodulation products. The reason is twofold: First, the mandrel is generally electrolyzed with a zincate or similar flashing that promotes deposition of the copper ion; if this coating covers the bonding surface of the insert, then a weak junction is formed that separates under stress. The second limitation occurs when an insert extends beyond the mandrel and electrical fields do not penetrate into the corner formed by the junction of the mandrel and insert; here a crease is formed that again separates under stress. Electroforming houses have the capability to overcome these obstacles, as quiet complex items have been built

and tested, so the reader should work with his supplier to insure the appropriate process is used.

Whenever broaching is used as an interior planing operation, the component has remained quiet. But whenever broaching is used to square an interior corner, copper particles are inevitably pressed into the orthogonal metal and IMP's produced. It is the conclusion of this study that EDM is the most reliable means of removing metal from an inside corner (e.g., the base of a transformer step) whenever milling leaves an unacceptable radius.

#### 2.4 Bonding Procedures

Rarely is a complex component made in one piece so the designer must specify a method of bonding the various parts together. The most reliable method is to place junctions where they do not intercept current flow, such as along the center of a waveguide topwall. By assembling TE<sub>10</sub> devices (e.g., filters) in this manner, bolts and machined surfaces are sufficient for quiet operation. During the study no IMP's were caused by such a junction.

The only other processes examined here were oven brazing, torch brazing and soldering for copper/brass components, and dipbrazing for aluminum. All processes were successful for some components and failures on others. The most common cause of failure was residual flux that after finding its way to the surface would corrode and separate the junction; unfortunately, this is a longer term effect and may not show up during early component tests. Here the designer must work with the brazier or welder and try to reduce the chance of residuals. Torch and oven brazing also anneal the material so the component no longer behaves elastically to external force and the long term behavior of flanges becomes unpredictable. Low temperature solders should be used only to establish electrical conductivity, not mechanical continuity since the long term creep strength is negligible in terms of flange forces. Aluminum dipbrazing tanks must be fresh and clean to avoid pits and bubbles along seams which often produced IMP's during the



program. All bolted connections fall into flange categories and should follow previous recommendations.

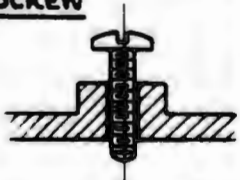
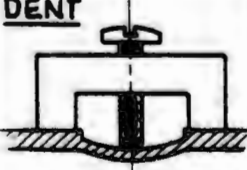
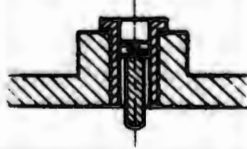
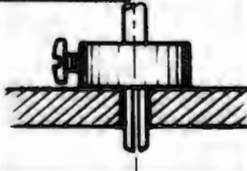
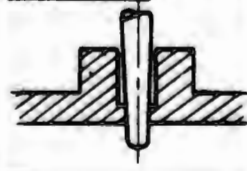
## 2.5 Tuning Approaches

For the bands over which this study operated (i.e., 7.25 to 7.75 GHz for receive and 7.90 to 8.40 GHz for transmit) tuning of some sort was mandatory for filters. Toward this end the study examined eight tuning methods from a mechanical standpoint, and of these tested five under high power. The five illustrated in Figure 2-3 are (1) the conventional screw, (2) controlled denting, (3) the precision screw, (4) the split pin, and (5) the taper pin.

The conventional screw is easily installed, inexpensive, versatile in its placement, and is easily controlled and recovered during tuning operations, but was one of the major sources of IMP's. The very nature of threads prohibits full contact between male and female counterparts and encourages burrs or filaments on the outer edges. Various sizes of threads and fittings from coarse to fine, from loose to tight, and from free to locked, were tried with nearly all attempts failing to meet linearity specifications. In very rare instances a quiet screw was obtained, but no correlation between IMP level and mechanical appearance or fit could be established. Soldering was also attempted by pretinning the hole and screw and then heating the unit after tuning. The attempt was not successful but with additional experimentation might have been a success. Nevertheless, the study concludes that the use of conventional screw should be discouraged.

Dent tuning has been quite successful as a quiet tuning method, but not so successful in providing tuning control. Dent tuned 18-cavity filters provided an initial quiet test bed for testing other better tuned filters, even though the passband VSWR of the dent tuned models was higher than required for normal deliverable feeds. The recoverability of copper or brass to an external force amounts to less than a few thousandths of an inch, so considerable experience and care is required of the technician who tunes a filter in this manner. For other less critical waveguide components dent tuning should be considered where wall thickness and configuration

FIGURE 2-3  
COMPARISON OF TUNING METHODS

METHOD	MANUFACTURING LEVEL	EASE OF TUNING	LONG TERM STABILITY	PROBABILITY OF NO IMP's <sup>*</sup>
<u>SCREW</u> 	STANDARD	STRAIGHT-FORWARD	POOR	< 5%
<u>DENT</u> 	STANDARD	REQUIRES MUCH PRACTICE & EXTREME CARE	EXCELLENT	> 99%
<u>PRECISION SCREW</u> 	PRECISION	STRAIGHT-FORWARD	POOR	< 5%
<u>SPLIT PIN</u> 	STANDARD	REQUIRES SOME CARE	FAIR	> 70%
<u>TAPER PIN</u> 	HIGH PRECISION	REQUIRES EXTREME CARE	EXCELLENT	> 95%
<u>OTHER</u> PRESS FIT COLLET EXPANDABLE PIN	PRECISION	VARIABLE	GOOD (EST.)	UNKNOWN

<sup>\*</sup> IMP'S BELOW -140 dBm FOR 10 KW TOTAL POWER

permit. The designer must know the limit of his material, however, and should stay well under stress levels that would fracture the metal. Over-stressed copper will generate intermodulation products.

Precision screws purchased from an outside vendor have no advantage over conventional screws as two threaded junctions now exist rather than one. Also, this type of screw with its non-contacting shaft is highly susceptible to small particles that may become lodged between wall and shaft, thereby further encouraging IMP's. During the program the precision screw was never quieted, and hence is not recommended in common transmit/receive areas.

The split pin was not intended to be an end of itself, but a means of initially tuning a complex device so that taper pins could be fitted later. However, whenever the hole was precision reamed and the taper pin free of burrs and with sufficient spring action to form good contact, the tuning was often free of IMP's. Hence, the designer should not discard this device as a final tuning method. He must, however, devise means of permanently locking the tuning in place and of keeping particles from between the split shaft.

The most reliable and stable means of tuning is the taper pin, which for this study was inserted into a pre-tuned filter and cut to the proper length to generate an estimated wall pressure of about 12,000 psi. Under these pressures any slight deformity or ellipticity is removed and full contact is achieved. Again, the designer must be sure all burrs and scratches are removed from the mating surfaces and surface polish is commensurate with material elasticity as suggested in Figure 2-1.

Of the other tuning methods, press fit pins are unacceptable for softer metals because of galling; collet tuning and expandable pins appear feasible but were not tested under RF conditions. There are without doubt many other methods of tuning that would be successful, but regardless of the detail approach, if the principles presented above are applied the designer should obtain a good estimate of the probability of success.

## 2.6 Test Facility Requirements

As a final point, the facilities required to adequately test components will be discussed. This will enable the reader to recognize what his test bed needs are for a program of equivalent frequencies and sensitivity. The first requirement, of course, is a high power amplifier capable of delivering 5 to 10 kilowatts of carrier power. The bandwidth must be at least 150 MHz if it is to transmit carriers at 7.90 and 8.05 GHz, the minimum separation to place a third order product in the receive band. It is desirable that the transmitter have a broader bandwidth than the minimum, preferably covering the entire 7.90 to 8.40 GHz band because results may be deceiving if shorts or filters cause a current null of either transmit carrier or intermodulation frequency to fall on a test junction. The broader bandwidth and frequency search remove critical phasing constraints.

The receiving or monitoring system should have a noise figure of 6 dB or better if signals in the -140 dBm range are to be studied. This means that a paramp or tunnel diode amplifier must precede the spectrum analyzer. Since thermal noise power is -174 dBw/Hz at room temperature (290°K), a 100 Hz predetection bandwidth on the spectrum analyzer preceded by a 6 dB NF amplifier will give a theoretical noise level of -148 dBm. The 8 dB margin is adequate for cable losses and other factors that cause the real sensitivity to deviate from theoretical. It is also recommended that a spectrum display similar to the HP 141T be used as the persistence capability is required to spot the IMP during the extremely slow scan rates of narrow bandwidth. The two unmodulated carriers used for driving the power amplifier must be stabilized to 1 part in  $10^9$  or better for the short term. Instability greater than this value will cause spreading of the spectral energy and an artificial reduction of the IMP level.

At least 200 dB of filtering over the 7.25 to 7.75 GHz band must be inserted between the HPA and the testing area if wideband amplifiers such as TWT's are used. Any lower value will cause transmitted IMP's to appear in the test region. If klystron amplifiers are used the filtering can be lowered to about 150 dB or less, depending on tube gain and output filtering

in the receive band. Between the bands (i.e., from 7.75 to 7.90 GHz) at least 100 dB of rejection is required, usually by a separate bandstop filter since the skirts of normal transmit/receive combinations leave an unprotected void at about 7.83 GHz. The energy from TWT HPA's passing through this window is of sufficient level to burn out the tunnel diodes.

A screen room of 80 dB isolation is recommended for the test area, the transmitting area, or both, since the IMP level "floating" in the vicinity of the transmitter is typically 60 dB above the noise level. Stray signals are invariably picked up by cabling and/or low noise test instruments.

In addition to the above recommendations there are, of course, other requirements for monitoring, amplifying and transmitting signals that are obvious to those who normally work with microwave equipment. These are not summarized here but can be derived from the body of the report, if necessary.

The experimental program originally intended to supplement the theoretical study, and through well controlled experiments support, deny, or categorize the various effects. Subsequent design could then specifically address the cause, rather than a general list of do's and don'ts. Unfortunately, testing facilities were far more non-linear than had been expected and manufacturing processes far more imperfect, so the majority of effort was expended in a continuing struggle to maintain a quiet test bed of sufficient sensitivity for the program. Ultimately a stable and quiet test facility arrived, but too near the end of the program to permit the completion of desired correlative tests. This is not to imply that the program was unsuccessful, for to finally achieve repeatable and reliable quietness in a test bed is a major accomplishment in itself. Furthermore, the results of measurements taken on defective components, coupled with data taken periodically on temporarily quieted facilities, still can be compared with some validity to the theory. If the reader remembers that ideally controlled experiments were not made and recognizes a range of uncertainty in the author's interpretation of happenings, then the following discussion is valid.

In relating the theory to experiments, each theoretical postulation is discussed individually and wherever practical related to particular results. Frequently the text refers to figures or equations in the various reports. Since both experimental and study reports use duplicate numbering systems, the reference is identified by ER and SR respectively (e.g., Figure 2.2-1 (SR) or Figure 4.3-5 (ER) refer to the study report and experimental report, respectively).

### 3.1 General Model

Section 2.0 (SR) develops the basic equations for the non-linear generating mechanism, assuming the transfer function is a polynomial of the  $m$ th order. Using only the first three terms of this polynomial, the response of Figure 2.2-1 (SR) is obtained, in which the IM level is plotted as a function of power ratio with total power held constant. This information is repeated

here as the solid line of Figure 3-1, and superimposed is the standing and traveling wave data of Figures 4.3-5 (ER) and 4.3-6 (ER). Both experiments and theory demonstrate a 2 dB/dB response to changes in the carrier closest to the IM product, and 1 dB/dB for the carrier farthest from the IM product. By extrapolating the linear portions of the curve, the crossover point (M) occurs for equal carrier ratios. The maximum IM level is obtained when the carrier nearest the IM frequency is about 3 dB greater than the remaining carrier. (Note that the level of all data is normalized to the level of the apparent extrapolated crossover point.)

Thus, the cubic-function model, as represented by equations 2.2-1 (SR), 2.2-15 (SR), and 2.2-22 (SR), appears to be a good one, particularly in describing 3rd order behavior.

The fifth order predictions are presented in the tunneling/filament-conduction discussion of paragraph 3.2.4 (SR), but are derived nevertheless from the above equations. Predictions here are for variation of between 15 dB and 30 dB per order for 200 watts, depending on assumed oxide layer thickness; no variation with power is indicated.

To compare the measured variations of higher order IMP levels the reader is referred to Figure 4.4-3 (ER) and Figures 6.5-1 thru 6.5-3 (ER). For input power levels of between 10 and 1000 watts the level difference between third and fifth orders ranges from 10 dB to as high as 50 dB. The consistency between theory and experiment is not clear here, but the reader should remember that in most tests the flanges and non-linearities were phased for the third order and coupling impedance could be substantially different for the fifth or higher order.

Even so, the wide range of values predicted by the theory is somewhat consistent with the wide range experienced during tests, so until further data is taken the equations are assumed to hold for higher orders.



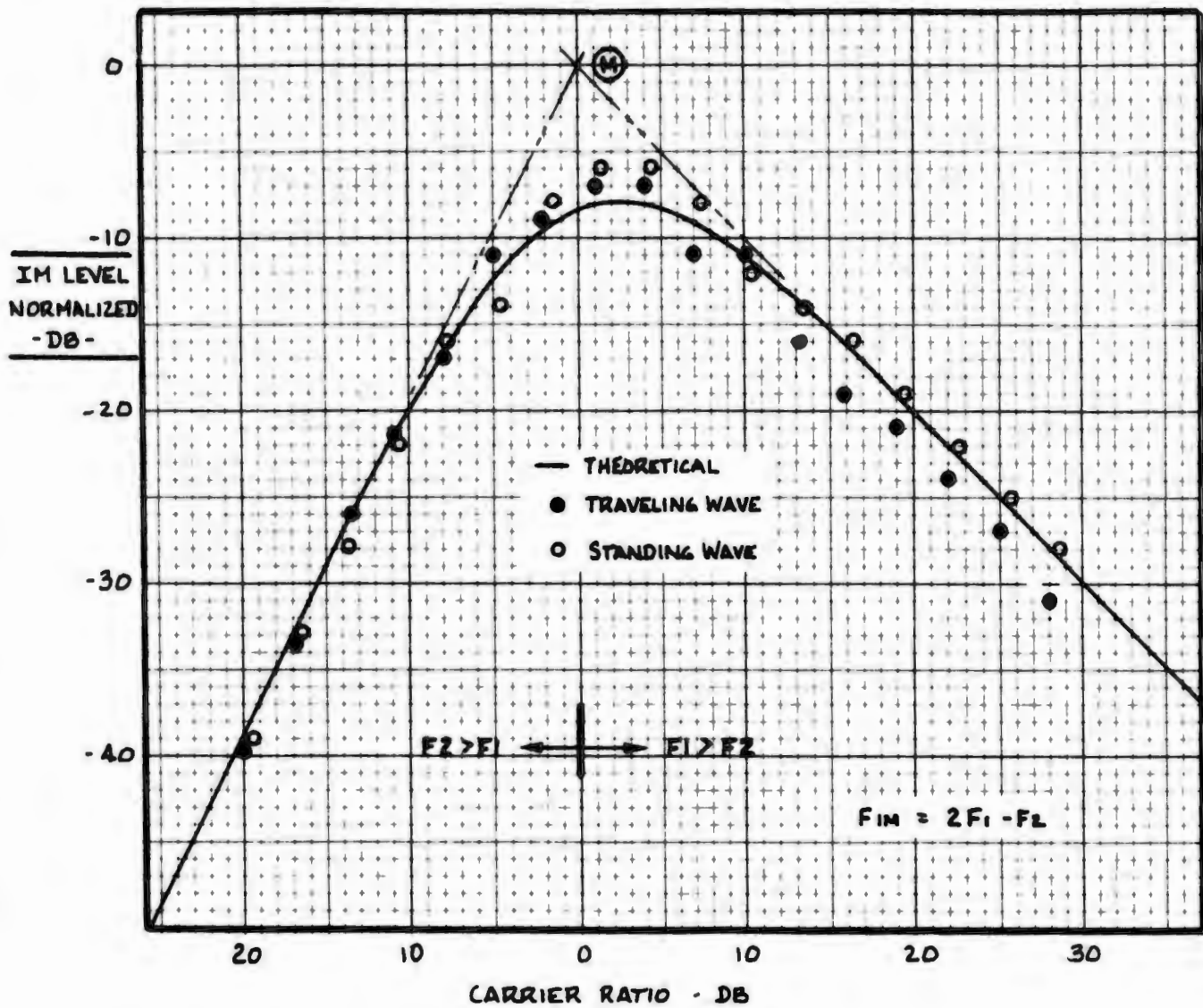


FIGURE 3-1 COMPARISON OF MEASURED & THEORETICAL IM MODELS



### 3.2 Flange Contact Model

A flange contact model is established in the various sub-paragraphs of paragraph 3.2.1 (SR) and illustrated in Figure 3.12 (SR). Regardless of the type of IM generating mechanism, whether semiconductor, tunneling, filament conduction or microdischarge, if a major non-linearity exists at a flange or similar junction, and if the flange model is correct, then a well defined behavior should be evident. The principal of the basic model is repeated in Figure 3-2 where current flow patterns for a progressively tightened flange are illustrated. If the flanges are only lightly touching, then contact is made only at ripples at the (A) level and full conduction current occurs in very few points (hence high current densities). As the flanges are tightened, more and more contacting points occur and the current is distributed.

All mechanisms described in the study are current dependent, so if the current density is decreased, either by lowering the RF power or increasing the number of contacting points, the effect on IM level should be nearly identical. This consistency is substantiated by Figure 6.5-1 (ER) where a coarse relationship between pressure (contact area) and IM level is observed. The curve labeled "Base Flat Flange" shows an intermodulation product at -105 dBm for 5-inch/lbs. bolt pressure, decreasing to -126 dBm above 20-inch/lbs. The shape of the curve agrees with the modeling principle in that the rate-of-change of the IM level is rapid at low bolt torques and slow at torques above 15 inch/lbs.; in the same manner the rate-of-change of the flange contacting areas of Figure 3-2 (and current distribution) is large for light contact and smaller for heavy contact.

The model is further confirmed by Figure 4.2-7 (ER) which presents data taken on flanges purposely made coarse with various sandpaper grit. These flanges were tested immediately after lapping (or sanding) so it is supposed that the oxide or contaminant levels were negligible. This graph indicates that a rougher surface produces higher IMP's, and that additional tightening ultimately makes the rougher surface equivalent to a smoother one (compare final rough flange test data to polished flat flange data). Again, the data supports the chosen model.

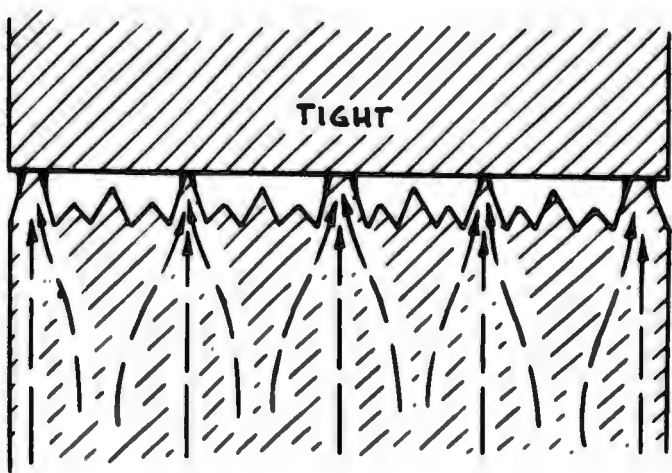
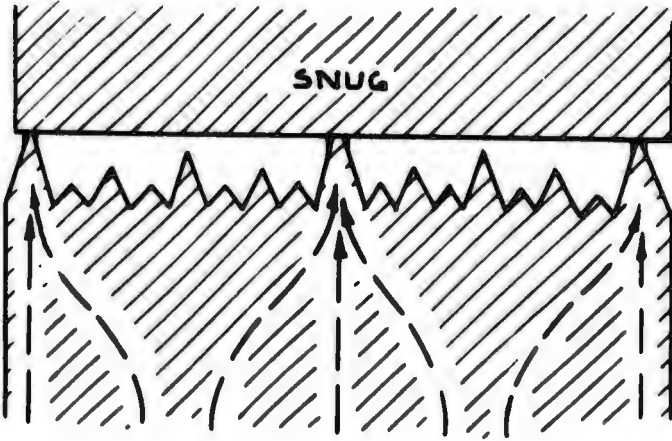
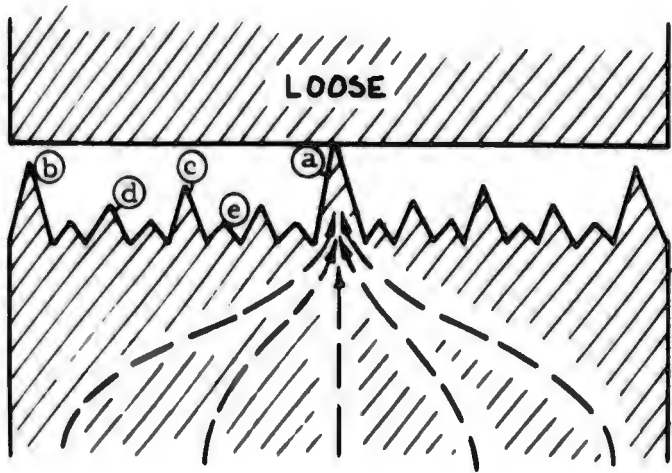


FIGURE 3-2

FLANGE  
CONTACT  
MODEL

Hence, from both an intuitive and experimental viewpoint the flange model appears valid and the "A-Spot" principles apply.

### 3.3 Semiconductor

The semiconductor theory assumes the flange is coated with an oxide layer of sufficient thickness and of appropriate material (or doping) to produce a depletion layer at the metal-oxide-metal junction. The conditions under which this theory would be verified are the following: (1) the non-linearity should be independent of atmospheric pressure, (2) the IM level should be somewhat dependent on D.C. bias level for high impedance contact, and (3) the level should be relatively independent of oxide layer thickness after a certain angstrom layer is established.

The vacuum chamber tests of paragraph 4.4.1 (ER) show that in closed waveguide the intermodulation levels are independent of environmental pressure and the oxide layer tests of paragraph 4.2.4.1 (ER) and paragraph 6.4 (ER) indicate that the level is independent of oxide layer thickness. These observations support the semiconductor theory. However, from the biasing tests of paragraph 5.6 (ER) there appears to be no relationship between applied D.C. voltage and intermodulation levels. Hence, since all three conditions are not simultaneously satisfied, it is assumed that classical semiconductor theory, per se, does not apply.

### 3.4 Tunneling

From a physical point of view, the tunneling models of Figures 3-29 (SR) and 3-30 (SR) more closely describe the metal junction than the previous semiconductor model. In most respects the tunneling phenomena should respond like the semiconductor, except the non-linearity (or tunneling current) is heavily dependent on oxide thickness as supported by Figures 3-45 (SR), 3-46 (SR) and 3-47 (SR) (repeated here as Figure 3-3). Thus, if tunneling were the dominant force at the -140 dBm level (or 200-210 dB below the carrier), then there should be substantial IM level variations for different metals and different oxide thicknesses. However, experiments

show that the IM level observed from flanges is independent of oxide thickness, whether the flange surface was exposed for only a few minutes after polishing, a few hours, days, or even months, as noted in paragraph 6.4.

While the range of intermodulation products expected from a new flange should vary substantially over the first 24 hours of exposure, actual measurements held relatively constant regardless of surface age at the levels indicated by the shaded areas of Figure 3-3. (Note that the theoretical curves assume optimum tunneling over the flange; however, the shunt characteristics of spot breakthrough would lower the curves to the levels of measured data. Nevertheless, it is change we are attempting to observe, not absolute level.)

It would also appear that a highly polished surface should be more susceptible to the tunneling effect than a rougher one, in that the flatter surface would distribute pressures more evenly and would be less likely to encourage shunting spots where metal penetrates the oxide layer. The rougher surface, on the other hand, would tend to operate on the "Parker Seal" principal, where fewer jagged peaks would break through and imbed in the mating surface. Again, if the polished flange results of Section 7.5 (ER) are compared with the rougher flange data of Figure 4.2-7 (ER), the converse appears to be the rule. Also, since the shunt capacitance across a smooth oxide layer varies linearly with distance (i.e., 3 dB coupling variation between  $20\text{A}^\circ$  and  $40\text{A}^\circ$  for copper), while the tunneling effect varies over 100 dB for the same change, it would appear that whenever intermod exists at a flange the change with surface age would be larger. In reality this relationship has not been observed.

Although the surface contact and blending mechanism is still not well defined, it is the contention of those performing the experiments that tunneling alone is not a significant cause of intermodulation at the levels or under the circumstances of this program. This is not to say, however, that tunneling cannot combine with other effects to produce the experimental observations.

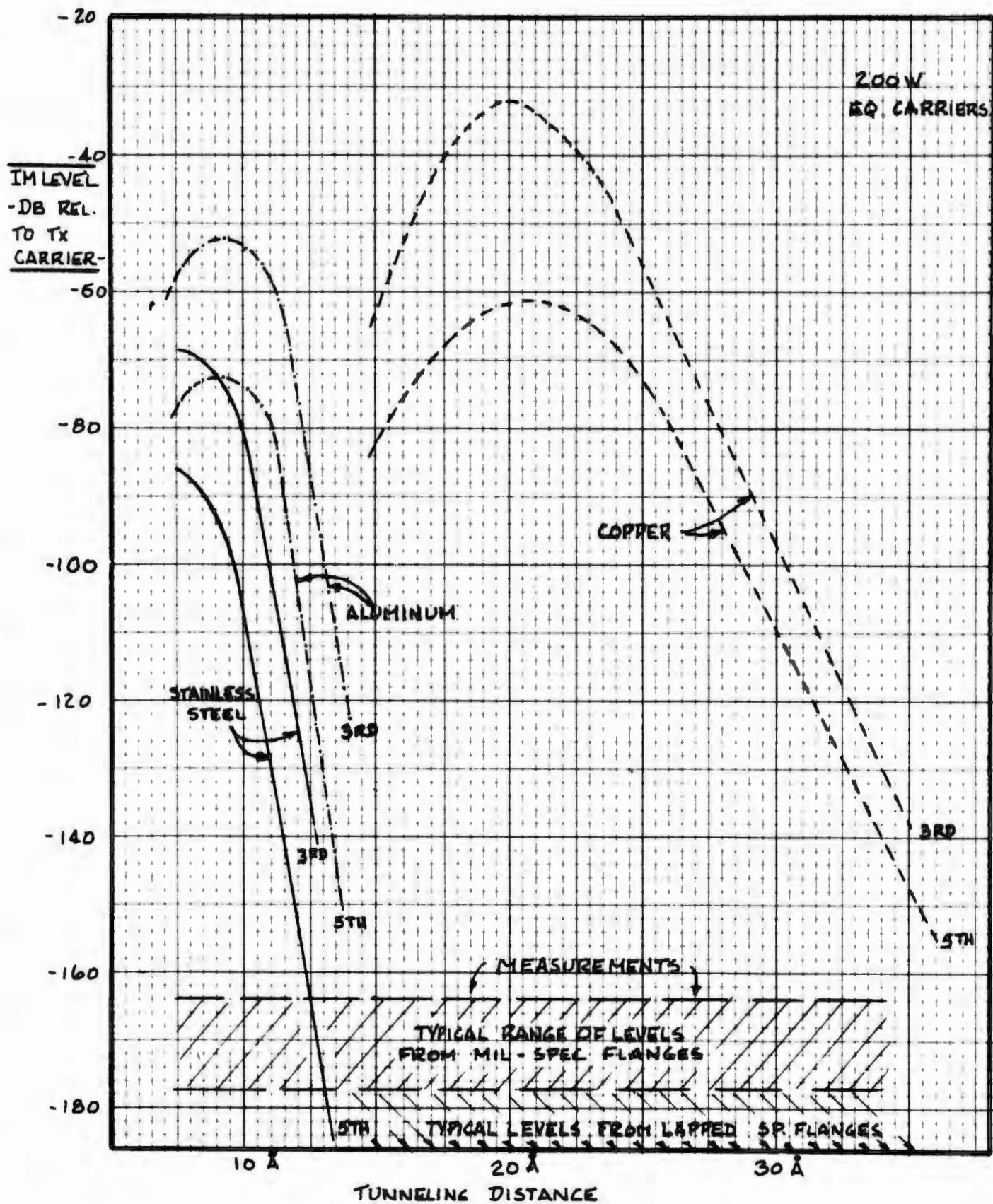


Figure 3-3

### 3.5 Filament Conduction

The Study Report only briefly mentions on pages 71 and 172 the existence of a phenomena called Filamental Conduction. The mechanism behind this occurrence is not clearly defined, but it is believed to be caused by microscopic filaments or whiskers which may promote a microdischarge, a non-linear inductance and resistance (referred to as the constriction inductance and resistance in paragraph 3.2.2 (SR)), or an exceptional tunneling effect if the filaments are tipped with an oxide. The study report, because of limited time and funds, arbitrarily lumps filamental conduction with the tunneling theory and discusses it as an entity no further.

After reviewing the behavior of flanges during tests it is felt that of all the areas presented, this one deserves considerable study and definition since its implied characteristics seem to agree quite closely with actual surface behavior of flanges. The rougher flange with sharper peaks and fewer contacting areas carrying high current densities is more likely to produce a non-linear constriction inductance than a highly polished flange. Furthermore, the high pressure contact (when computed or estimated full contact is reached on the microinch scale) would tend to compress filaments and make them less influential. During testing it has been observed on several occasions that small burrs or hairs (about 0.001" long or less) on or near the flange corners greatly enhance the susceptibility of a flange to create intermods. The broached surfaces of Figure 6.3-7 (ER) likewise produced IM's whenever scratches or metal filings were imbedded in the metal. Even in electroformed parts that fracture or fault, as described in paragraph 6.3.1 (ER), filaments are likely to be produced.

Thus, from a "compatibility with data" standpoint, filament conduction with constriction impedances appears to be a prime intuitive suspect since it would be relatively (1) independent of environmental pressure, (2) independent of oxide thickness, (3) dependent on contact pressure, (4) dependent on surface smoothness, and (5) independent of D.C. bias, all of which are characteristics of the experimental behavior.



### 3.6 Gaseous Conduction Phenomena

From an ionization breakdown point of view the theory suggests that under no circumstance will conventional breakdown or arcing occur in the waveguide and, therefore, no intermodulation products are possible from this source. On page 126 (SR), however, an exception is noted for the slot antenna case whenever the traveling wave passes a topwall slot orientated perpendicular to its direction of travel. In this case breakdown would occur at 6 KW for a 1 mm gap or less, or (by extrapolation) at 10 W SW for a 0.003 inch gap.

Experimental evidence points to the discharge as the major cause of intermodulation products in the "Cox" phenomena region, but of insignificant importance for the work at Philco-Ford. The vacuum chamber tests of paragraph 4.4.3 (ER) show an IM fluctuation with environmental pressure, but only if a deliberate gap is established between flanges. In this case the characteristic peaking of non-linearity is seen around 1 torr with a decrease in level for pressures below 1 torr. However, with no intentional air gap between flanges the intermodulation level remained constant for all pressures, indicating that some other mechanism predominates.

Similarly, corona discharge can and does occur in the waveguide, as noted in paragraph 6.3.3.2 (ER), where a brilliant glow has actually been observed within the waveguide. Under this condition the IM level increases to the Cox levels (some 100+ dB above typical levels). Again, however, the vacuum tests suggest that the corona discharge or related effects are not the significant cause of low level IM's.

### 3.7 Analogous Luxembourg Effect

In paragraph 3.3.2 (SR) the theory predicts an intermodulation level of -230 dB for a 10 meter waveguide filled with dry nitrogen, dropping to -390 dB if either water vapor or oxygen are present. The experiments cannot dispute this claim since such levels are far below the sensitivity of present measuring equipment. It is apparent, though that since quiet

systems have been obtained at levels of -210 dB relative to the stronger carrier, the Analogous Luxembourg Effect is insignificant.

### 3.8 Water Vapor - Non-Linear Absorption

Paragraph 3.3.3 (SR) discusses water vapor and concludes that for a 1% vapor content (about 80% relative humidity) the IM level from a 10-meter line would be about -152 dB below a 6 KW carrier or -85 dBm. Since all experiments have been run under low humidity (<30%) and with short lines, the theory cannot either be supported or denied. However, on occasion water loads have been used (reference paragraph 4.2.4 (ER), "Traveling Wave Tests"), and the system has been quiet to below -130 dBm at 5000 W, so if the water is non-linear it absorbs its own intermodulation products.

### 3.9 Waveguide Thermal Conduction Modulation

The theory presented in paragraph 3.4.1 (SR) concludes that an intermodulation product of -298 dB below a 1 KW carrier is expected for a wave modulated by thermal conduction inertia in a 40-foot line. Again, since experimentation has demonstrated quiet systems, even with high power in heated waveguide, the importance of this phenomena is placed in its appropriate insignificant position.



SECTION 4.0

TESTING PROGRAM - PHASE I

(AS PERFORMED APRIL - MAY 1972)

## 4.1 LOW POWER SCREEN ROOM TESTS

### 4.1.1 Description of Test Area.

Originally, the IM Study Program intended to isolate intermodulation generating mechanisms, and determine how these mechanisms were influenced by fabrication and environmental variations. Hence, the first series of tests were initiated under highly controlled laboratory conditions, where generating and receiving equipment were isolated from each other, and test flanges were of controlled flatness and surface tolerance.

Two screen rooms were used to provide isolation between equipment. With all generating and combining equipment in one room and measuring equipment in the other, a quiet environment for flange tests was insured. To pass RF signals from one room to the other and still maintain screen room integrity, an assembly of copper-plated plates, waveguide and flanges was fabricated and installed as shown in Figure 4.1-1. Flanges were brazed to WR 137 waveguide and all joints were sealed with a non-hardening conductive paste.

The screen rooms were of welded steel (solid panel) construction. Although not measured, the estimated isolation between rooms was 150 dB.

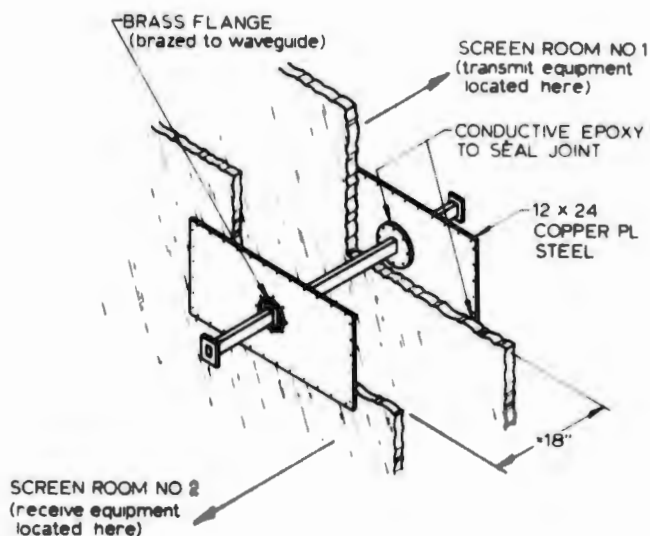


**FIGURE 4.1-1**  
**RF SEALING METHOD**

#### 4.1.2 Screen Room Test Setup

For screen room tests, the equipment shown in Figure 4.1-2 was used in the following configuration:

Generator Frequencies	7.90 GHz   Typical 8.05 GHz
Power Output	≤ 1 watt/carrier
Test Waveguide	WR 137
Test Flanges	CPR 137F (1/2" thick)
Monitored Frequency	7.75 GHz ( $2F_1 - F_2$ )
Paramp Noise Temperature	140°K (approx)
System Sensitivity	-140 dBm/1000 Hz (referred to test flange)
Field Distribution	Full standing-wave

#### 4.1.3 Screen Room Test Results.

##### 4.1.3.1 Closed Waveguide.

With two 3.5" sections of rectangular waveguide and one section of convoluted flexible waveguide inserted between the transmit and receive filters, no discernible intermodulation product was present when all flanges were tightly bolted. Furthermore, when two additional sections with circular cover flanges were added (8 ft. and 12 ft, respectively), the third order intermod was still not observed.

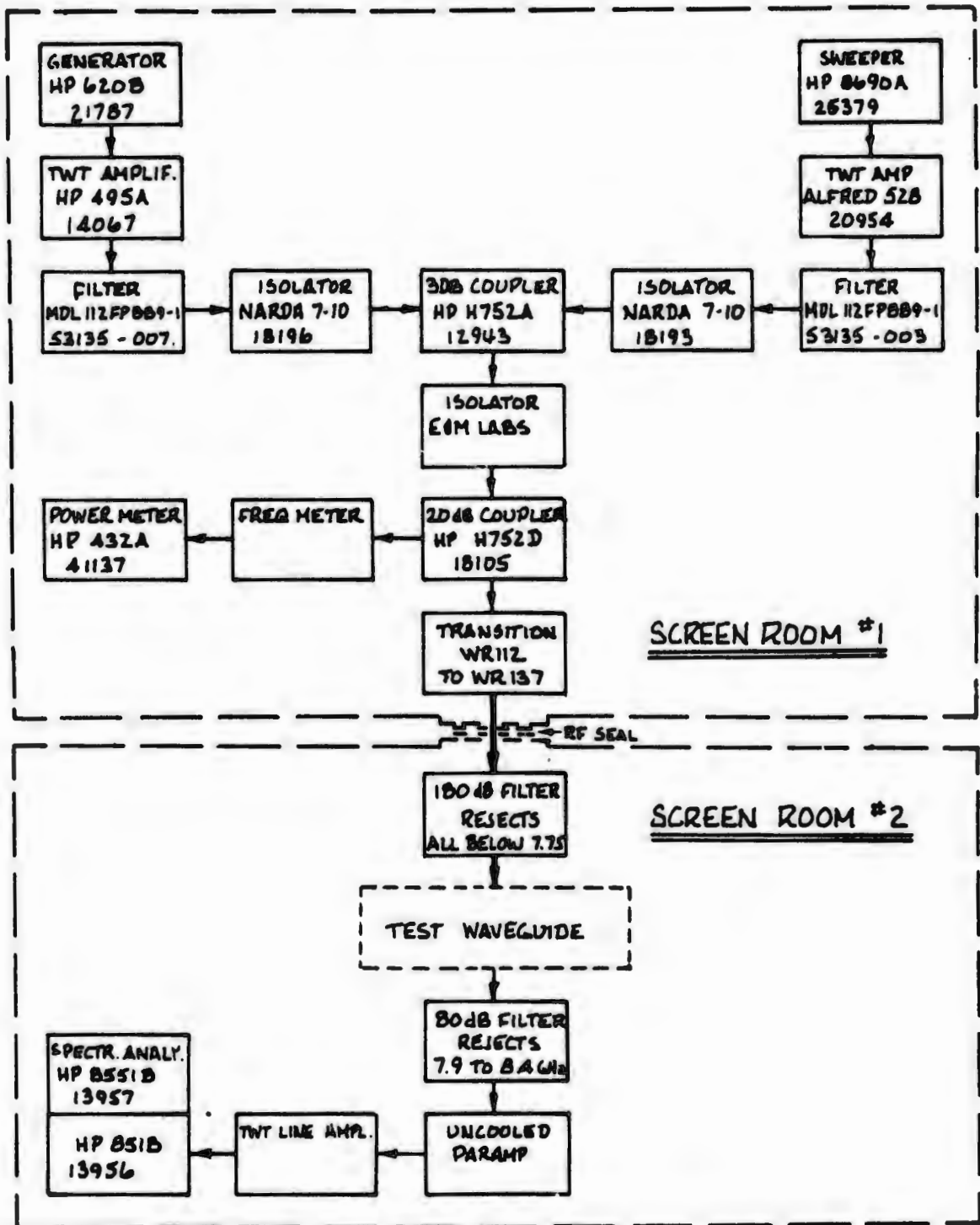


FIGURE 4.1-2  
SCREEN ROOM TEST SETUP

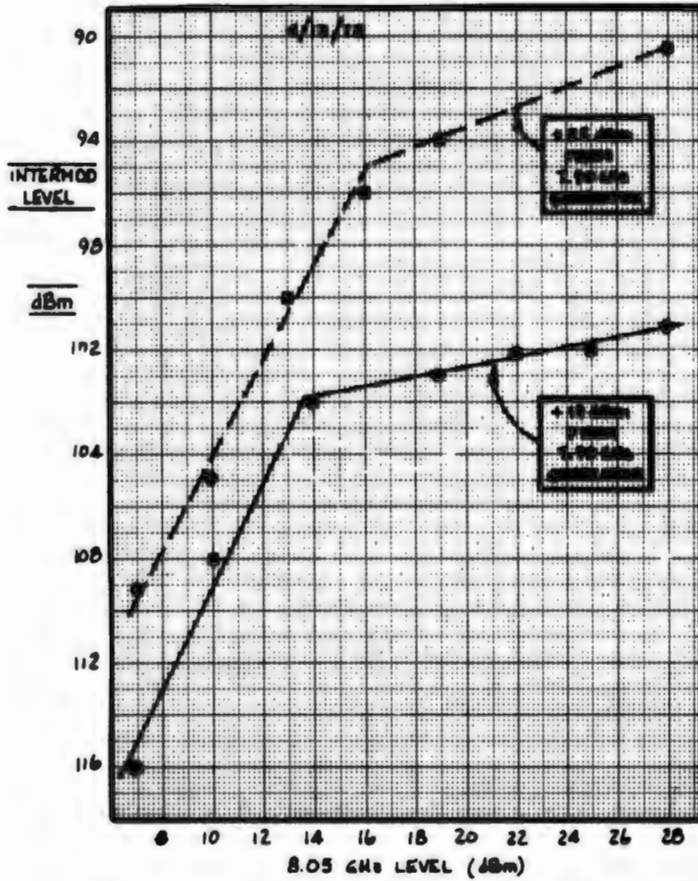
#### 4.1.3.2 Open Waveguide.

One of the CPR flanges was unbolted and contacting surfaces separated. No intermod was observed providing there were no loose metallic objects in the vicinity of the flange. However, by placing loose bolts, washers, or lightly contacting metal objects near the opened flange, the third order intermod could be generated. A similar effect occurred with loose bolts placed in the flanges. The intermod level during these external coupling tests was typically -130 to -120 dBm, but was too unstable for recording.

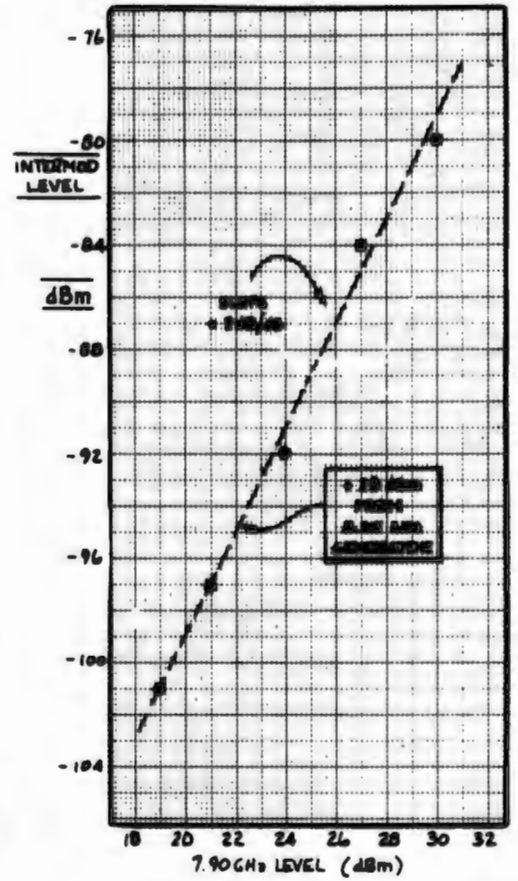
#### 4.1.3.3 Objects Within Waveguide.

A strong intermod was obtained by placing a loose bolt within a sealed waveguide. Here, signals up to -80 dBm were readily generated. Because this was the first evidence of stable intermods in controlled test lines, the power level was varied, and data taken as shown in Figure 4.1.3.

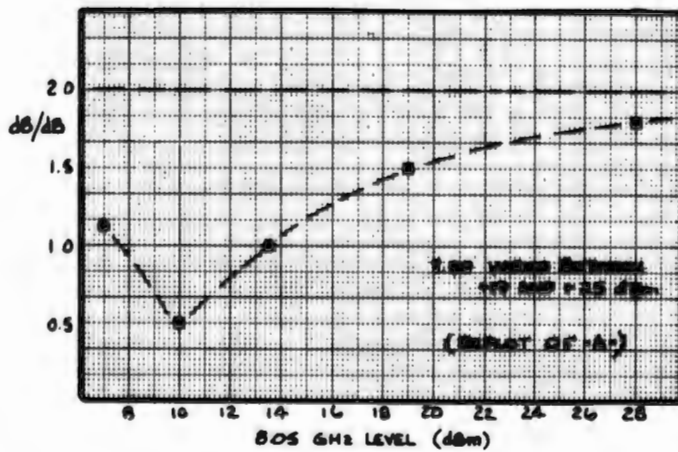
Two points are of significant interest here: (1) For the 8.05 carrier fixed at +28 dBm, variations in the 7.9 carrier level produce a 2 dB/dB response in the intermod level as shown in Figure 4.1.3-B. This follows higher power responses described in paragraph 4.2.3. However, as the 8.05 level falls below +28 dBm, the intermod variation no longer holds the 2 dB/dB relationship with the 7.9 carrier as shown in Figure 4.1.3-C. Whether this indicates a threshold effect is not known because of insufficient data points; however, future tests should re-examine this low level behavior. (2) There appears to be a leveling of the intermod level as the 8.05 level comes within 6 dB of the 7.9 GHz level as shown by Figure 4.1.3-A. (This agrees with higher power data in Section 6.2.)



A - INTERMOD VARIATION WITH 8.05 GHz LEVEL



B - INTERMOD VARIATION WITH 7.9 GHz LEVEL



C - SLOPE OF INTERMOD LEVEL WITH 7.9 GHz VARIATIONS

Reproduced from best available copy.

FIGURE 4.1-3  
EFFECT OF BOLT IN WAVEGUIDE

#### 4.1.4 Receive Filter Short Location.

The inability of test 4.1.3.1 to produce intermods was inconsistent with previous HT/MT measurements that had shown high intermod levels for one watt of carrier power. It was suspected that intermod levels were functions of field gradients at contacting points, so an investigation of the waveguide field distribution commenced to defined voltage and current peaks with respect to junctions.

In the setup of Figure 4.1-2, transmit signals are effectively shorted (or reflected) by the receive filter and create standing waves with a varying point of origin. The data presented in Figure 4.1-4 establishes the location of the first null within the receive bandpass filter over the lower portion of its reject band. By determining guide wavelength, the remaining field and current distribution within the waveguide is known.

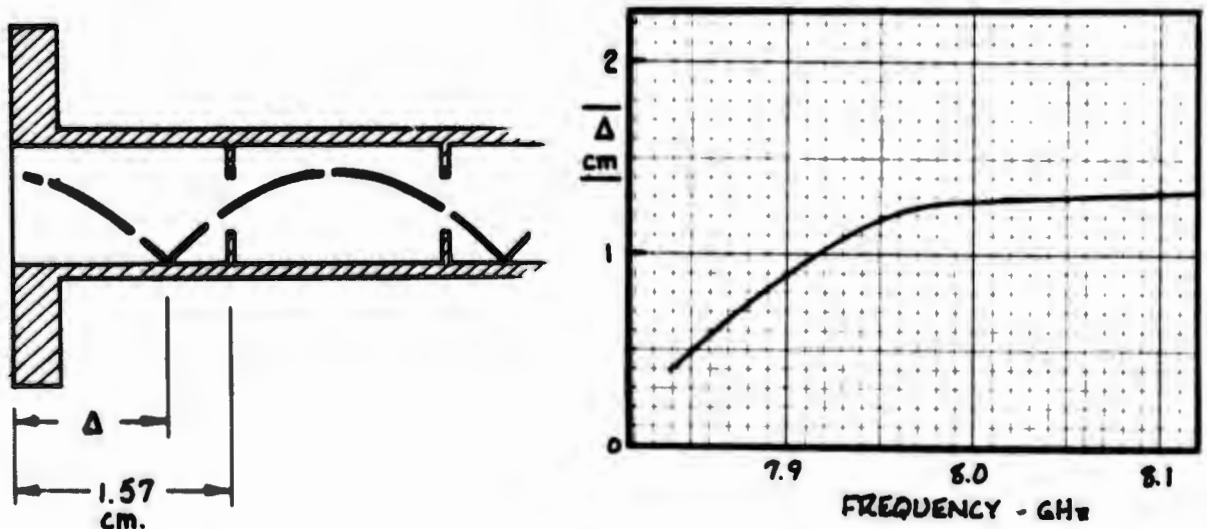


FIG. 4.1-4 SHORT LOCATION - HT/MT RECEIVE FILTER



#### 4.1.4 Receive Filter Short Location.

The inability of test 4.1.3.1 to produce intermods was inconsistent with previous HT/MT measurements that had shown high intermod levels for one watt of carrier power. It was suspected that intermod levels were functions of field gradients at contacting points, so an investigation of the waveguide field distribution commenced to defined voltage and current peaks with respect to junctions.

In the setup of Figure 4.1-2, transmit signals are effectively shorted (or reflected) by the receive filter and create standing waves with a varying point of origin. The data presented in Figure 4.1-4 establishes the location of the first null within the receive bandpass filter over the lower portion of its reject band. By determining guide wavelength, the remaining field and current distribution within the waveguide is known.

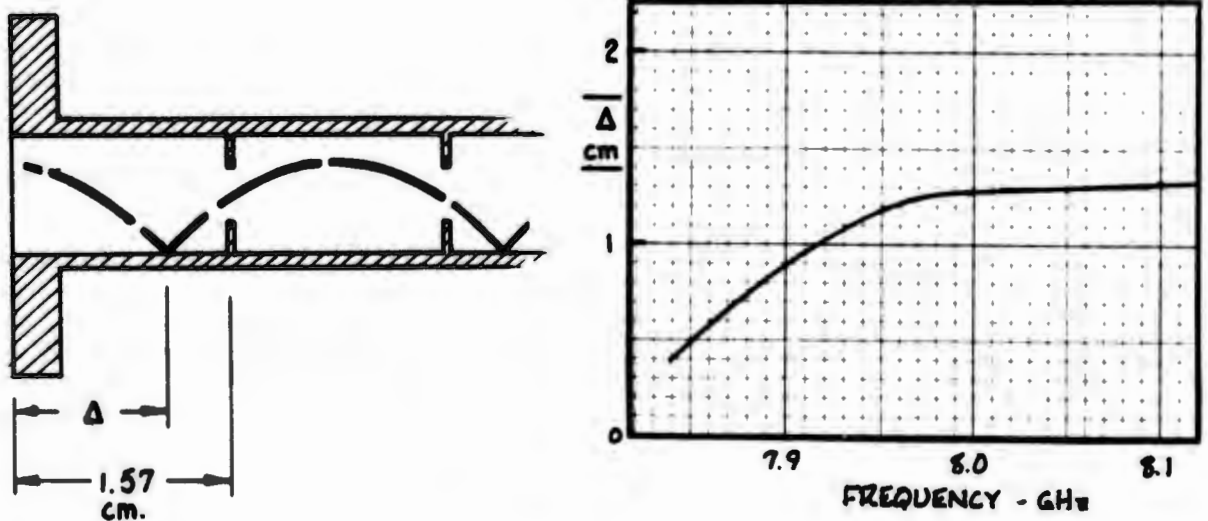


FIG. 4.1-4 SHORT LOCATION - HT/MT RECEIVE FILTER

#### 4.1.5 Transmit Filter Short Location.

During the test program, the transmit filter was not considered an influence on the level of intermodulation products. Nevertheless, measurements were made to establish an effective short location for the filter reject band, as shown in Figure 4.1-5.

More recently, the effect of the transmit filter on intermods has been reconsidered. Any source which introduces a new frequency into the waveguide is affected by the impedance at the point of entry. Since a short in one arm of the waveguide will vary the line impedance at any point from zero to infinity, it is appropriate to recognize the transmit filter location in future tests. (The location of the transmit filter could also affect the relative levels of the various orders of intermodulation products, particularly where only a few flanges are in the test setup.)

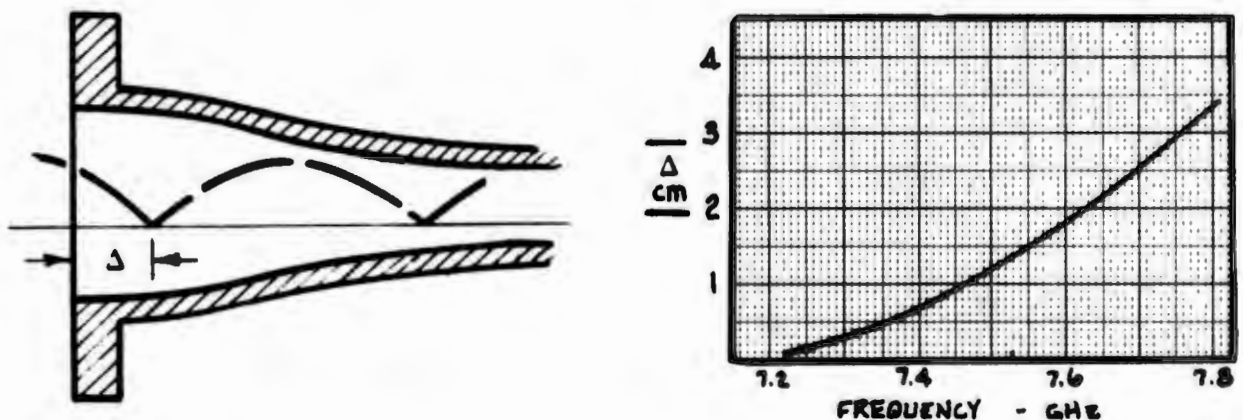


FIGURE 4.1-5 SHORT LOCATION - HT/MT TRANSMIT FILTER

## 4.2 HIGH POWER WAVEGUIDE TESTS

Believing that increased power would create intermods in closed waveguide, the setup was moved to the HT/MT antenna area. The MT Low Power Amplifier (LPA) provided capability to 2 KW and the High Power Amplifier (HPA) provided capability to 6 KW.

### 4.2.1 Standing-Wave Tests.

The equipment was again arranged in the standing-wave (fully shorted) configuration as shown in Figure 4.2-1. Flanges (1), (2), (3), and (4) were subjected to 100 watts of power, equivalent to 400 watts at the field and current peaks. As in the laboratory tests, no intermods were discernible, even with untightened flanges.

At this point, the filter short-position data was used with guide wavelength to plot actual field position within the waveguide. The results are shown on the following page.

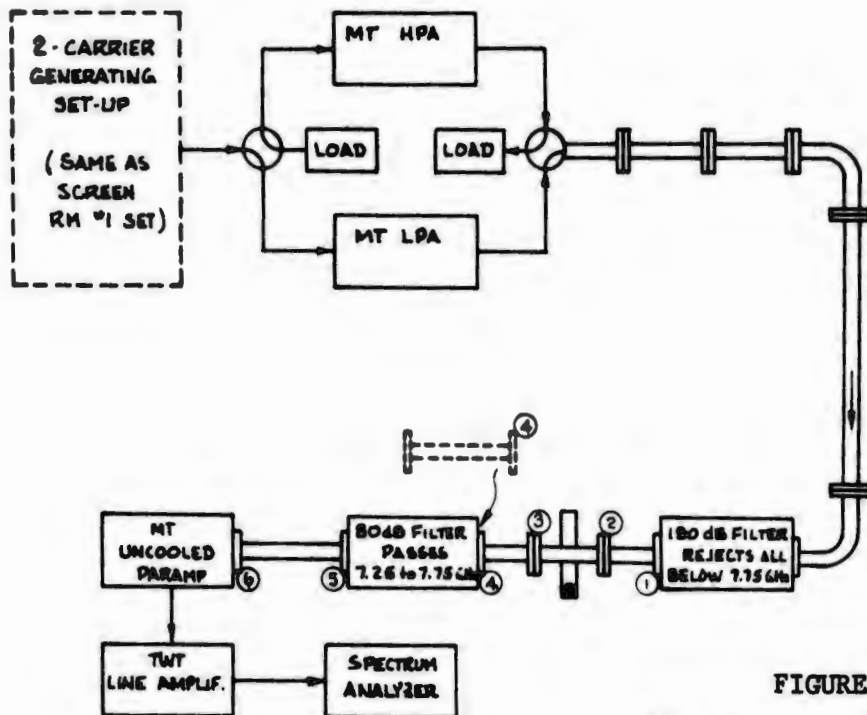
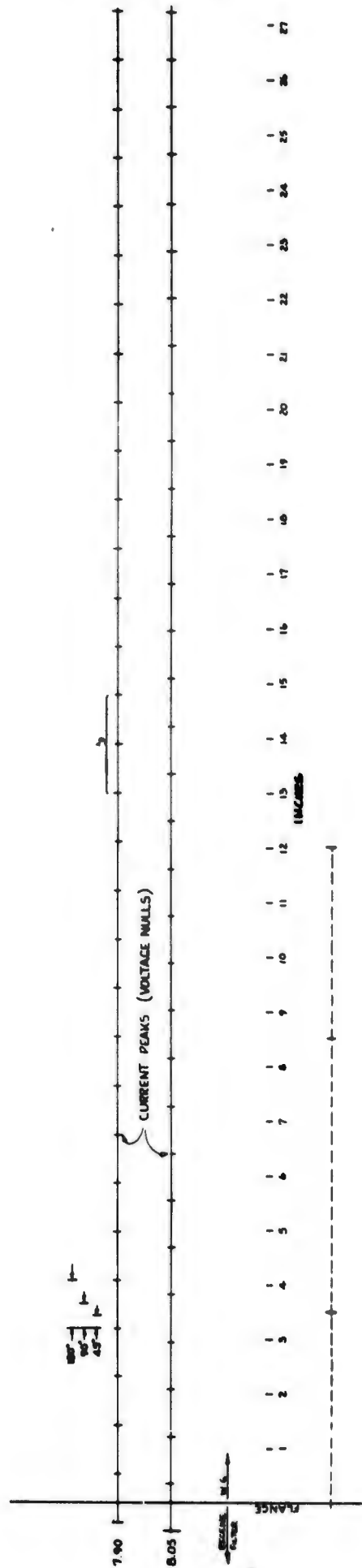


FIGURE 4.2-1  
HIGH POWER STANDING WAVE SETUP

The nulls of the waveguide fields for the test line of 4.2-1 are shown in Figure 4.2-2 for 7.90 and 8.05 GHz. The locations of flanges (1), (2), (3), and (4) are indicated on the dashed line and fall 3.5, 8.5 and 12 inches from the filter flange. Note that flange (4) lies near voltage peaks of both carriers, and if intermods were related to field strength, they should be generated in the 5.1-1 arrangement. Since no intermods were observed, it is assumed that flanges should lie on current peaks (or voltage nulls). Flanges (1) and (2) are positioned on 7.90 GHz current peaks, but are on 8.05 GHz current nulls. Since both carriers do not simultaneously excite the non-linearity, no intermod is expected.

In looking at Figure 4.2-2, current peaks of both sources agree at a point  $27 \frac{3}{8}$  inches from the receive filter flange. Hence, an additional section of waveguide was inserted at flange (4) to shift flange (3) to the current peak (note that flange (4) is also on a current peak because of the  $2\lambda$  separation). With the flanges optimally located, intermods were present at about the -70 dBm level.



**FIGURE 4.2-2**  
**WAVEGUIDE FIELD DISTRIBUTION**

#### 4.2.2 Soft Copper Gasket Design.

At this point soft copper gaskets were fabricated for sealing waveguide flanges in the test portion of the waveguide. These gaskets mated with the CPR 137F flanges and were made with a raised edge of between 0.005 and 0.010 inches, as shown in Figure 4.2-3. The material was OFHC copper, annealed by placing in a 1400<sup>o</sup>F oven for three hours, quenched, and etched to remove all oxides. A test gasket, after softening, had a softness rating of 49, based on Rockwell 30T test using a 1/16 inch diameter ball.

By inserting copper gaskets in flanges (1), (2), (3) and (4) of 4.2-1 third order intermods were progressively suppressed to below the noise level (about -130 f<sub>o</sub> to -135 dBm). Gaskets of two thicknesses were made: 0.25 inch and 0.06 inch, each equally effective in quieting flanges. Because of their location with respect to current peaks, flanges (2), (3) and (4) had the greatest effect on the intermod. These tests confirmed that longitudinal currents in conjunction with a small non-linearity in the conducting medium produce intermodulation. (See Section 5.2.4 for gasket limitations.)

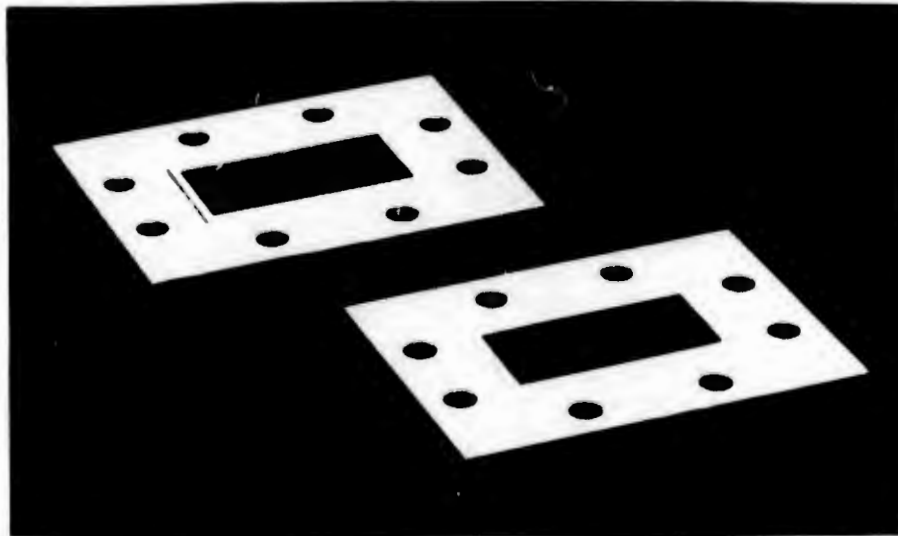


FIGURE 4.2-3  
SOFT COPPER GASKETS

### 4.2.3 Power Level Effect.

The copper gasket at flange (3) was removed and the power varied from 3 to 100 watts under the full standing wave condition. The intermod varied by 2 dB per dB of input power as shown in Figure 4.2-4. (During these tests, 75% of the power was applied to the 7.90 carrier and 25% to the 8.06 carrier at all levels; this ratio appeared to give the strongest intermod).

The level of the intermod depends on the assumed vs. actual gain of the paramp/TWT combination. Stability varied throughout the test, but a mean loop gain of 50 dB (including cables) was assumed. Consequently, the real level of the intermod may vary  $\pm 5$  dB from the levels indicated.

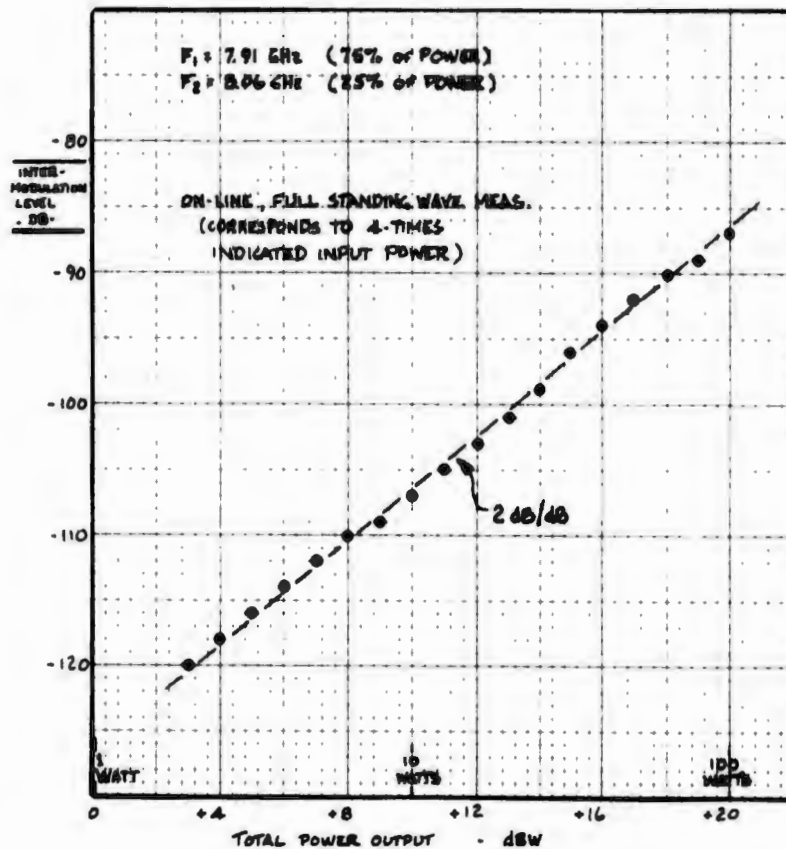


FIGURE 4.2-4  
POWER LEVEL EFFECTS  
(STANDING WAVE)



#### 4.2.4 Travelling Wave Tests.

The standing-wave tests previously described were limited in power level by the rating of the LPA isolator. To extend the power capability, the test setup was revised by adding a water load and placing the monitoring system off-line, as shown in Figure 4.2-5. In this manner, the LPA was used to 2.5 Kw levels, and the HPA to 6 Kw levels.

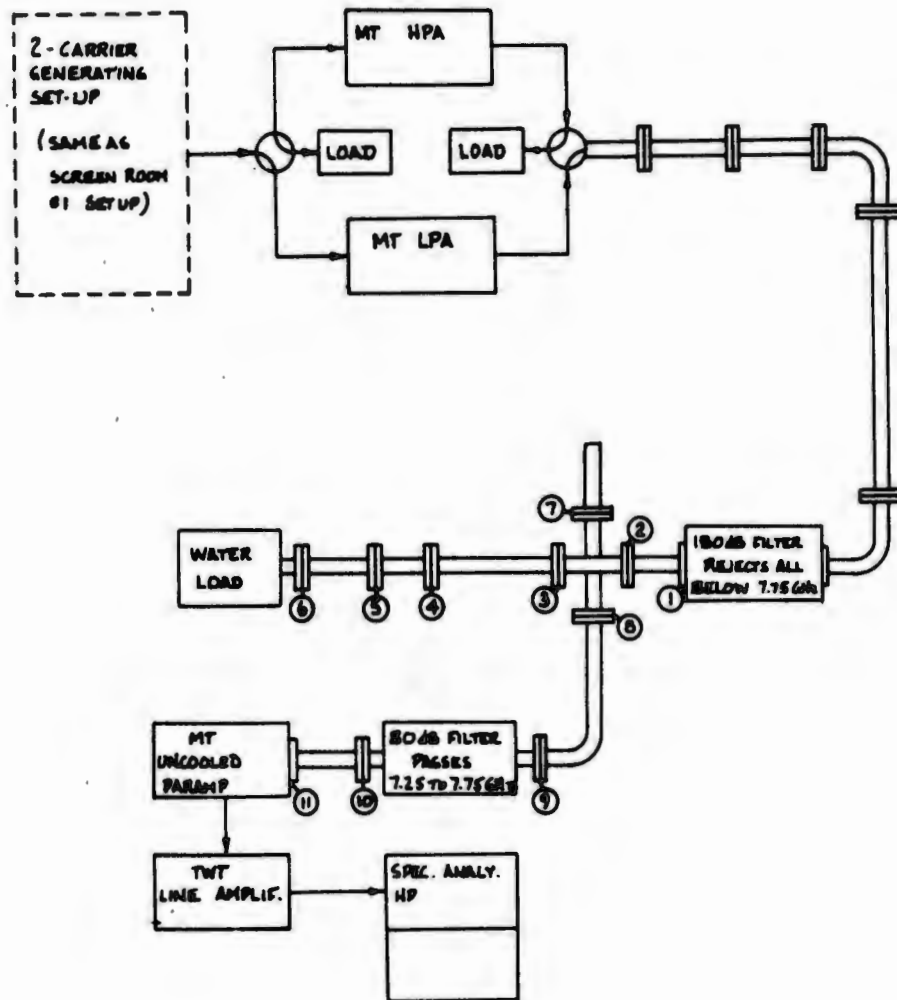


FIGURE 4.2-5  
HIGH POWER TRAVELING WAVE SETUP

#### 4.2.4.1 Smooth Flange Tests

A series of tests were made in the previous setup under two conditions: (1) a coaxial 20 watt load at flange (7) , and (2) a 200 watt waveguide load at flange (7) . The results are shown in Figure 4.2-6.

With the coaxial load, the intermod levels were consistently higher than for the waveguide load; in fact, the noise from the coaxial adapter dominated all others. Also, the intermod was less predictable with coax and varied whenever the load was removed and reinstalled. (These effects agree with previous measurements on the HT/MT system that showed all coaxial components to be strong sources of intermodulation.)

With a waveguide load, intermods decreased in magnitude as copper gaskets were added to on-line flanges. With a fully gasketed system, the intermod was reduced below visible sensitivity. It was also noticed that coaxial connectors or ungasketed flanges before the transmit filter or after the receive filter caused no measurable problem. Also, one copper gasket was heavily coated with oxide by heating to 1000<sup>o</sup>F and quenching; this gasket appears to be as effective as the clean ones in quieting the flange.

Note that primary line intermods are reduced by the crossguide coupler and are really 30 dB stronger than indicated.

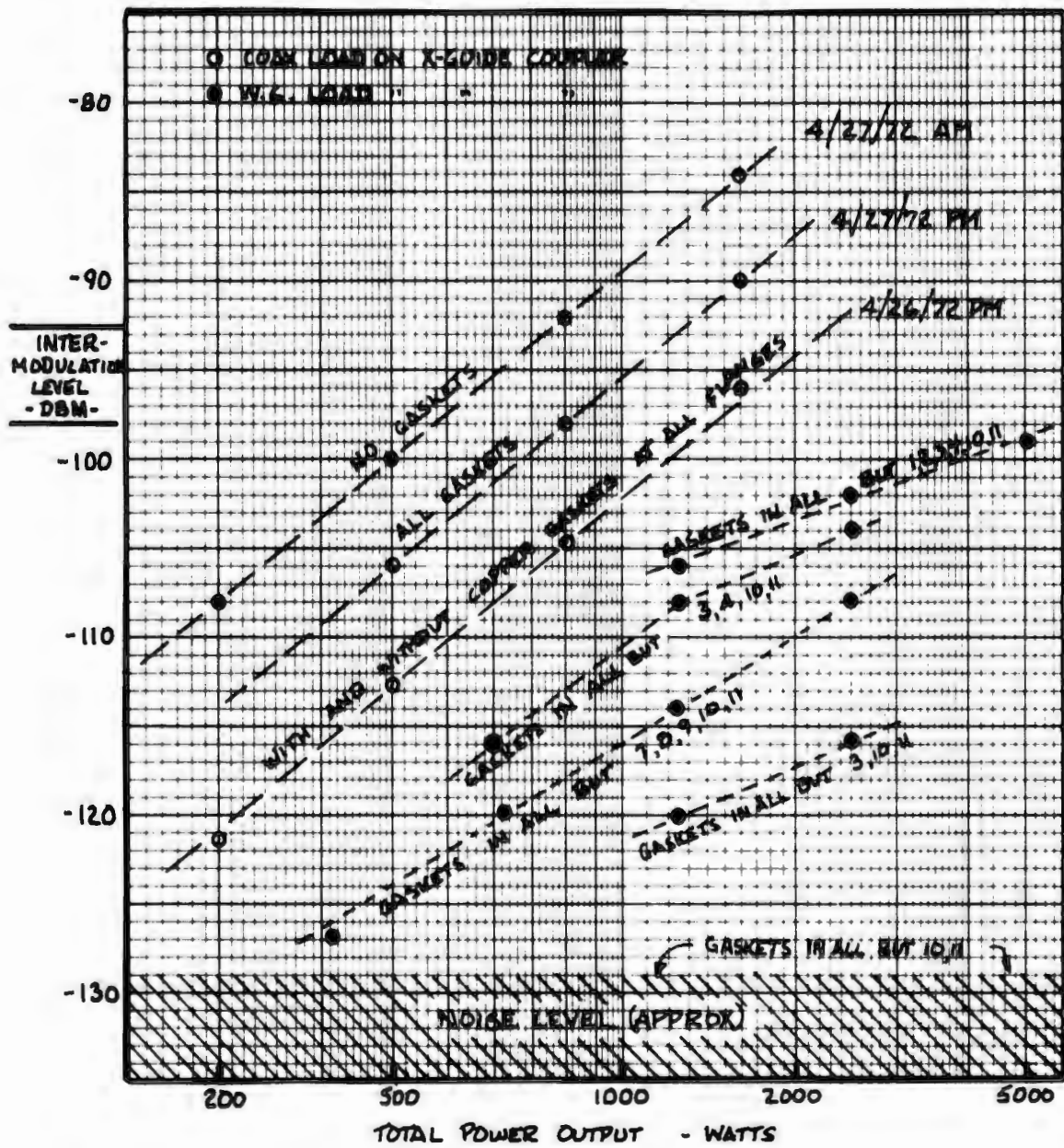


FIGURE 4.2-6  
 TRAVELLING-WAVE TEST #1 (HIGH POWER)

#### 4.2.4.2 Coarse Flange Tests

One series of tests were made to see if flange surface finish and grain had any effect on intermod level. Using the setup of 4.2-1 and inserting an ungasketed test flange at point (3) produced the variations shown in Figure 4.2-7. Only three cases were examined: E-vector scratches as produced by one pass over #240 grit emery cloth; H-vector scratches produced the same way; and a polished surface produced by figure 8 lapping on #600 emery cloth.

The upper three curves were made with flanges "snugly" tightened (probably about 20 inch pounds applied to the bolts). The final two curves were made with flanges heavily tightened (probably greater than 40 inch pounds). In general, it appears as though the E-vector scratches produce quieter flanges than H-vector ones, and a polished flange is best of all.

The reader should notice the change of intermod slope with applied power for smooth vs. coarse flanges, and for snug vs. tight flanges. The slope, which varies between 1 dB/dB and 2.67 dB/dB, might suggest a multiplicity of mechanisms that are either enhanced or suppressed by flange texture.

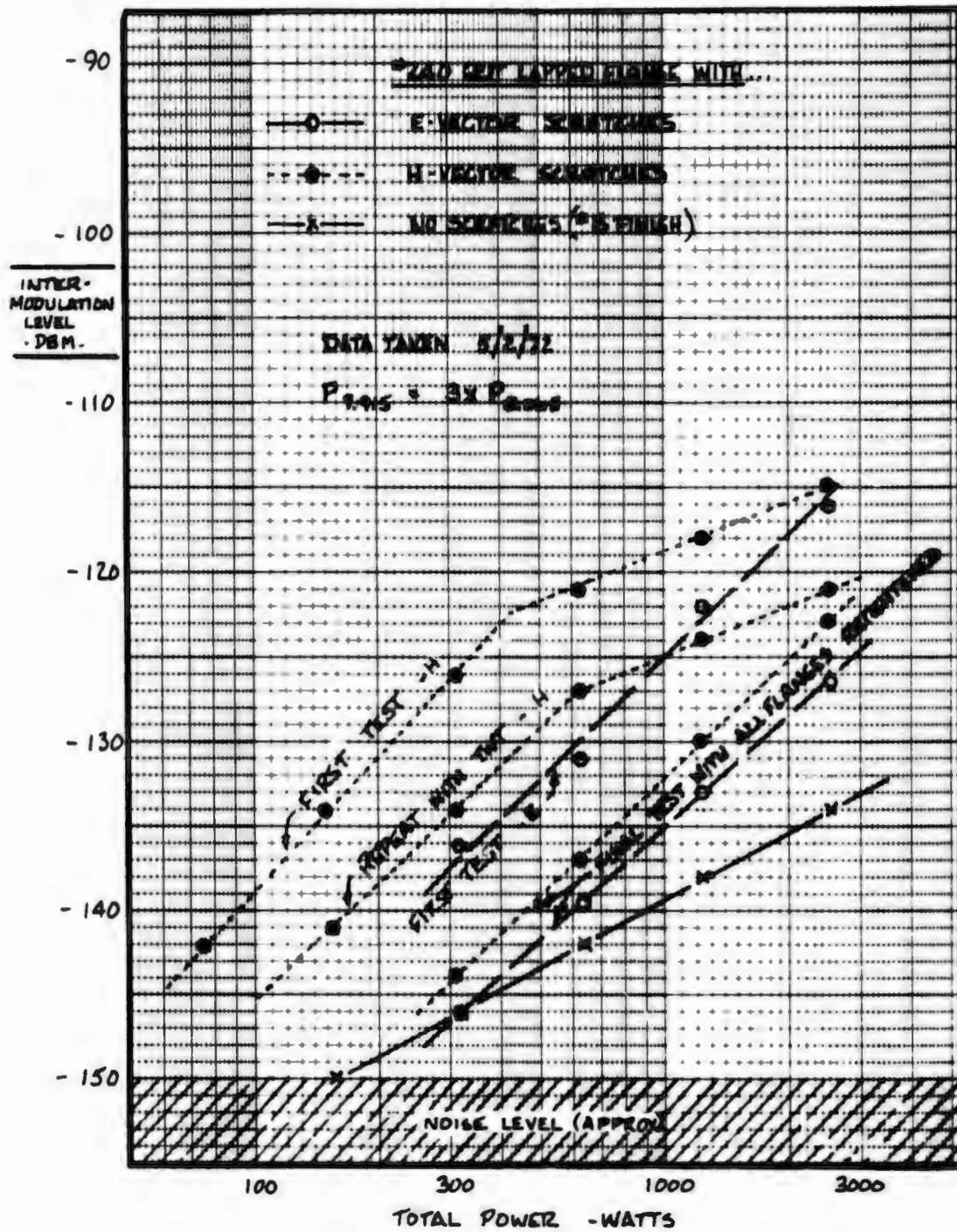


FIGURE 4.2-7

TRAVELLING-WAVE TEST #2 (HIGH POWER)

#### 4.2.4.3 Matched Discontinuity Tests

Standing-wave measurements indicated that high current densities accentuate intermods. To confirm this, while the transmitter and waveguide remained matched, several matched discontinuities were fabricated. These inserts were  $\lambda_g/2$  long and were stepped in the E-plane, H-plane, and E- and H-planes, as shown in Figure 4.2-8.

The rise in intermod level over a plain flange was not significant. For the worst case of an E- and H-plane step, the intermod rose about 6dB as shown in Figure 4.2-9. (This could be attributed to the added junction rather than the step.) However, when soft copper gaskets were inserted on both sides of the discontinuity, the intermod did not diminish. This was the only case when intermods were not suppressed in test lines by copper gaskets.

These tests support claims that discontinuities of waveguide flanges caused by lateral displacement accentuate current density and should be minimized by precision pinning of flanges whenever junctions are in areas common to receive and transmit signals.

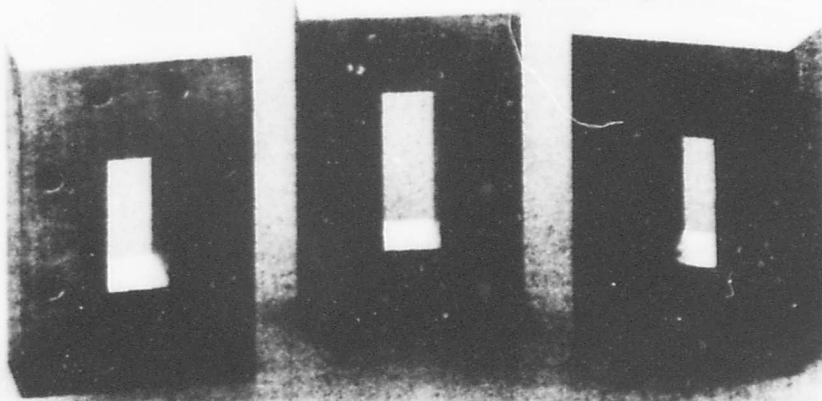


FIGURE 4.2-8  
MATCHED DISCONTINUITIES

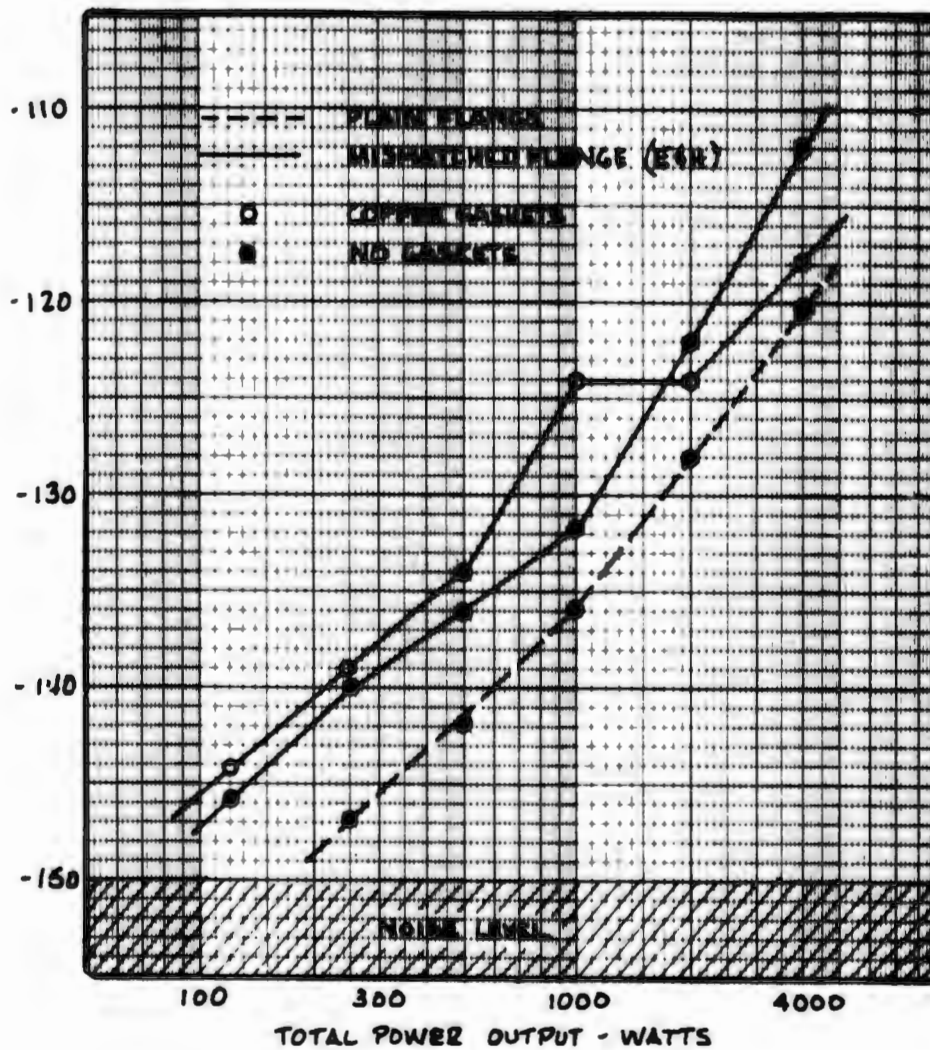


FIGURE 4.2-9  
EFFECTS OF MISMATCHED FLANGE



#### 4.3 HIGH POWER FEED ASSEMBLY TESTS

Horn castings and a polarizer assembly of the HT type were obtained and installed between the two MT vans, as shown in Figure 4.3-1. The transmit arm was connected to the HPA through the 180 dB high pass filter (not shown), while the receive arm was connected to the bandpass filter and the paramp (lower center of picture). The setup was identical to Figure 4.2-5 except the crossguide coupler and water load are replaced with the polarizer and horn, respectively.

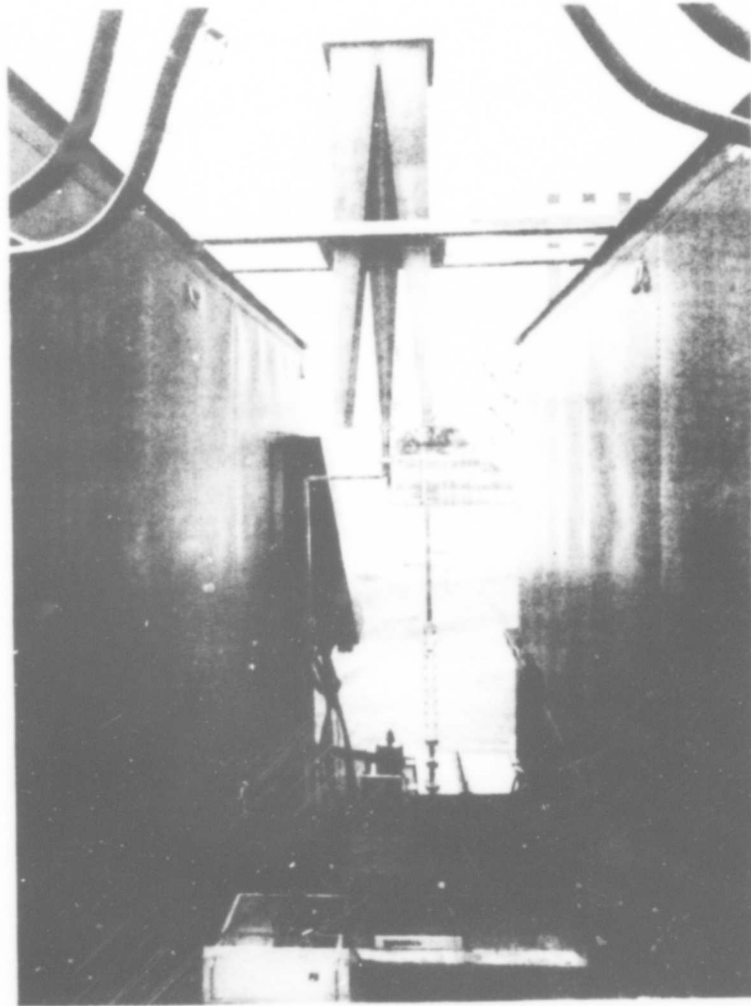


FIGURE 4.3-1  
HORN/FEED TEST SETUP

#### 4.3.1 Feed Tests

Data taken through the horn/polarizer, with copper gaskets in all rectangular waveguide gaskets but no gaskets in the feed itself, showed intermods as high as -70 dBm for 6 Kw input. With the feed fully gasketed (i.e., soft copper inserts as shown in Figure 4.3-2), the intermod only decreased about 6 dB. The data for these cases are shown in Figure 4.3-3 for powers of 10 w to 6 Kw. The intermod/carrier slope for both travelling wave cases is about 2.5 dB/dB, somewhat different than the 2 dB/dB experienced with the standing-wave tests.

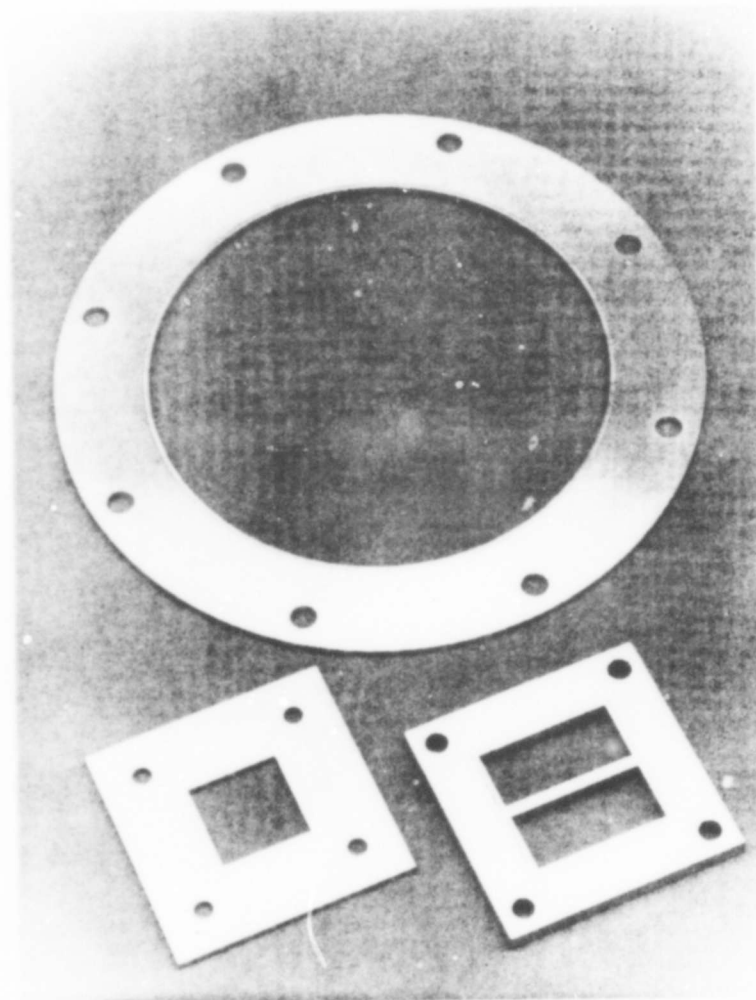


FIGURE 4.3-2  
HORN GASKETS (SOFT COPPER)

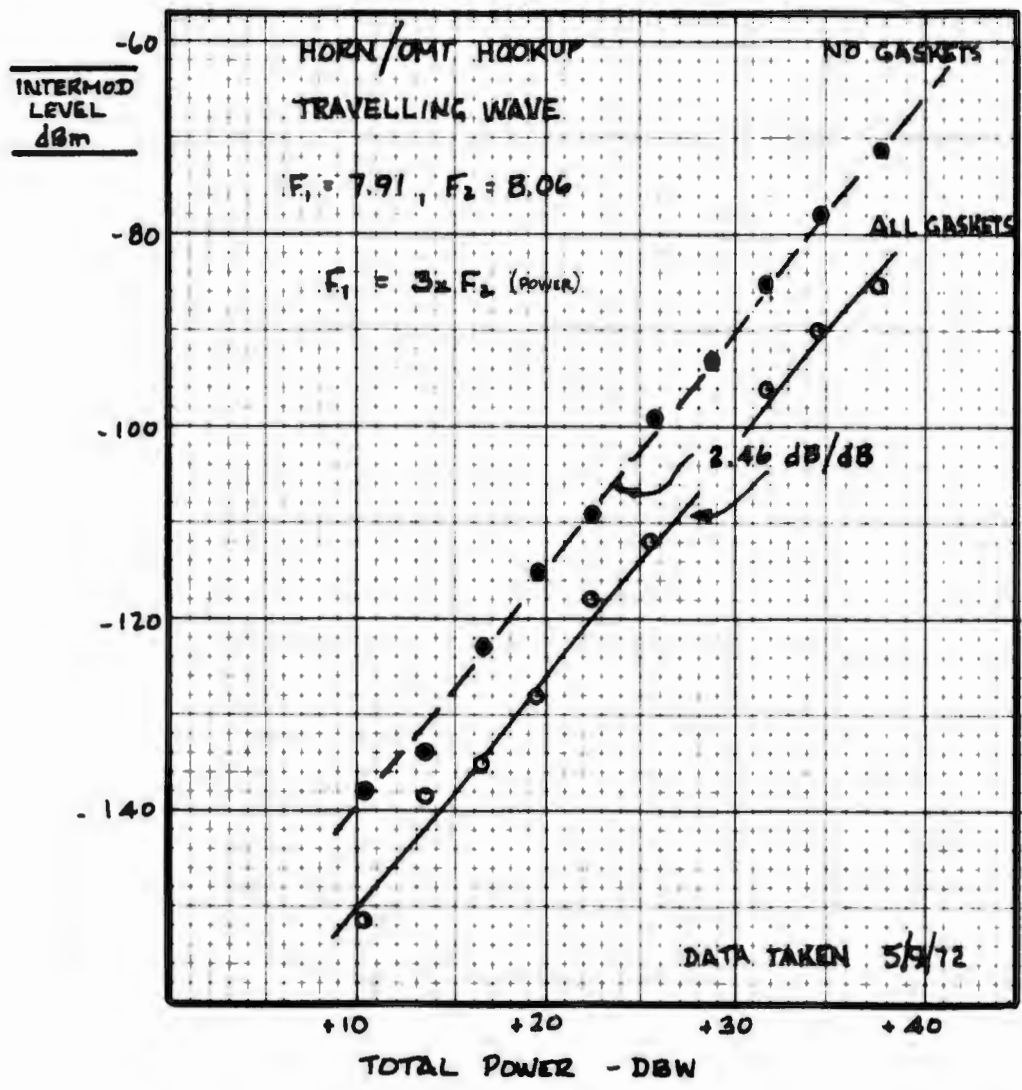


FIGURE 4.3-3  
FEED TEST RESULTS

The reason the intermods did not vanish when copper gaskets were added to the horn became obvious when the enlarged photographs of Figure 4.3-4 were taken. A and B illustrate two areas of the large circular flange between two sections of the horn casting. In the first, a clear outline of the raised edge of the copper gasket is apparent, and shows that the applied pressure was adequate to produce reasonable contact. However, the second shows no clear impression, indicating that contact was poor and intermods probably were still being generated.

Figure 4.3-4C shows a portion of the small square flange at the horn throat. Although the impression of the copper gasket is pronounced, voids and scratches appear in the casting that could encourage intermod generation. Also, because of insufficient bolt holes, special clamps have been fabricated to provide more evenly distributed pressure over the flange surface.

A third source of intermods may have been the interface between the polarizer and waveguide. As shown in the lower right hand corner of Figure 4.3-1, the polarizer requires a bifurcated gasket that has insufficient contact pressure at its center. A lack of pressure along the bifurcation which separates the transmit and receive lines would not only promote intermods, but would also increase direct coupling in an area where 30 dB isolation is desired. To overcome this limitation, the flanges will be soldered together for subsequent tests.

Reproduced from  
best available copy.



FIGURE 4.3.4A  
GOOD PORTION OF  
UPPER FLANGE

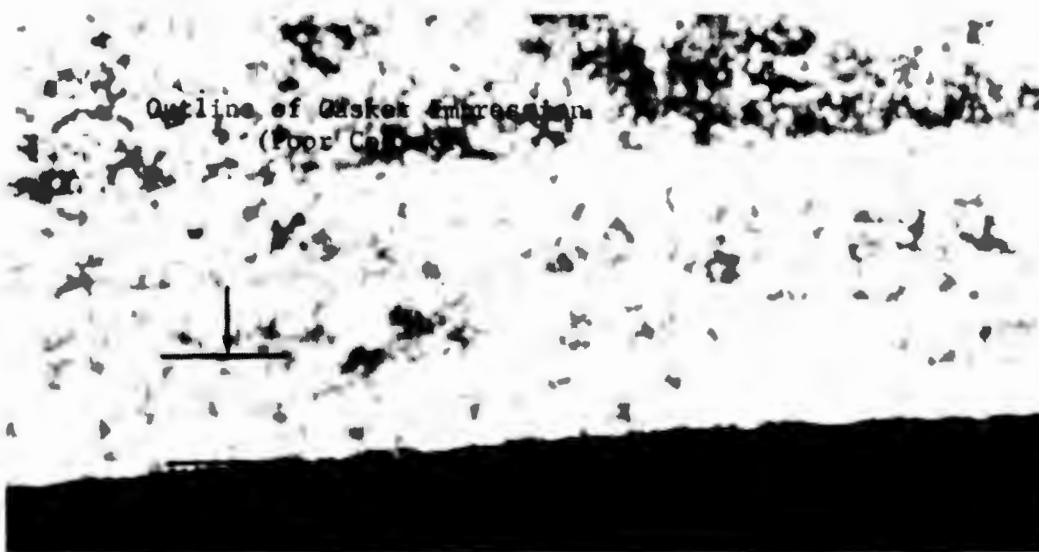


FIGURE 4.3.4B  
POOR PORTION OF  
UPPER FLANGE



FIGURE 4.3.4C  
THROAT FLANGE

FIGURE 4.3-4  
ENLARGED PHOTOGRAPH OF HORN FLANGES

#### 4.3.2 Effect of Single Carrier Variations

As an aid in the establishment of a non-linearity curve, the effects of single carrier variations were observed. The results shown in Figures 4.3-5 and 4.3-6 indicate that the lower carrier has more influence on the intermod level than the upper. In the limit, the intermod level appears to fall off 2 dB/dB for 7.9 GHz variations, and 1 dB/dB for 8.05 GHz variations. For a given input power level, the peak intermod level is achieved when the lower carrier is twice as strong as the upper.

Standing-wave slopes appear no different than those for travelling waves (matched load), but it is particularly interesting to note that mismatched lines produce significantly stronger intermods than matched ones (e.g., 50 watts into a standing-wave pattern yield the same intermod levels as 2000 watts into the horn).

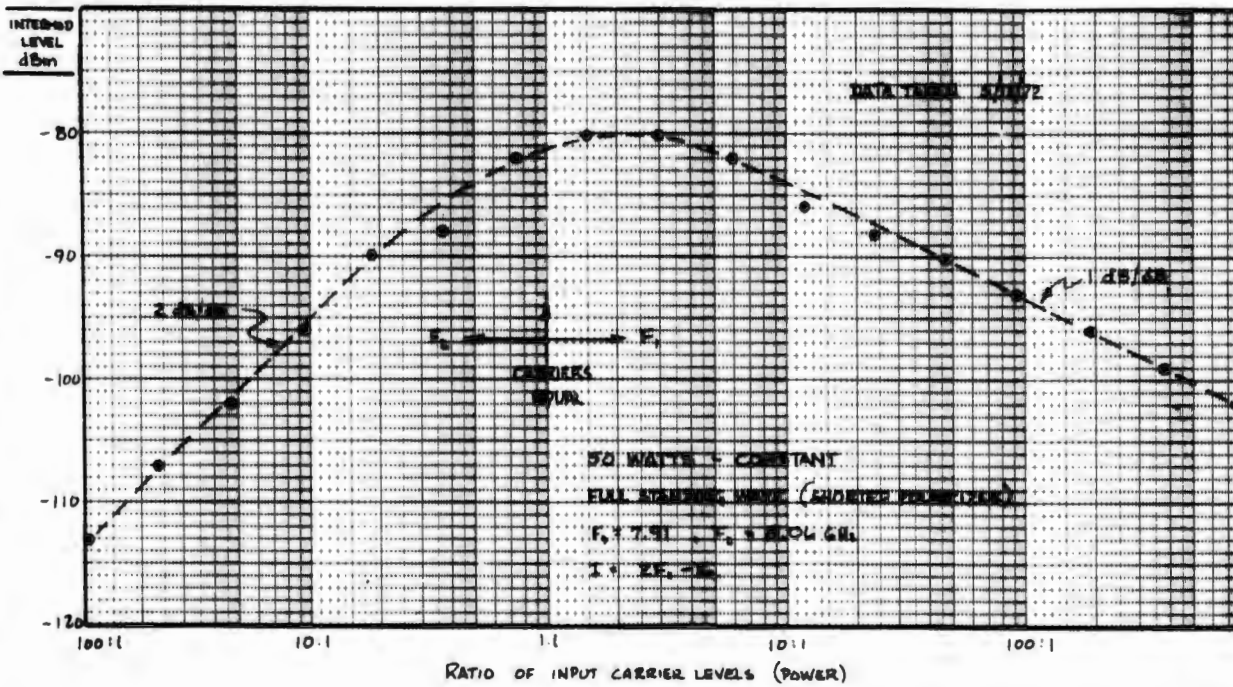


FIGURE 4.3-5 CARRIER RATIO EFFECTS (STANDING WAVE)

Reproduced from best available copy.

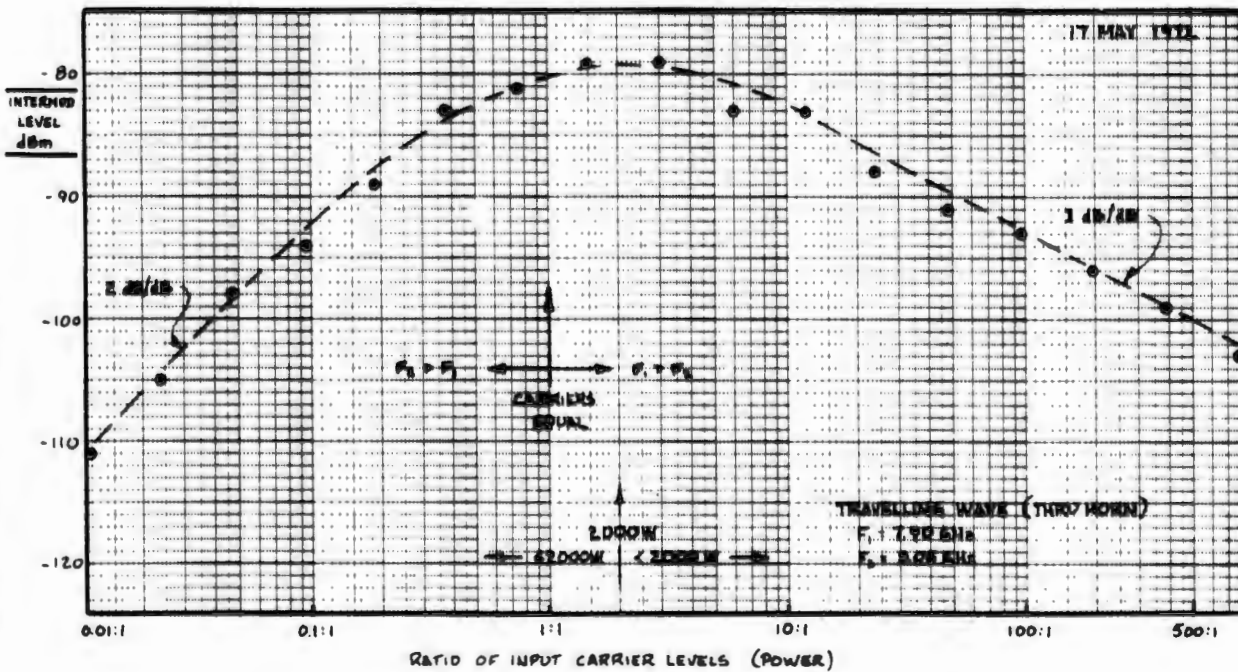


FIGURE 4.3-6 CARRIER RATIO EFFECTS (TRAVELING WAVE)



#### 4.4 LOW POWER VACUUM TESTS

Test waveguide and filters were assembled in a vacuum chamber to test the effect of air (and the lack thereof) on the non-linear mechanism. Since the facilities did not permit high power in the chamber (no convection cooling), the waveguide was configured for a full standing-wave distribution, as shown in Figure 4.4-1. The paramp was not available for this test so a tunnel diode amplifier (TDA) was used to achieve sensitivity.

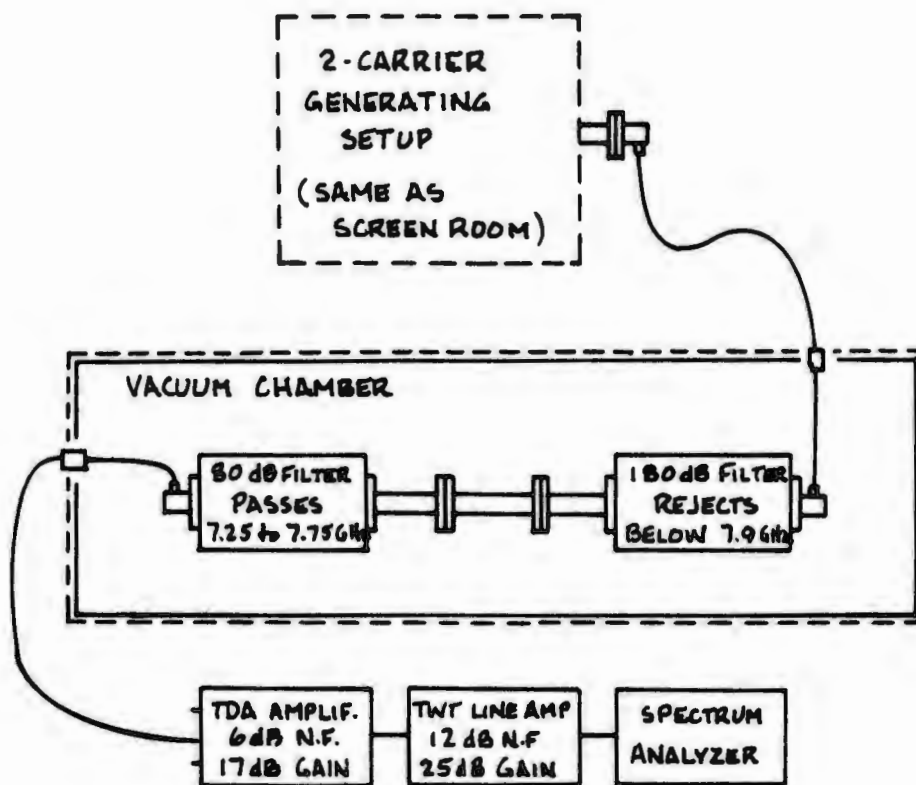


FIGURE 4.4-1  
VACUUM CHAMBER SETUP

#### 4.4.1 Air Gap Tests

The first series of tests were made with a variable gap in the waveguide flange (shims added). During the tests there appeared to be some relationship between flange gap, pressure and intermod level as shown in Figure 4.4-2. As the pressure dropped, points were periodically taken that show an intermod level increase between 1 and 10 torr; the magnitude of which varied with gap size. With no gap as shown by the lower curve, the intermod was independent of pressure.

Unfortunately, there are insufficient data points to draw a definite conclusion, but it appears as though ionization flow or microbreakdown is not the principal cause of intermod in a closed waveguide system, but could become significant if substantial air gaps are present (for example, at a choke flange). Additional tests should be made in this area.

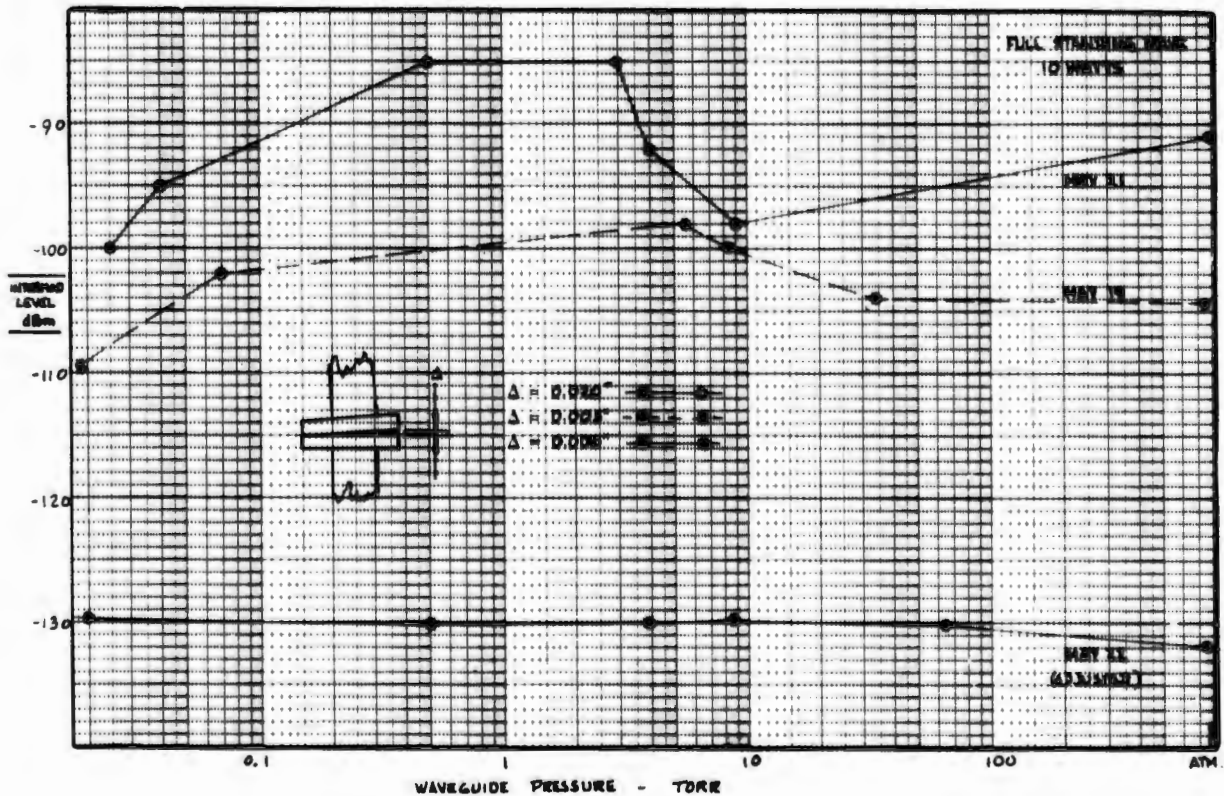


FIGURE 4.4-2  
VACUUM/GAP EFFECTS

#### 4.4.2 Higher Order Intermod Levels

During the vacuum tests, other orders of the intermodulation phenomenon were observed as indicated in Figure 4.4-3. Regardless of the separation of the primary carriers (150 MHz or 100 MHz) and regardless of pressure, each level appears to fall off by about 10 to 15 dB relative to the previous level. Because of the narrow bandwidth required to achieve -140 dBm sensitivity, higher orders near the noise level were not located, but still may have been present. Higher power tests planned for the future will provide more equivalent sensitivity.

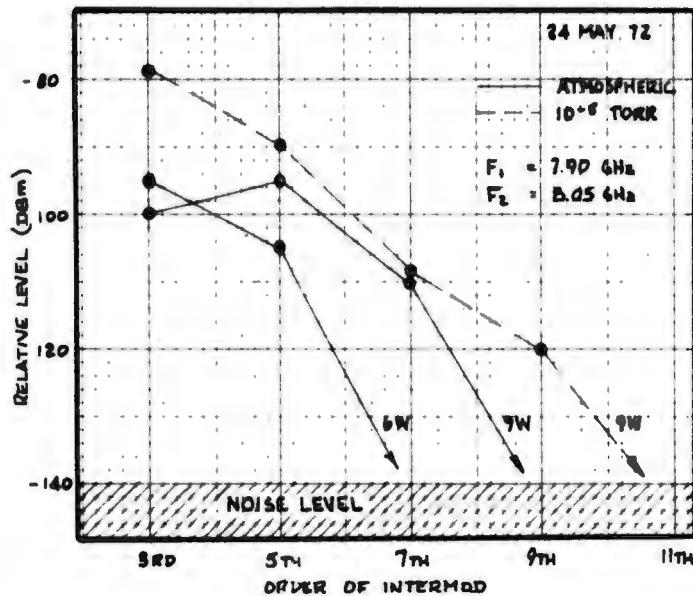
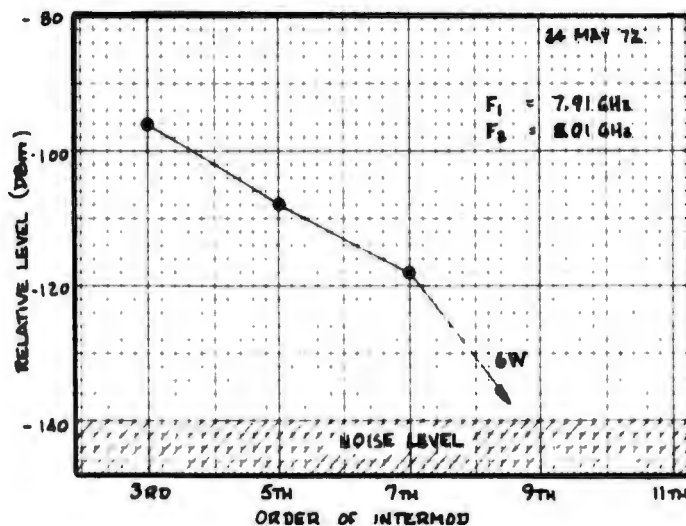


FIGURE 4.4-3  
HIGH ORDER INTERMOD LEVELS



#### 4.4.2 Higher Order Intermod Levels

During the vacuum tests, other orders of the intermodulation phenomenon were observed as indicated in Figure 4.4-3. Regardless of the separation of the primary carriers (150 MHz or 100 MHz) and regardless of pressure, each level appears to fall off by about 10 to 15 dB relative to the previous level. Because of the narrow bandwidth required to achieve -140 dBm sensitivity, higher orders near the noise level were not located, but still may have been present. Higher power tests planned for the future will provide more equivalent sensitivity.

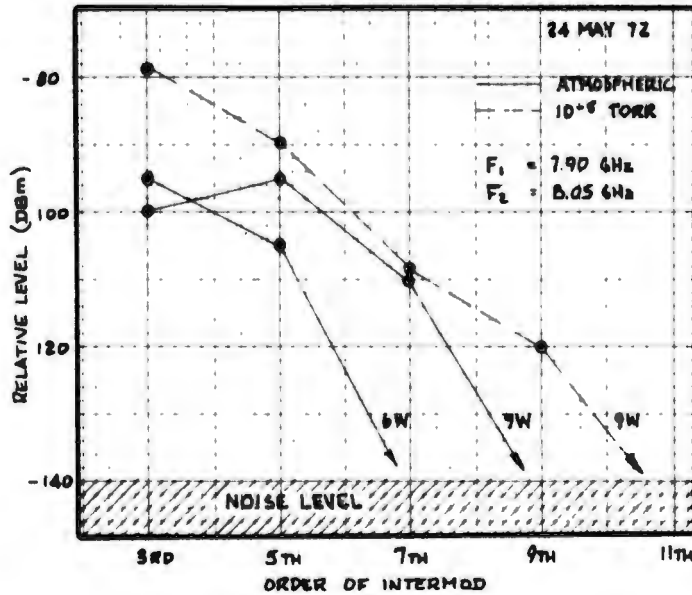
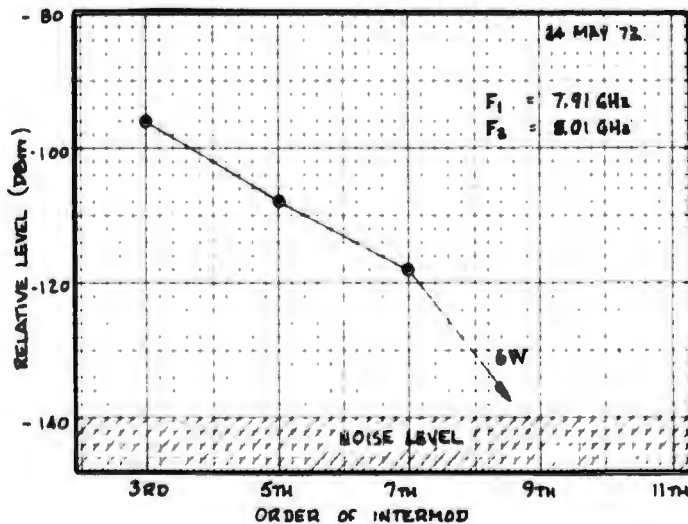


FIGURE 4.4-3  
HIGH ORDER INTERMOD LEVELS



#### 4.4.3 Closed Waveguide Tests

Notice that in Figure 4.4-2, there were no data points taken between 65 and 760 torr. To remedy this, the closed waveguide test (with phasing section added to shift current peak to flange) was repeated, and the vacuum drawn at a slower rate. At an equivalent altitude of 10,000 feet ( $\approx$  500 torr) there was a pronounced drop in the intermod level; beyond this point, the level picked up and stabilized at about 100 millibars. With further decrease in pressure, the intermod remained stable except for a fixed drift which may have been caused by carrier level or frequency variations.

However, before significance can be placed on this phenomenon, the tests should be repeated with some control on mechanical motions within the chamber, as well as stabilization of the generator.

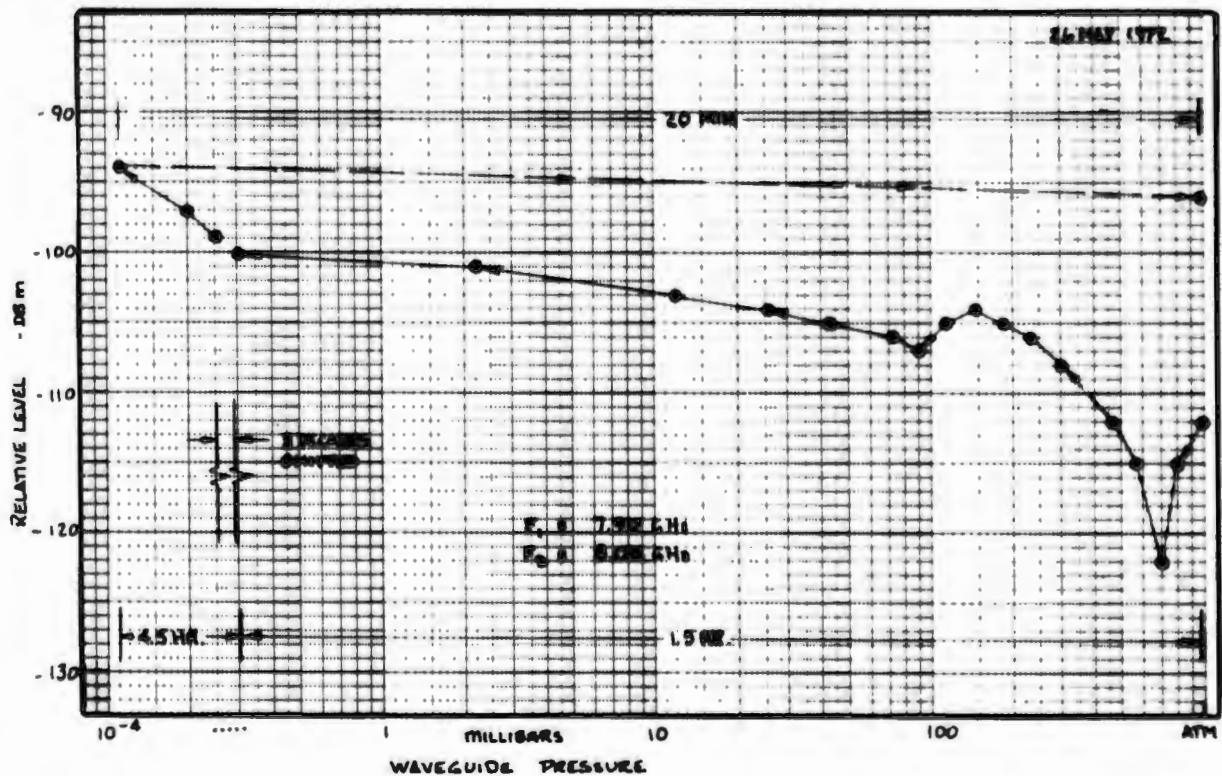


FIGURE 4.4-4  
SLOW PRESSURE-DROP EFFECTS

#### 4.5 COLLECTION OF MATCHED LOAD DATA

All data shown on previous graphs and some additional (but somewhat redundant) data for matched load conditions are collected in Figure 4.5-1. These points include measurements for horn and waveguide setups and for a variety of flanges and conditions wherever intermods were clearly measurable. Even though conditions varied considerably, data points show a remarkable consistency throughout the power range. It is particularly notable that if an intermod existed at all above 2Kw, it was stronger than -100 dBm (for the wide range of gasketing and flange type one would expect a spread of data all the way to the noise level; since this was not so, the existence of a threshold is suggested).

The mean of all data points (i.e., equal number of points, above and below the line) is indicated by the dashed line. The slope is 2.5 dB/dB for the matched load tests.

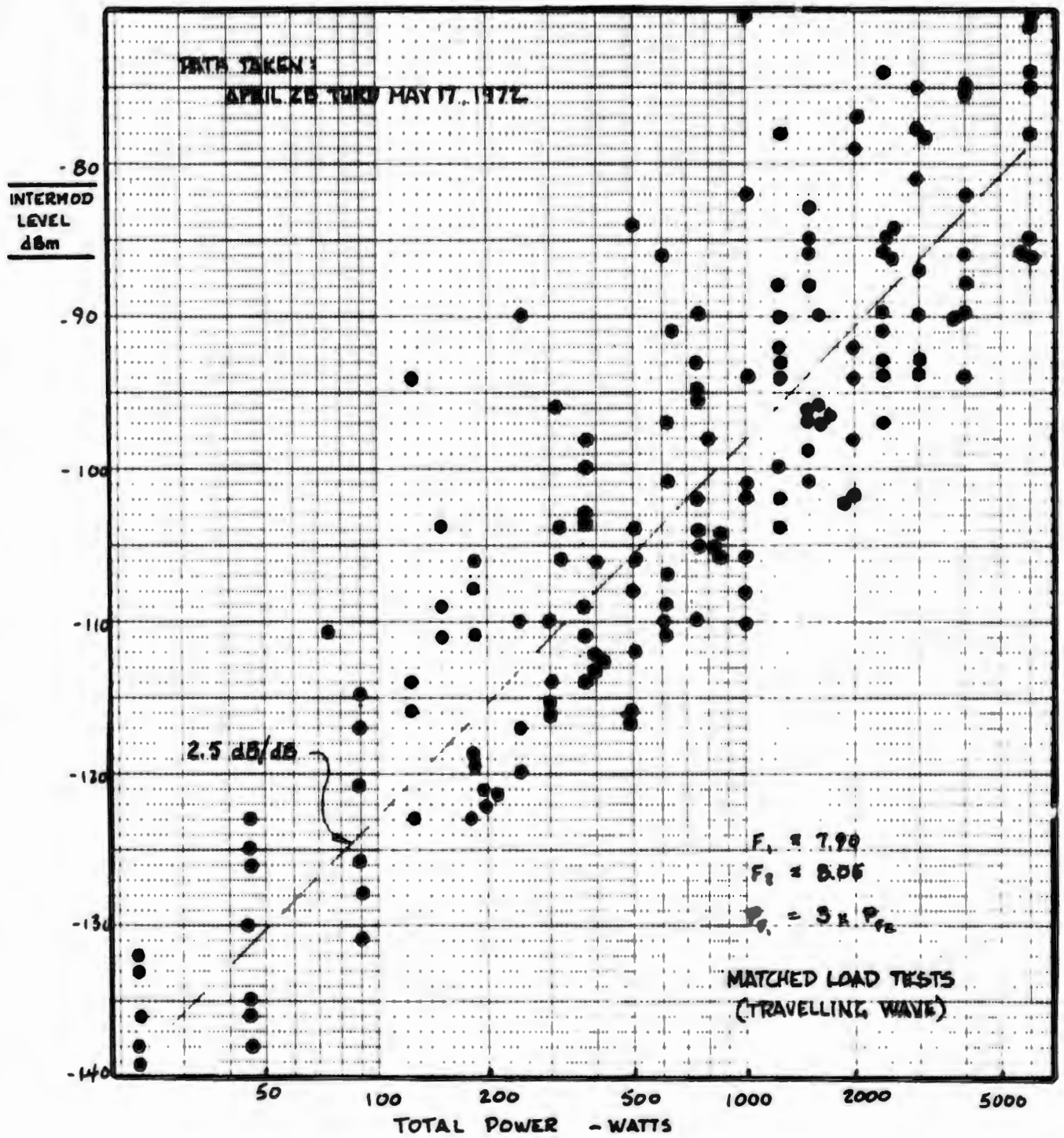


FIGURE 4.5-1  
COLLECTION MATCHED LOAD DATA



**SECTION 5.0**

**TESTING PROGRAM - PHASE II**

**(AS PERFORMED JULY - SEPTEMBER 1972)**

## 5.1 Test Facilities

The site equipment used for tests during the first testing phase was no longer available to the program after May, so new facilities and equipment were obtained. The Life Test HPA provided by the customer became the source of high power, and was installed in the Developmental Test Facility (DTF). In the DTF a screen room was available for waveguide tests, and roof-mounted structures were available for feed tests as shown in Figure 5.1-1. For the MSC-46 tests described in Paragraph 5.5.1, the lower waveguide was extended through the screen room doors to the absorbing enclosure assembled for the dieguide feed.

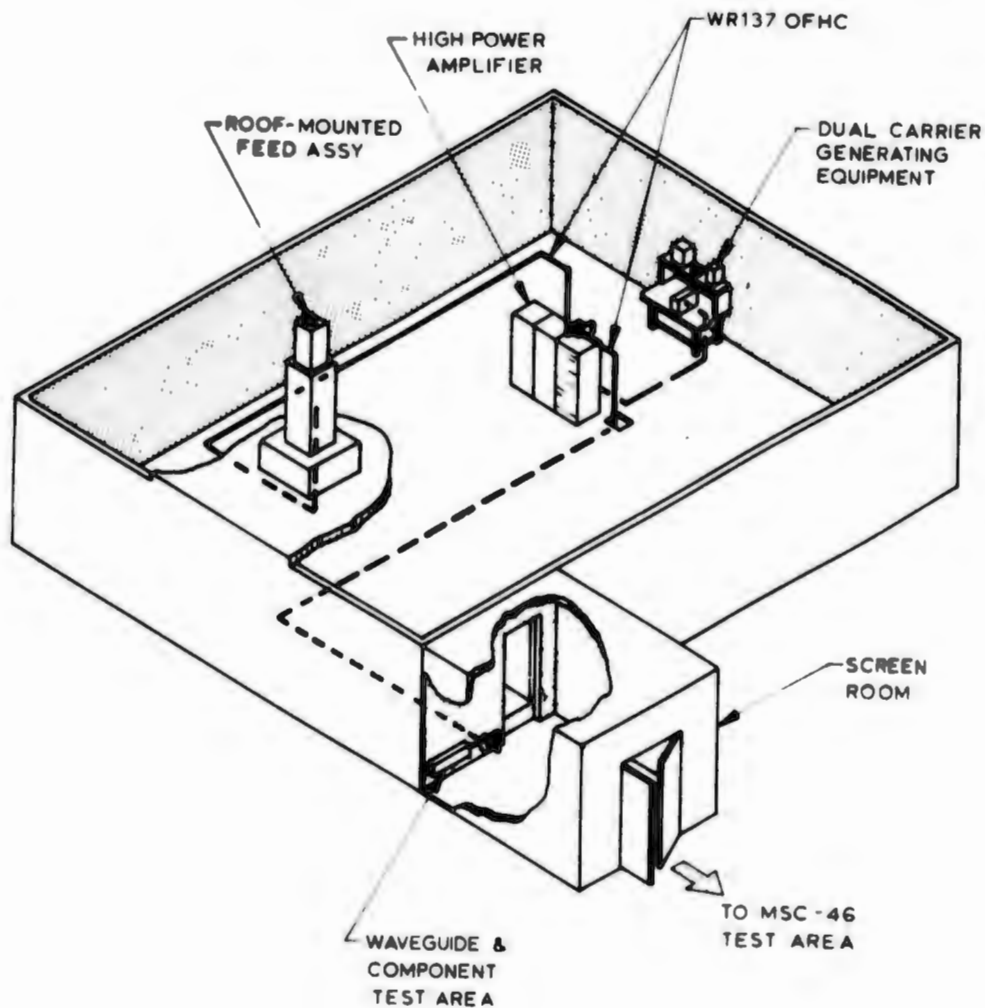


FIGURE 5.1-1  
DTF TEST FACILITIES

5.1.1 Equipment Block Diagram

Throughout the second testing phase, the same setup was used as shown below in Figure 5.1-2. A waveguide switch at the output of the HPA enabled power to be instantly switched from the roof area to the screen room area depending on test requirements. The maximum power used during any test was 6000 watts (HPA output), and the minimum sensitivity was -150 dBm on the roof and -140 dBm in the screen room.

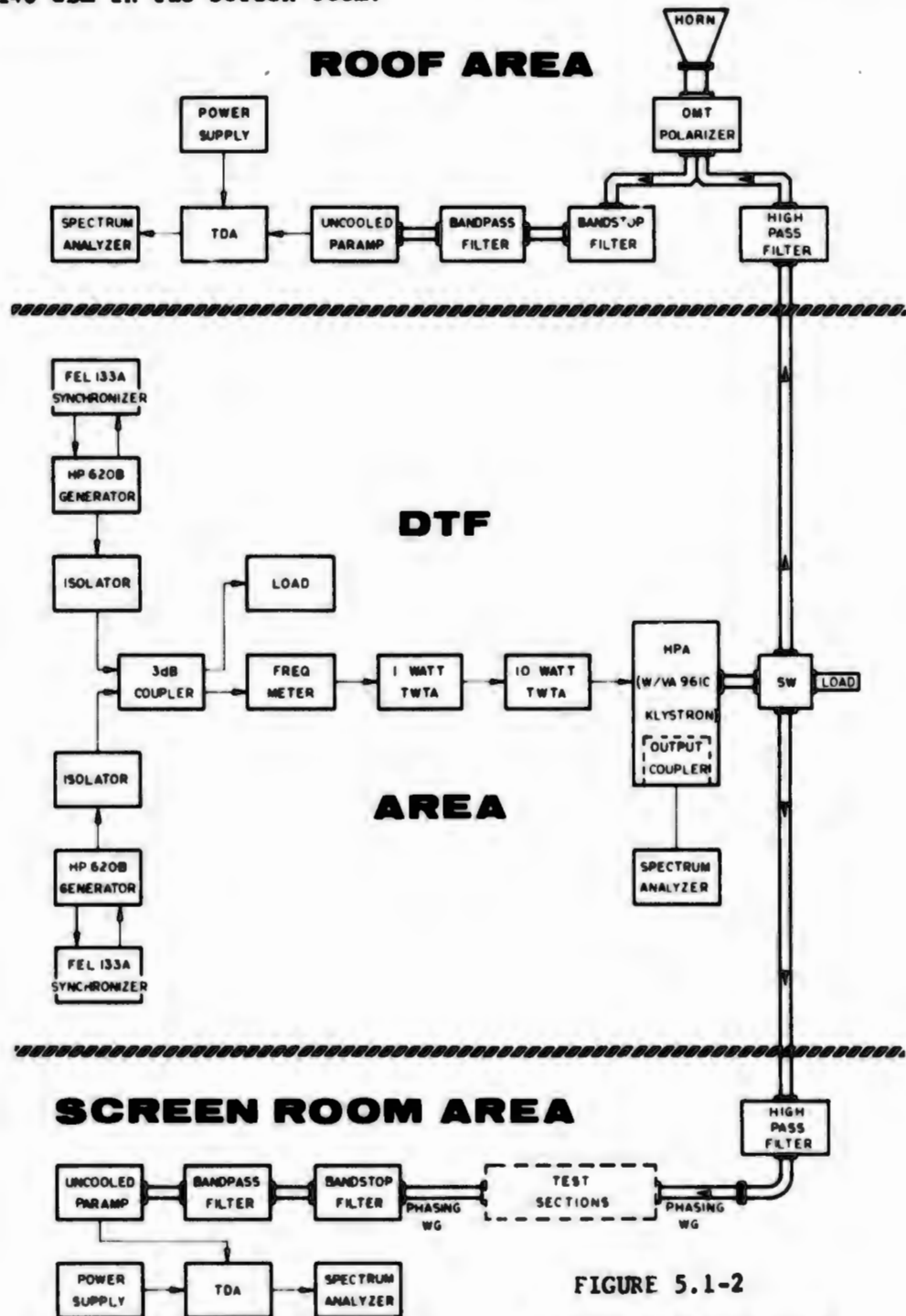
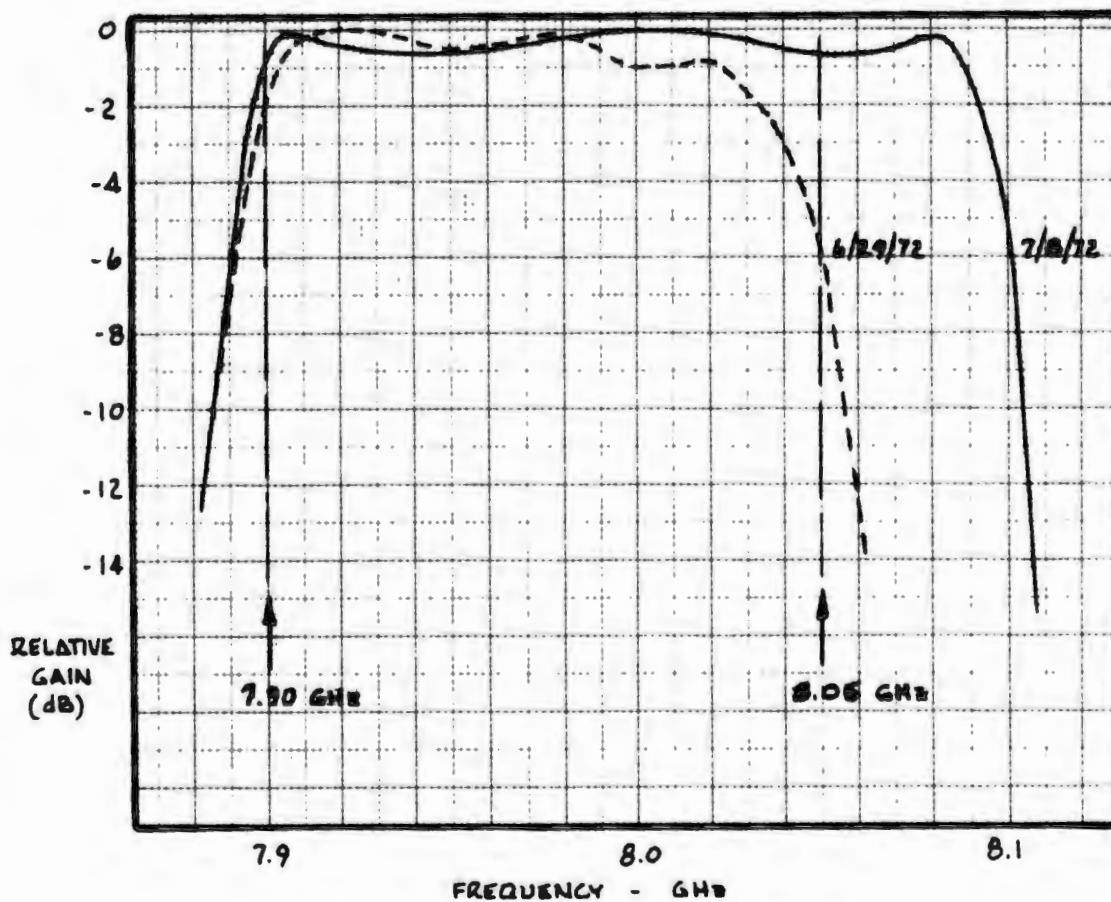


FIGURE 5.1-2  
PHASE II BLOCK DIAGRAM

### 5.1.2 Retuning the HPA Klystron

The bandwidth of the standard Varian 961C klystron is restricted to about 120 MHz to maximize output. Unfortunately, the 150 MHz separation between bands requires an amplifier with a bandwidth of at least 150 MHz if the third order intermod is to fall into the receive band, and preferably wider for some flexibility of transmit frequency. So the tube was returned to Varian and broadbanded as shown by the response of Figure 5.1-3. In the broadband state the maximum power measured at the calorimetric load was 6.8 kw @ 7.91 GHz; gain was 31 dB; ripple was 0.8 dB. However, the tube was only used for about five weeks before the filament failed; tests had to be continued with a narrow band replacement.



RETUNING EFFECT ON HPA GAIN

FIGURE 5.1-3

RETUNING EFFECT ON HPA GAIN

### 5.1.3 Transmit Filter

Following the return of the borrowed (deliverable) filter, a new transmit high pass filter was fabricated by tape-controlled machines here at Philco-Ford. Because of machine limitations, the filter length was lowered to 40 inches instead of 52 inches.

The filter was machined from solid brass, copper-plated for low loss and finned for heat dissipation as shown in Figure 5.1-4. For high power operation, the filter was encased in a polyethylene sleeve that guided forced air along the finned areas. The assembly was tested to 5 kw without excessive heating and without evidence of intermodulation products. This new filter provided an estimated 145 dB of rejection as extrapolated from measured skirt data shown in Figure 5.1-5. Fortunately, the lower rejection of the test filter compared to the deliverable unit was acceptable for the klystron HPA amplifier since its worst case receive band intermodulation level is at least 45 dB below the carrier total input power. VSWR is better than 1.2:1 as shown in Figure 5.1-5.

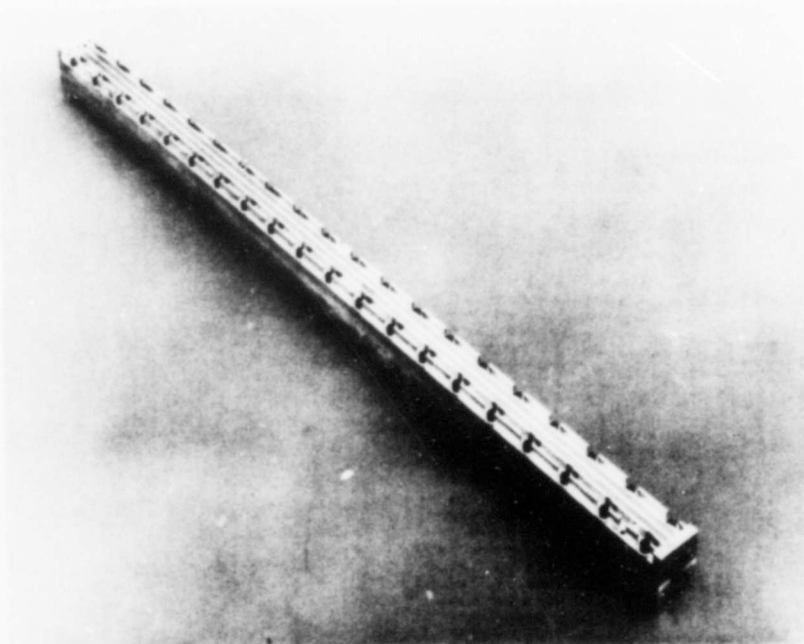


FIGURE 5.1-4  
HIGHPASS FILTER

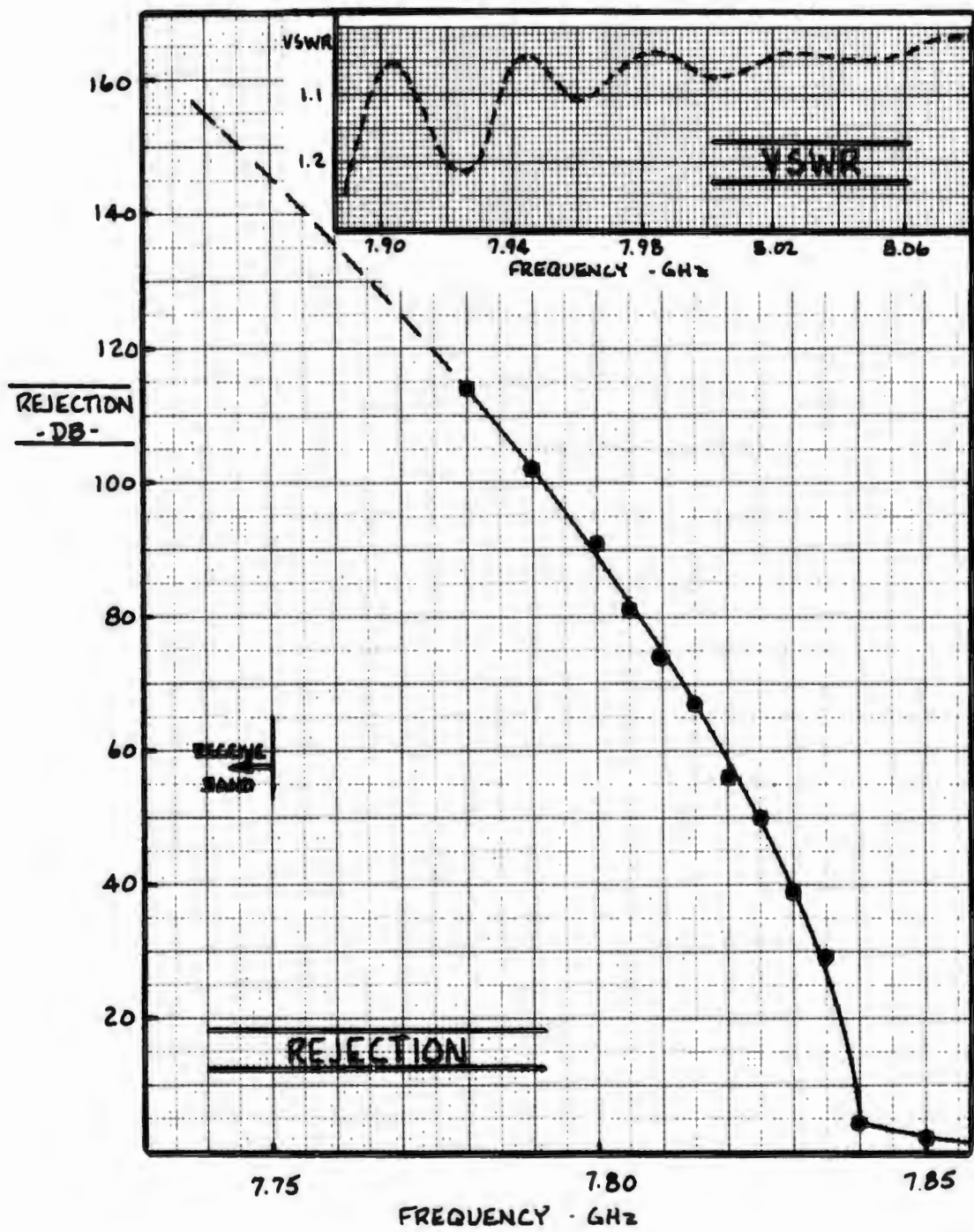


FIGURE 5.1-5  
MACHINED TRANSMIT FILTER RESPONSE

#### 5.1.4 Receive Filter

A new receive filter was built for the test program to replace the borrowed unit which had to be returned to site. The test filter was an identical copy of the 18-cavity Chebychev original, except tuning was changed slightly as shown below. This change was necessary to eliminate a hole in the reject characteristics of the transmit and receive filters that occurred at about 7.825 GHz between the two operating bands. Here less than 30 dB of combined rejection occurred and noise generated by the transmitter passed into the paramp (or TDA), and caused the amplifiers to saturate at high power levels. By retuning the cavities the response was shifted downward in frequency and the rejection increased to about 70 dB. No further interference from out-of-band noise was noticed in subsequent tests. VSWR was 1.2:1 or less for the modified unit.

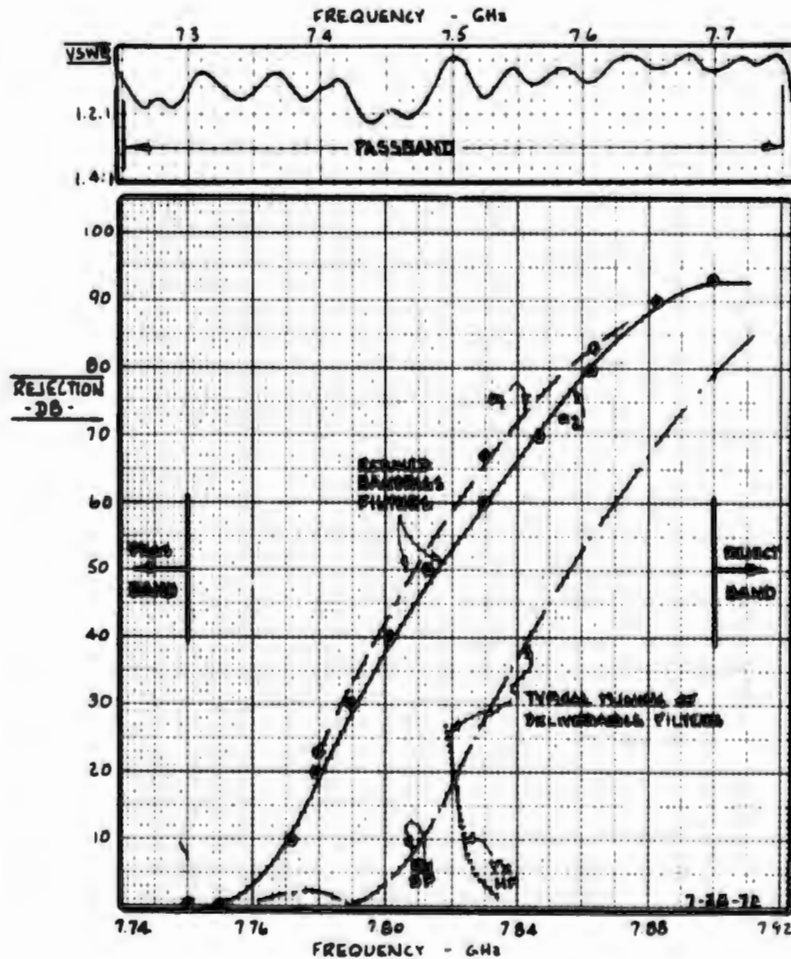


FIGURE 5.1-6  
RECEIVE FILTER RESPONSE



## 5.2 Waveguide Flange Examination

There has been no in-depth analysis of flange stresses, pressures, and distortions within this study, but we have taken a brief look at the approximate average pressures developed over the flange contacting surface and how these relate to the seating of gaskets. Subsequent text in this section summarizes observations.

5.2.1 Bolt Loading Curves - Predominantly, 10-32 and 1/4-28 bolts were used on flanges examined during this study. The curves presented below relate total bolt loading (axial pull) to applied torque for dry and lubricated threads, while circles indicate recommended maximum loading for the applicable SAE grades. Dry threads are used on all setups.

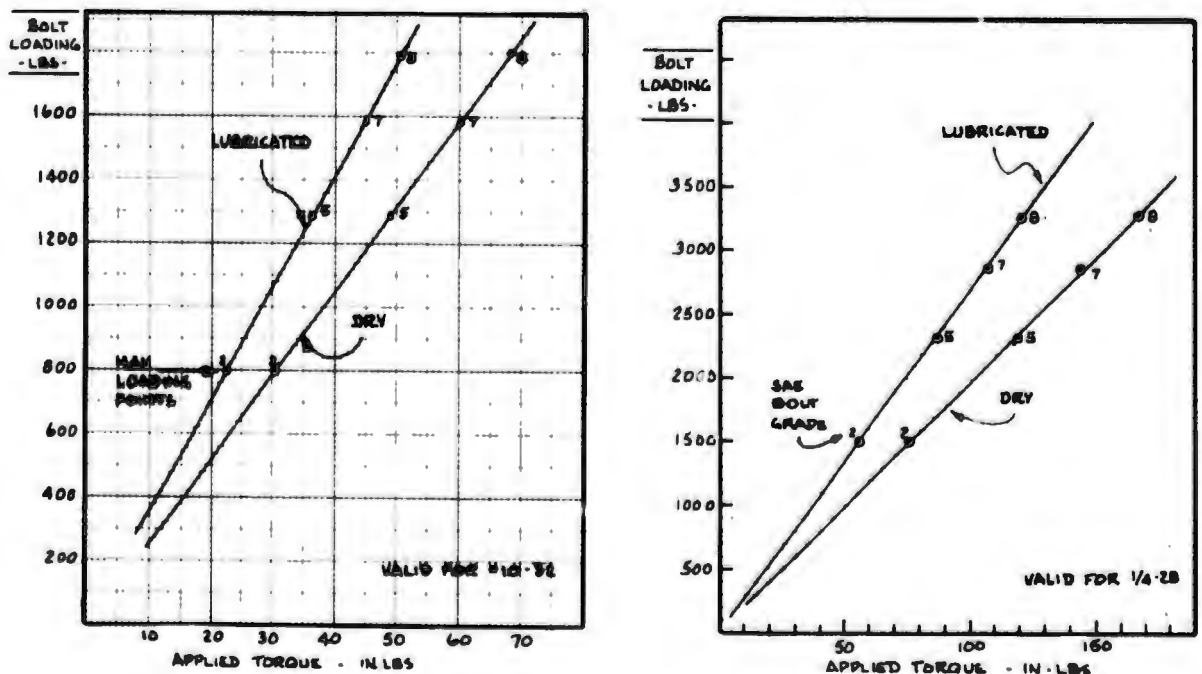


FIGURE 5.2-1  
BOLT LOADING CURVES

5.2.2 Standard Flange Appearance (UG 1356/U) - The enlarged photograph (3x) of a standard off-the-shelf UG 1356/U flange shown here effectively illustrates one of the reasons why standard flanges produce intermods. This flange meets MIL-F-3922 specifications for surface finish and flatness, but in its present condition would produce intermods in the -100 to -120 dBm range for kilowatt input levels. The two faulty areas are edge roughness and the normal machining grooves shown within the circle. Lapping after brazing would certainly be recommended for high power multicarrier systems.

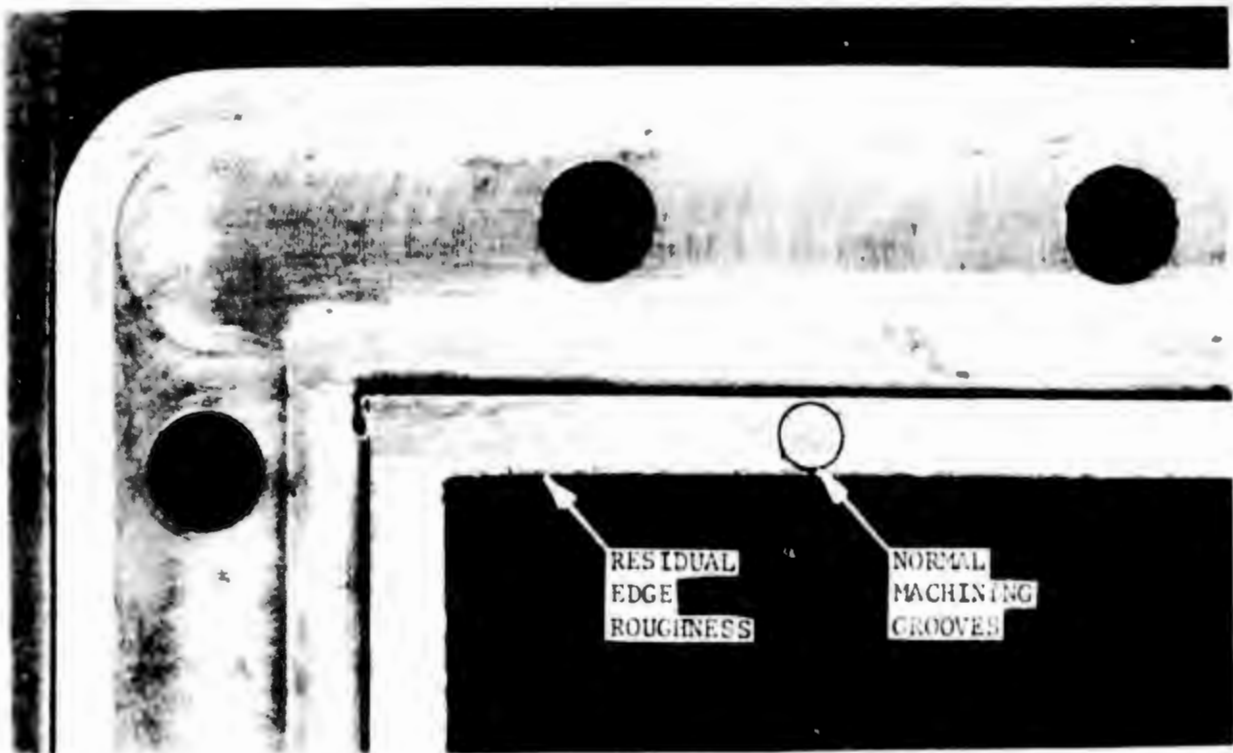


FIGURE 5.2-2  
STANDARD UG 1356/U FLANGE

### 5.2.3 Flange Plating Problems.

In setting up the dielguide feed, a problem that might present a dilemma to field personnel was observed. The CPR 187G flange on a WR187-to-WR112 transition had been plated to lower galvanic action between the brass transition and the aluminum waveguide to which it mated. As shown in the figure below, the flange arrived with the plating chipped in some spots and oxidized in others. Now the installer has a problem: if he installs the flange as is, intermods will be produced; while if he laps the flange, the plating will be removed and corrosion will be encouraged.

Since oxidation is unavoidable and flange scratches likely, plated flanges on any dismantable portion of a high power multicarrier feed should not be allowed. (For MSC 46 tests the flange was lapped as intermod suppression dominated corrosion effects for the short term).

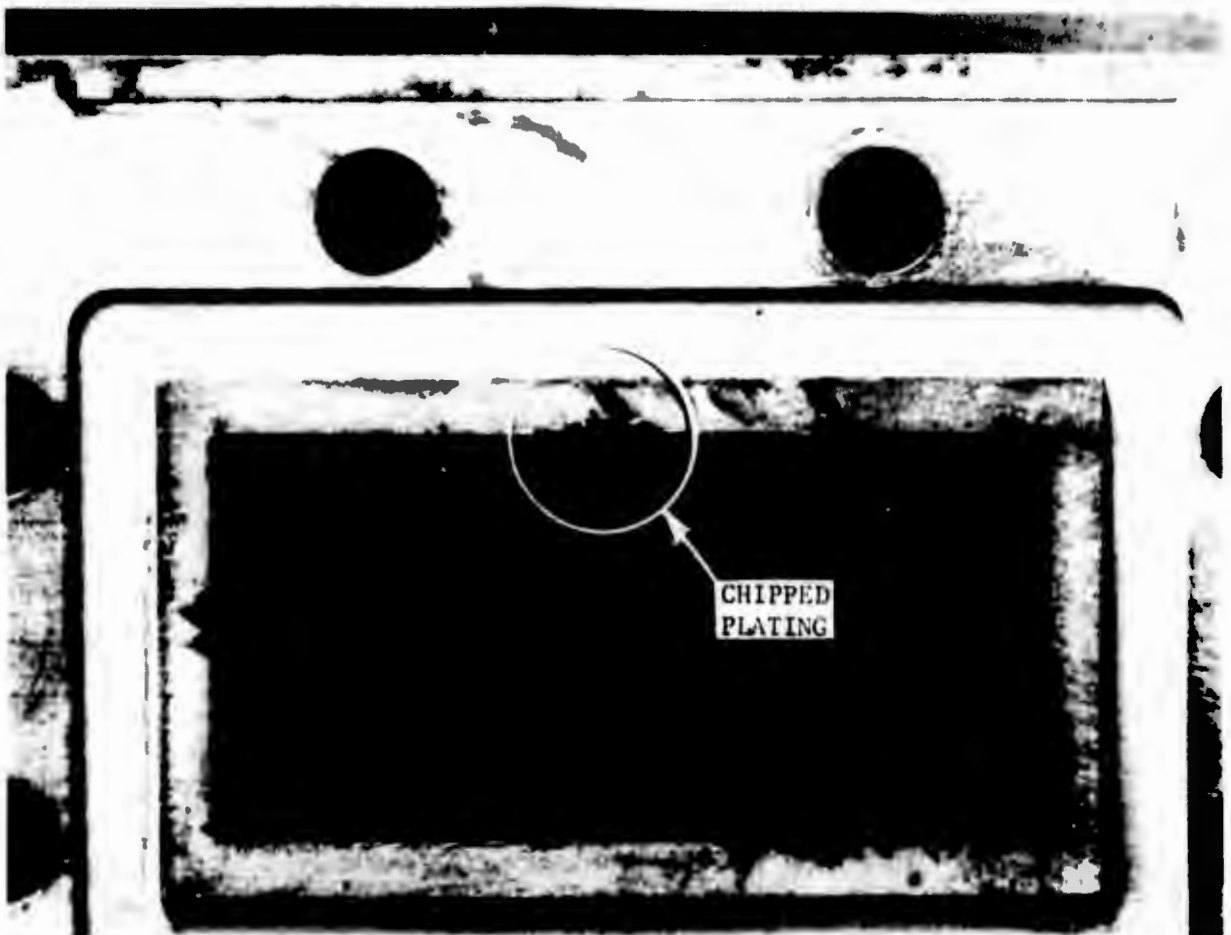


FIGURE 5.2-3  
PLATING DEFECT ON MSC-46 FLANGE

#### 5.2.4 Estimated Contact Pressure

The amount of pressure required to produce total contact of mating surfaces can be estimated in the following manner. It is first assumed that the mating surfaces have standard roughness as defined by ASME standards, with a peak-to-peak deviation of about four times the average or rms value. It is also assumed that the surface texture is applied to a gasket, and ideally smooth surfaces compress the softer material until surface deviations are flattened elastically as indicated below. (In a normal flange arrangement both surfaces are rough and both absorb energy elastically, so the results obtained with one smooth rigid surface should hold in a real situation.) Since the gasket is being compressed from both sides, only one half of the thickness (or .125" for the gaskets commonly used in the IM study) must absorb the total roughness.

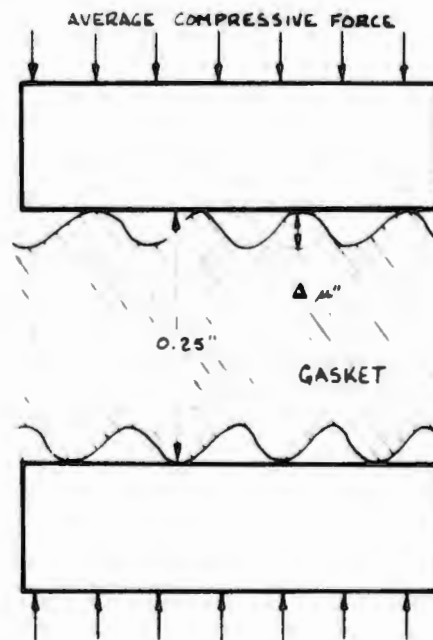


FIGURE 5.2-4  
FLANGE PRESSURE MODEL

The modulus of elasticity of both brass and copper is  $17 \times 10^6$  lb/in<sup>2</sup>; to elastically flatten the surface requires approximately

$$P = \frac{17 \times 10^6}{0.125} \times 4 \times 10^{-6} = 545 \text{ psi/microinch}$$

Therefore, if material elasticity were the only phenomenon working to our advantage, the required bolt torque as a function of surface roughness is as shown in Figure 5.2-5. Relating these curves to the bolt loading curves of Figure 5.2.1, it is seen that the flat flange, even with an 8 microinch surface, will never produce total contact (i.e., the bolts will strip before sufficient torque is applied). Similarly, the standard UG 1356/U grooved flange, illustrated in Figure 5.2-2 as having a 63 microinch finish, will also never attain complete contact. In fact, only when the grooved flange surfaces are polished to 8 micro-inches can the total contact be achieved.

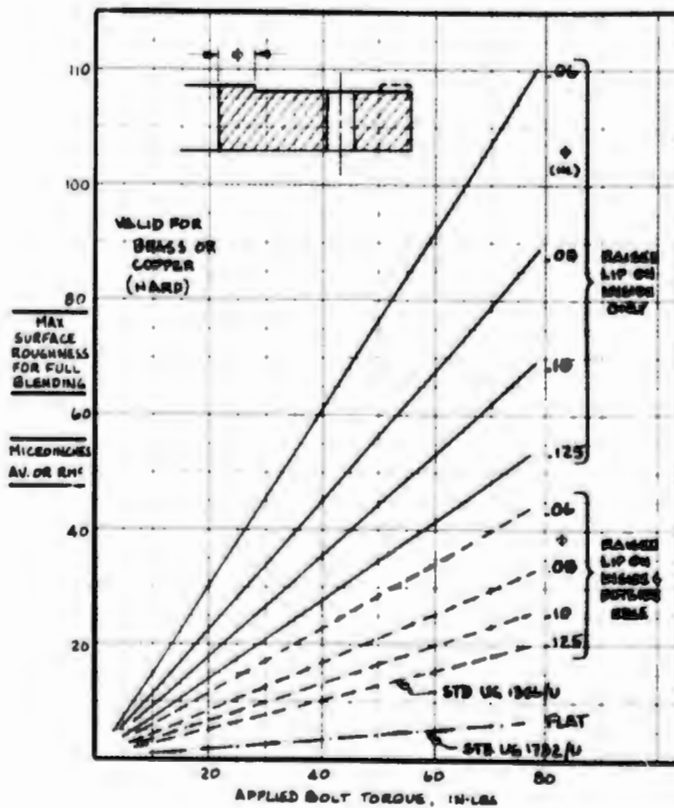
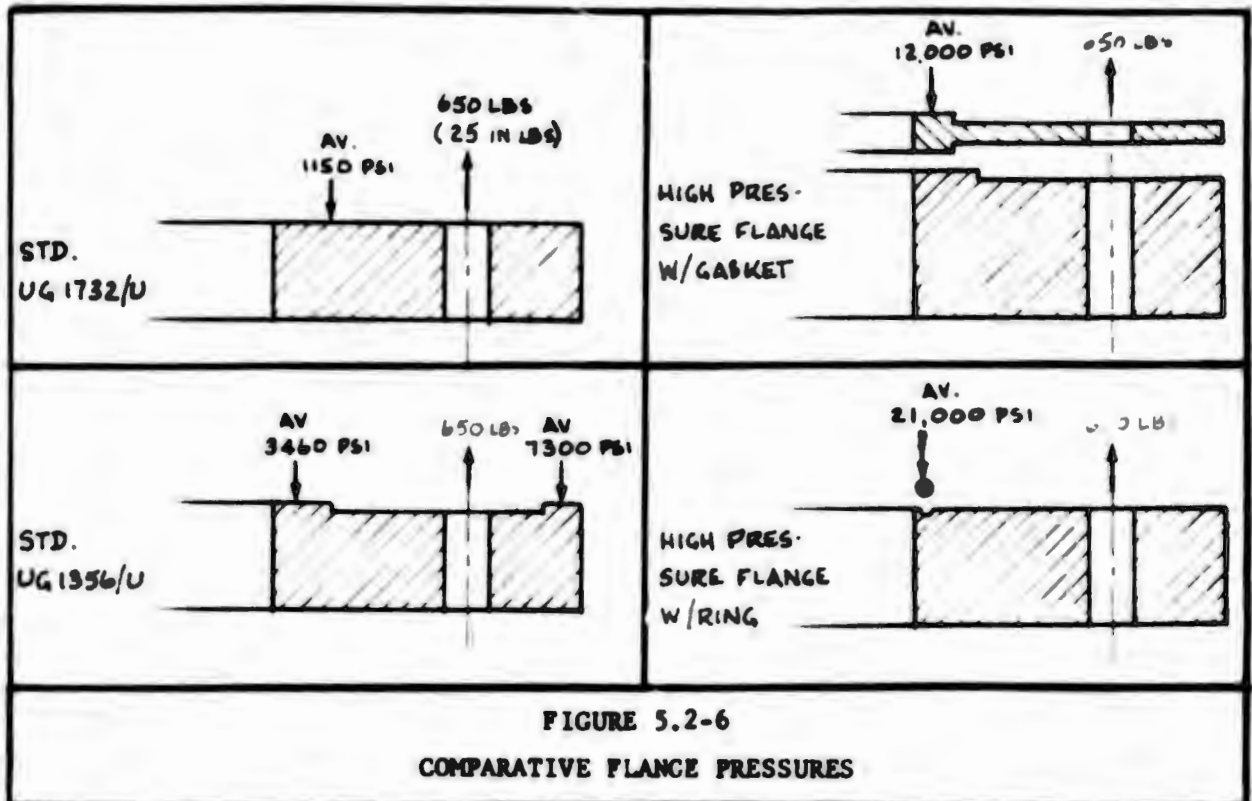


FIGURE 5.2-5.

FLANGE PRESSURE  
REQUIREMENTS

The above discussion also demonstrates the advantage of having a raised lip around the flange to concentrate applied force to a small area. The smaller the contacting area the less torque must be applied to the bolt to produce good contact. A comparison of estimated average surface pressure for various flange types tested during the IM study is shown in Figure 5.2-6 for 25 inch-pounds of applied pressure; here the advantage of concentrated pressure is apparent.



The preceding discussion is based only on hardened materials. If a fully annealed copper gasket is used then full blending comes much sooner for the first application of pressure. If the yield point is assumed to be 11,000 psi for 0.5% permanent deformation then the amount of pressure required to produce full contact over peak-to-peak surface deviations of 1250 microinches or less is 11,000 psi.

The compressibility of softened copper gaskets is demonstrated by Figure 5.2-7 in which the measured deflection of two copper gaskets is related to pressure. Sample #1 is a new gasket and at 11,000 psi the deflection is about 1500 microinches, and increases to 0.014 inches at 40,000 psi. Sample #2 is a used gasket and has no measurable deflection at 11,000 psi and about 0.007 inches at 40,000 psi. A comparison of the two results confirms that soft copper gaskets are effective only once for rough surfaces; after initial use, the smoothness of contacting surfaces reverts to the requirements imposed by Figure 5.2-5.

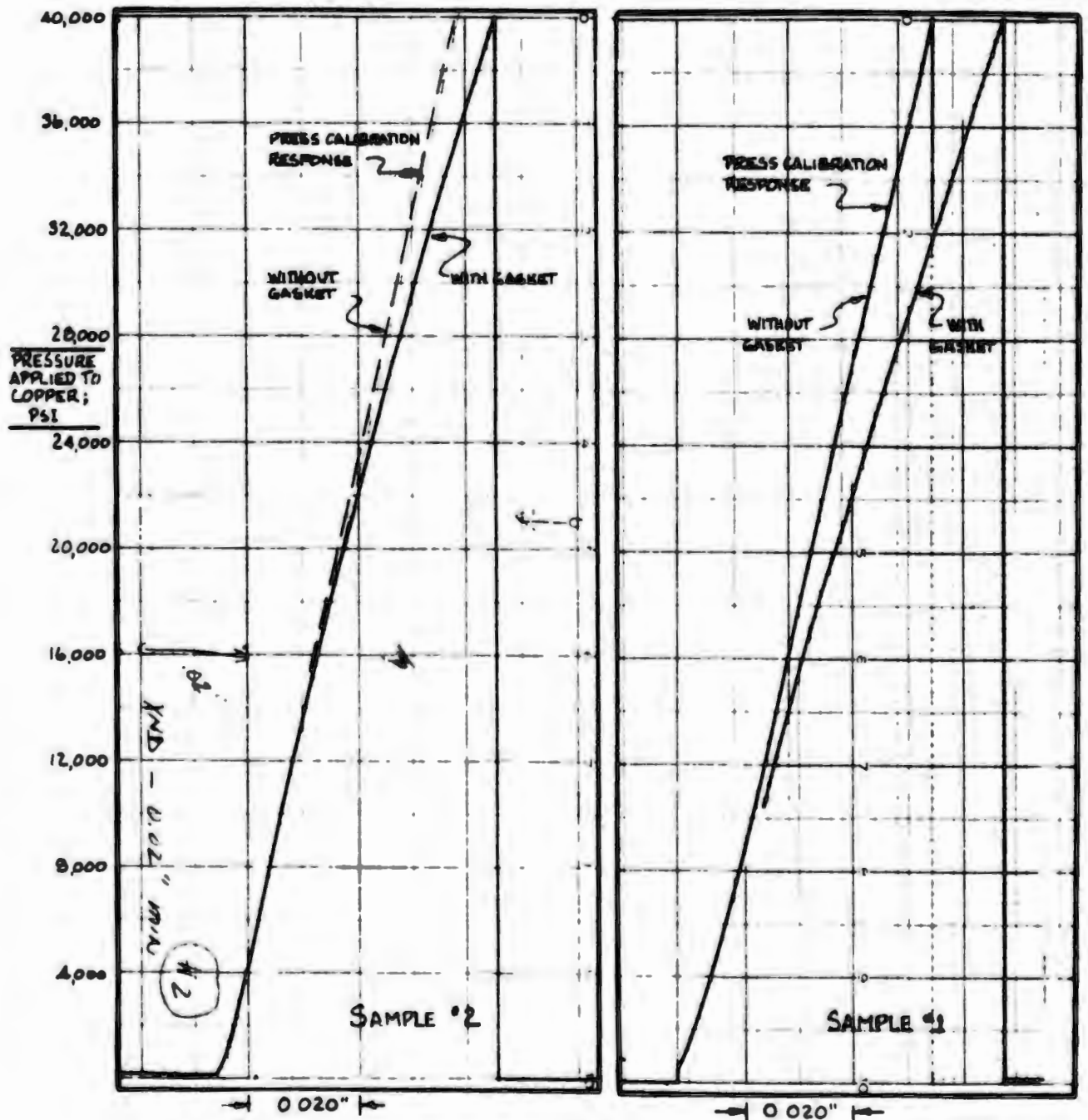
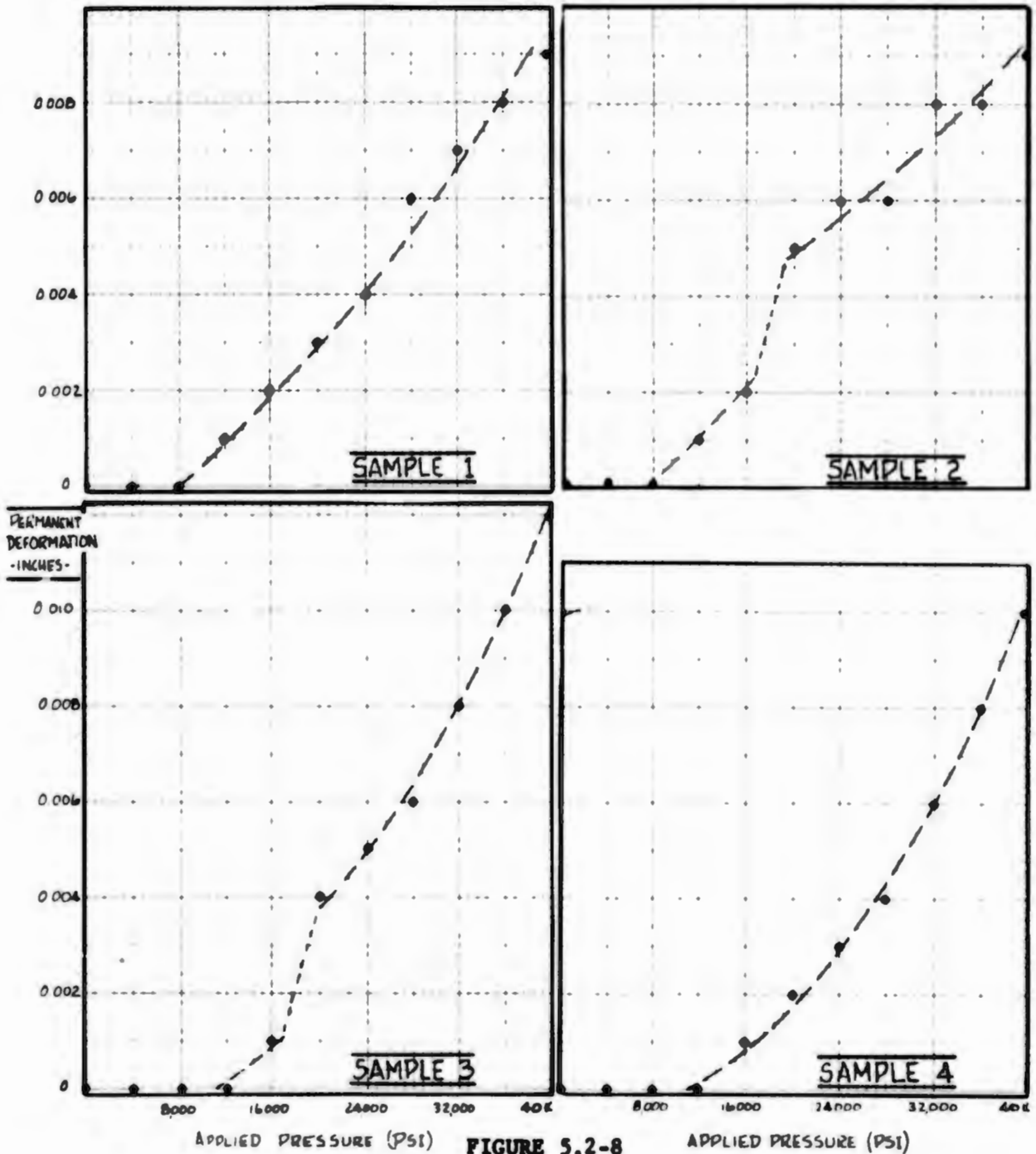


FIGURE 5.2-7  
COPPER GASKET COMPRESSIBILITY



Additional sample gaskets #3 through #6 were also tested, except the deflections were observed in 4000 psi increments as shown in Figure 5.2-8 rather than for the continuously increasing pressure shown previously. The permanent deformation was about 0.001" for pressures on the order of 12,000 psi for samples 1 and 2 (the expected value for soft copper), and for pressure of 16,000 psi for samples 3 and 4. The implication here being that the annealing process may not be uniform from item to item.



APPLIED PRESSURE (PSI) **FIGURE 5.2-8** APPLIED PRESSURE (PSI)

**INCREMENTAL COMPRESSIBILITY CURVES**

In this second phase of the experimentation, the gasket design used a raised lip thickness ( $\phi$ ) of about 0.06". Since this corresponds to a total contacting surface of only 0.25", 12,000 psi is achieved with only 15 inch pounds of bolt torque. To prove this physically, many flanges were assembled and the intermod levels monitored as bolt torque increased. In all cases where flanges were clean and gaskets were new, intermods that existed at 10 inch pounds vanished when the pressure was raised to 15 inch pounds.

This information can be related to lip thickness of any value by the graph below, which shows the bolt torque required to reach the yield point for various gasket configurations.

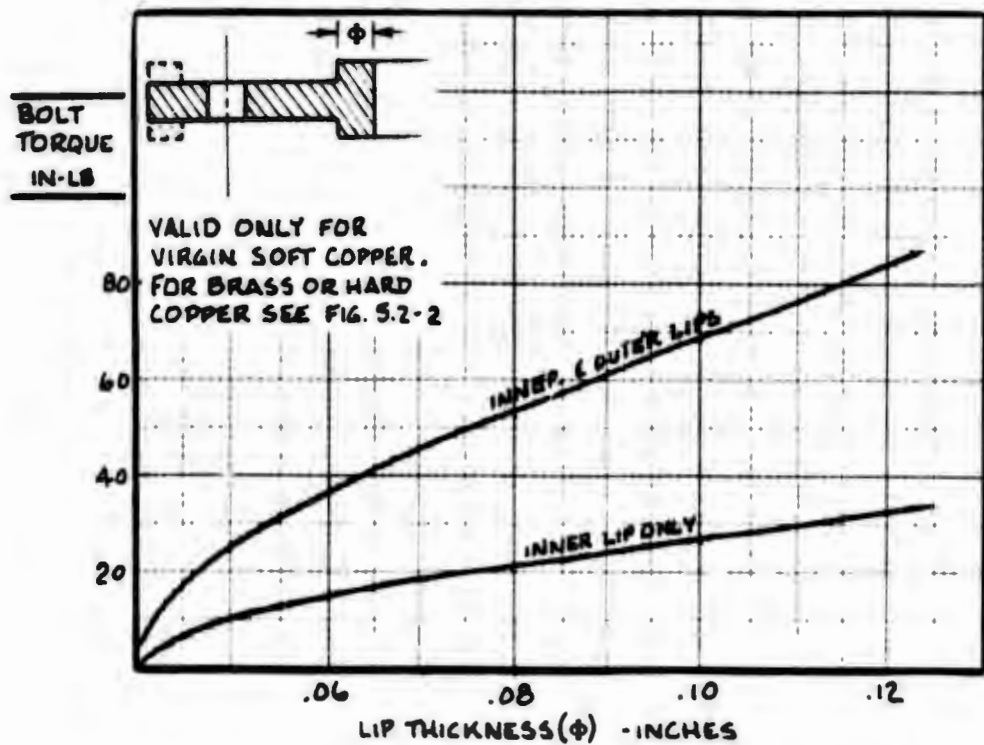


FIGURE 5.2-9  
BOLT TORQUE REQUIRED FOR YIELDING

Only one other effect was observed in placing copper gaskets with only inner edges between standard flanges: with no support on the outer edge, the flange would distort severely as the bolts were tightened. The cause is related to the brazing process, in which the flange is heated to annealing temperatures and the yield point is lowered to about 19,000 psi. When tightening the bolts to 25 inch pounds (for example) the stress levels exceed the yield point by nearly 2:1, and the flange yields.

The distortion can be prevented by doubling the flange thickness as illustrated below. With this design modification stress levels within the flange remain below the yield point and distortion is negligible.

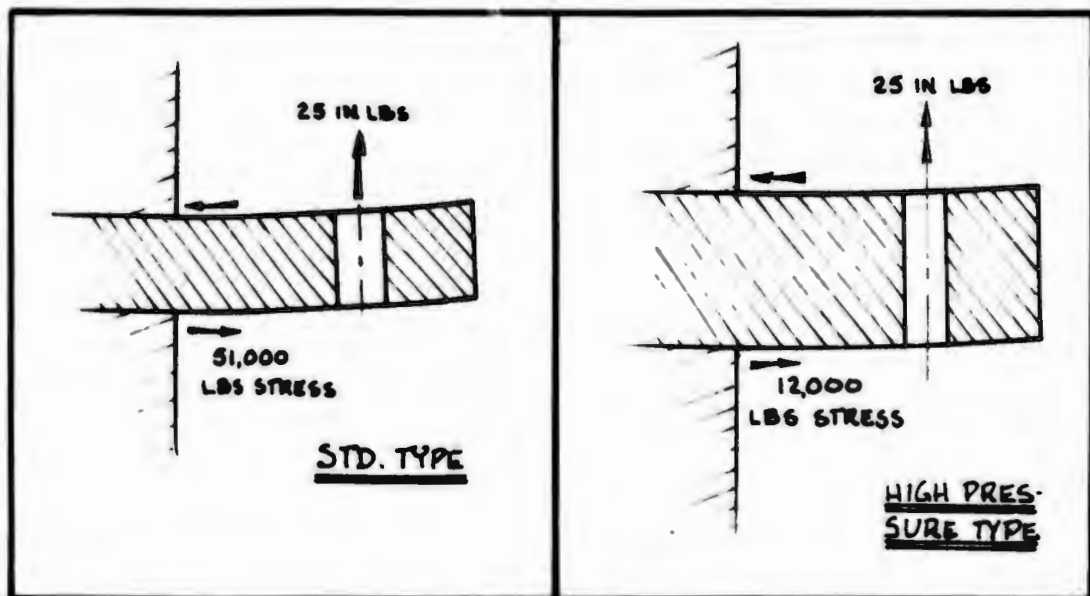


FIGURE 5.2-10  
FLANGE WARPAGE

### 5.3 Filter Studies

During the July - September portion of the study, receive filter tuning screws produced intermodulation products that were not eliminated by modifications. This section presents the problems, the devices, and the experiments conducted to pin-point and remove tuning intermodulation sources.

### 5.3.1 Receive Filter Intermods

High power tests performed in July revealed that intermodulation products were being generated by the receive bandpass filter. (This filter is identical in dimensions and manufacturing method to the quiet MT filter used on earlier tests.) The HT filter and a fourth filter of the same design were obtained and all units produced intermods. The tuning screws of one of the newer filters were removed and the intermods vanished; thereby removing blame from the longitudinal split along the filter axis, the flanges, and the cavity walls.

Subsequent tests in which one screw was inserted independently into each cavity revealed a varying sensitivity to intermod levels as shown below. With the transmitter located at cavity #18 intermods were observable in a generally decreasing manner as the cavities progressed into the filter; however, with the transmitter located near cavity #1, intermods were observable in only 5 cavities and not necessarily related to field strength in those cavities. It was interesting to note that no intermod could be generated in cavity #2 while very strong intermods were produced by cavity #16.

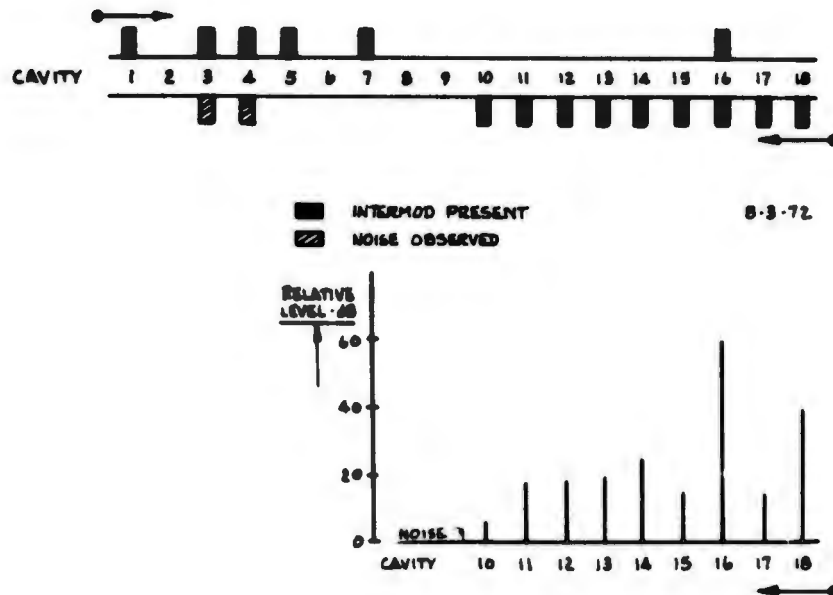
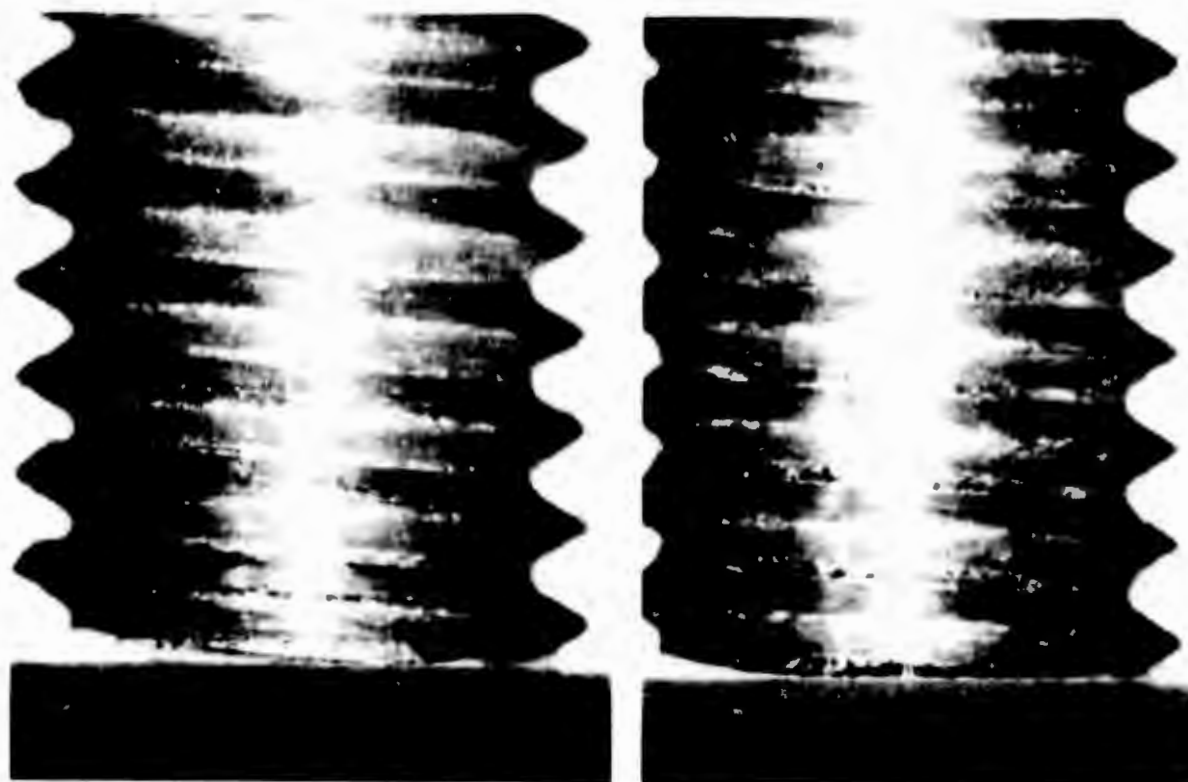


FIGURE 5.3-1  
RELATIVE CAVITY INTERMOD LEVELS

5.3.1.1 Thread Comparison - With such a significant difference in intermod levels between cavities #2 and #16 some readily apparent difference was expected under a microscope. However, the photographs of Figure 5.3-2 reveal no significant difference between the threads of the noisy cavity and the quiet one (photos shown are 15x). However, at higher magnifications microscopic traces of copper or copper-oxide particles from screw friction were observable, occasionally forming small muddy smears as they blended with minute traces of machine oil. However, this debris was present in all threads, quiet and noisy alike; so the difference may have depended upon the presence or absence of small oxide particles at the last thread on the waveguide end of the tuning screw.

The filter was then subsequently cleaned by an ultrasonic process to remove microscopic debris and vacuum dried. Further testing showed little or no improvement in intermodulation level.



CAVITY #2

CAVITY 16

FIGURE 5.3-2  
THREAD COMPARISON

### 5.3.1.2 Tuning Screw Comparison

Believing that tightness would be the solution to noisy screws, a new set of oversize copper and brass screws were manufactured and tested without a significant improvement in intermod levels (typically -80 to -115 dbm at 100 watts). Some precision tuning screws made by Johannsen Manufacturing Corporation of Boonton, New Jersey and shown in Figure 5.3-3 below, were purchased and inserted in one of the filters. These screws are provided with an outer sleeve, and a tight fit is obtained by an expanded fine thread on the inner tuning probe. Each sleeve was carefully hand-fitted to its cavity and secured rightly in position (the two-filter halves were also soldered together for added rigidity). During tests, intermods were produced at the -80 dbm level at 100 watts equivalent to the strongest previously obtained. This high intermod level might be expected in that the commercial screw has two interfaces that may be non-linear: one between the sleeve and the waveguide and another between the tuning element and the sleeve, each of which can produce intermods.

Finally, a filter was taken apart, the threads tinned, and the assembly tuned with tinned screws; after tuning the unit was placed in an oven until the solder flowed. When tested, intermods were still present but at a lower level ( $\approx 120$  dbm @ 100 watts). Solder flow (which was minimized to prevent detuning) was apparently insufficient to fill all voids or envelope all oxide particles between threads.

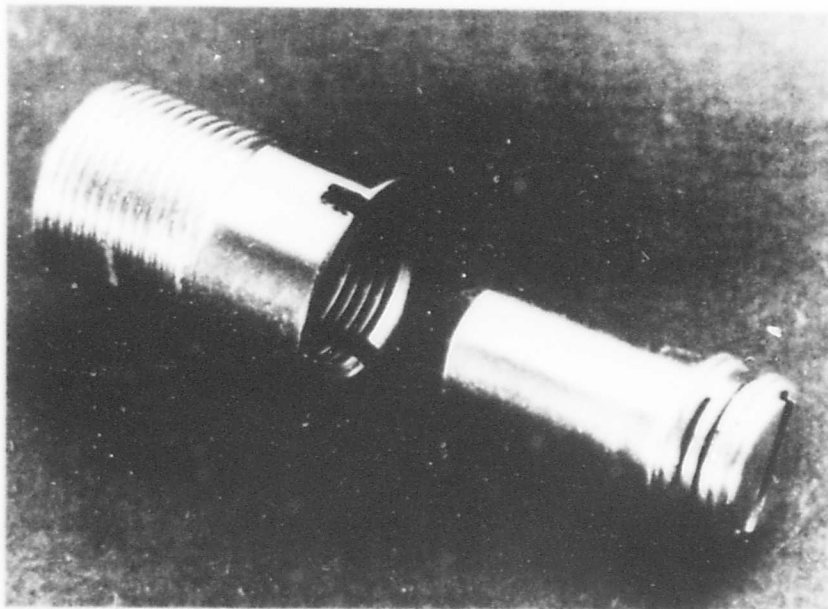


FIGURE 5.3-3  
JOHANNSEN TUNING SCREW



### 5.3.2 Filter Tuning Methods Experiments

Since tuning screws performed unreliably during the intermodulation study, other means of tuning waveguide components were investigated. Three methods were checked here; two for mechanical suitability and one for both mechanical and electrical characteristics. These methods were press-fit, compression-locking, and controlled-dent tuning.

5.3.2.1 Press-fit Tuning - The first method, press-fit tuning, was examined with the intent of initially tuning a filter with screws and then replacing each screw (one at a time) with a press-fit cylinder. This method would require tuning holes that are threaded only part of the way and reamed the remaining distance. The test fixture consisted of a block of OFHC copper as shown in Figure 5.3-4 and two dozen copper cylinders. Tolerance allowance ranged from 0.0001" clearance to 0.0005" interference. In assembling, no lubricant was used.



FIGURE 5.3-4  
PRESS FIT TUNING SCREW

When pins were pressed into holes 1 through 6, there was some blooming of the test block due to severe galling of pins 1, 4 and 5 (pin 4 is shown in an enlarged view below). Pin #1 galled badly when it was removed, and blooming of this hole increased.



Reproduced from  
best available copy.

FIGURE 5.3-5  
GALLING EFFECTS

Pins 1, 2 and 3 were removed and reinstalled to check repeatability of press-fit. After seven cycles, the fit was judged no longer dependable, and after 10 cycles all fits were only finger-tight. However, wherever new pins were installed in holes requiring high initial forces, the second installation was loose. When new pins were installed in holes requiring little initial torque, subsequent insertions were like new. For ranges in between, it appears as though repeatability of fit is inversely proportional to initial insertion force.

Overall, galling and blooming occurred in eight of the twelve samples, and from appearances, galling is probably as detrimental to intermodulation generation as screw-threads. (However, selective fitting and the use of a suitable lubricant could improve repeatability of fit. Dissimilar metal pins would help reduce galling but may encourage electrolytic corrosion.) Because of the inconsistent contact of wall and pin, the press-fit approach was pursued no further. However, a variation of the press-fit pin, the taper pin, was examined further in paragraph 6.3.3 and found to be an acceptable device from galling, contact, and intermodulation viewpoints.

5.3.2.2 Solid Collet Tuning - The second experiment incorporated locking sleeves to make a press-fit contact between holes and tuning pins when driving screws were tightened. The test fixture assumed the appearance shown below and was built to test pull strength, continuous contact, removability of tuning pins and distortion of surfaces. The block and sleeves were made of OFHC copper; pins and screws were commercial steel parts. Pins and sleeves were held to  $\frac{.0000}{.0004}$  clearance by drawing tolerance; the cone angle (included) of the collet was  $60^{\circ}$ ; wall thickness of sleeve was 0.031 nominal. Calculated stress levels in the sleeve were about 3600 psi compression, and shear forces in the block were about 4000 psi.

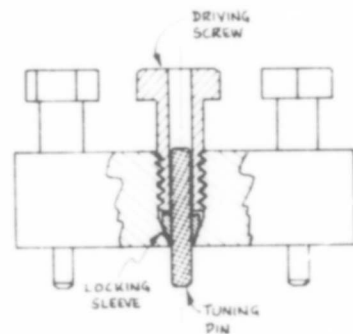


FIGURE 5.3-6  
COLLET TUNING EXPERIMENT

Several eccentricities surfaced in the initial assembly, none of which affected the experiment; however, if this method were to be implemented, the sleeve should extend into the waveguide a few thousandths with the hole cone sharp at the interior surface. This hole will no doubt be slightly egg-shaped or three-lobed but strain deflections would close any resultant gaps quite well. It is only by this method that full contact could be achieved between wall and pin.

The grip of the collet with finger tightening of the screws was evident. At an estimated 30-inch pounds of torque the friction lock was very positive. Repeated applications had an insignificant effect on the torque or grip at this level. Deflections of the block face (waveguide interior) was evident only by highlight differences when viewed at the appropriate angles.

Positioning each tuning probe to within  $\pm 0.001$  (as required to minimize VSWR) by hand sliding would be virtually impossible and would require an additional holding fixture. The tuning fixture in conjunction with close tolerances and complex pieces make this method expensive but it is mechanically feasible. Next development would be to put one or more of these into a straight waveguide to test for intermod generation and tuning versatility, although this step was not taken in this program.

5.3.2.3 Dent Tuning - It is apparent from the previous discussion that all cracks and burrs are not necessarily removed by tight fitting probes. Hence, dent-tuning was investigated as a means of eliminating all internal material discontinuities. To confirm that controlled dent-tuning provides a satisfactory range of adjustment, the single cavity test section shown in Figure 5.3-7 was thinned and subsequently dented by an externally-mounted screw. The resonant frequency of the device was monitored from its unperturbed state to the heavily dented (0.18") state shown in Figure 5.3-8.

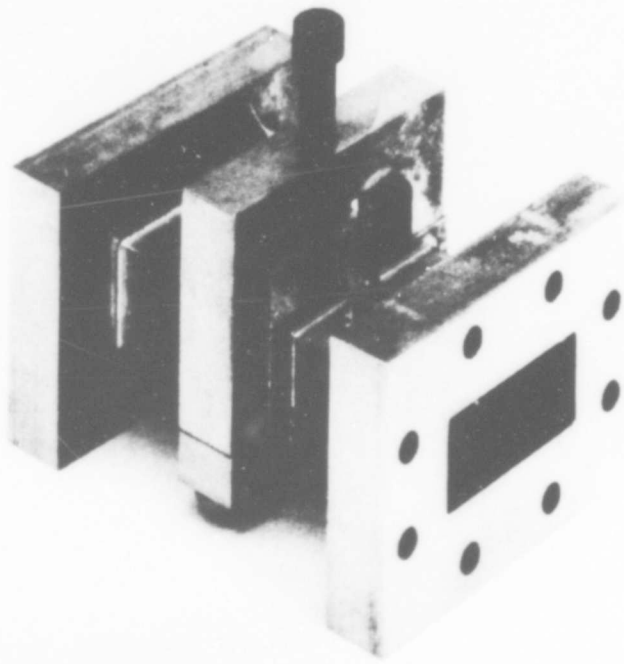


FIGURE 5.3-7  
TEST CAVITY

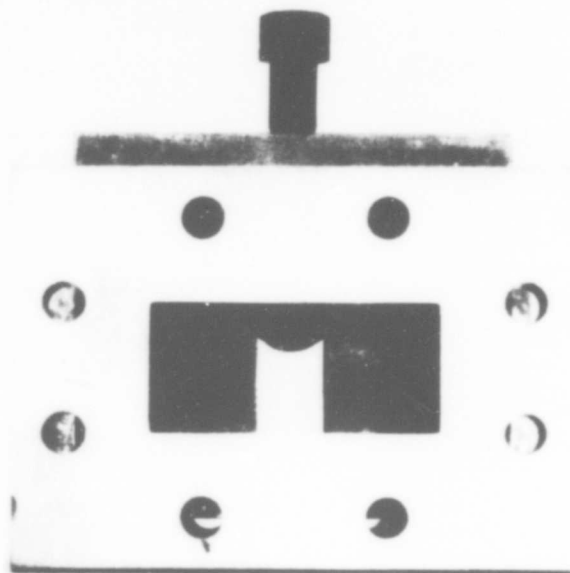


FIGURE 5.3-8  
TUNING EFFECT

The monitored items were center resonant frequency, skirt response, and recoverability as functions of the tuned screw position. The results plotted in Figure 5.3-9 show that the thin walled (0.030") copper permits cavity tuning over a 500 MHz range without fracturing the material, and that the resulting dent is well-formed and confined to the region immediately surrounding the screw. Residual elasticity of the copper remains at about 0.008" for the entire adjustment range, which restricts the permitted tuning overshoot to 30 MHz (or about 1/4 turn of the screw). This range should be sufficient providing extreme care is used during the tuning process, although the range can be doubled by adding another tuning screw to the lower wall of the cavity.

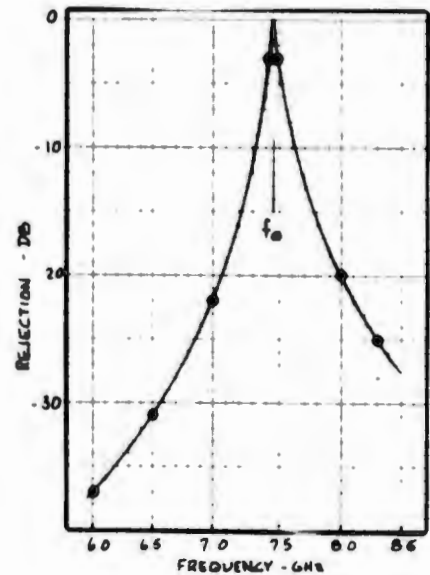
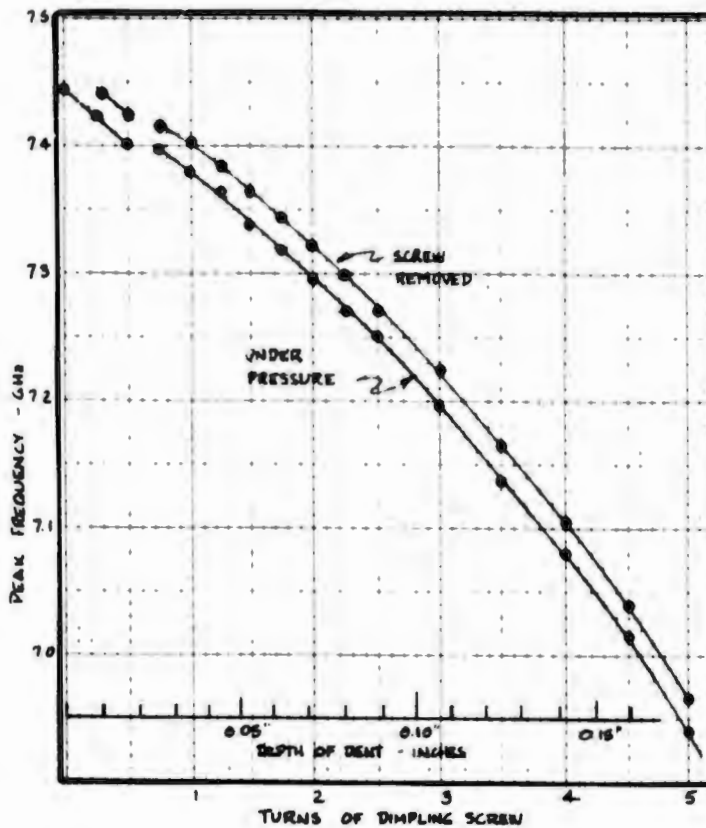


FIGURE 5.3-9  
CAVITY TUNING RESPONSE

### 5.3.3 Bandstop Filter

As a temporary solution to the filter tuning problems, a bandstop filter was fabricated as shown below to remove one of the transmit carriers from the receive filter. The cavities were made separately and tuned to 7.9 GHz by grinding each cavity base, and the assembly was torch soldered to remove all seams.

For two weeks the bandpass/bandstop filter combination worked satisfactorily even though only one end of the bandstop filter was quiet. (When carriers approached from the opposite end, intermods were generated.) The setup did not remain quiet, however, beyond the initial two-week period. On

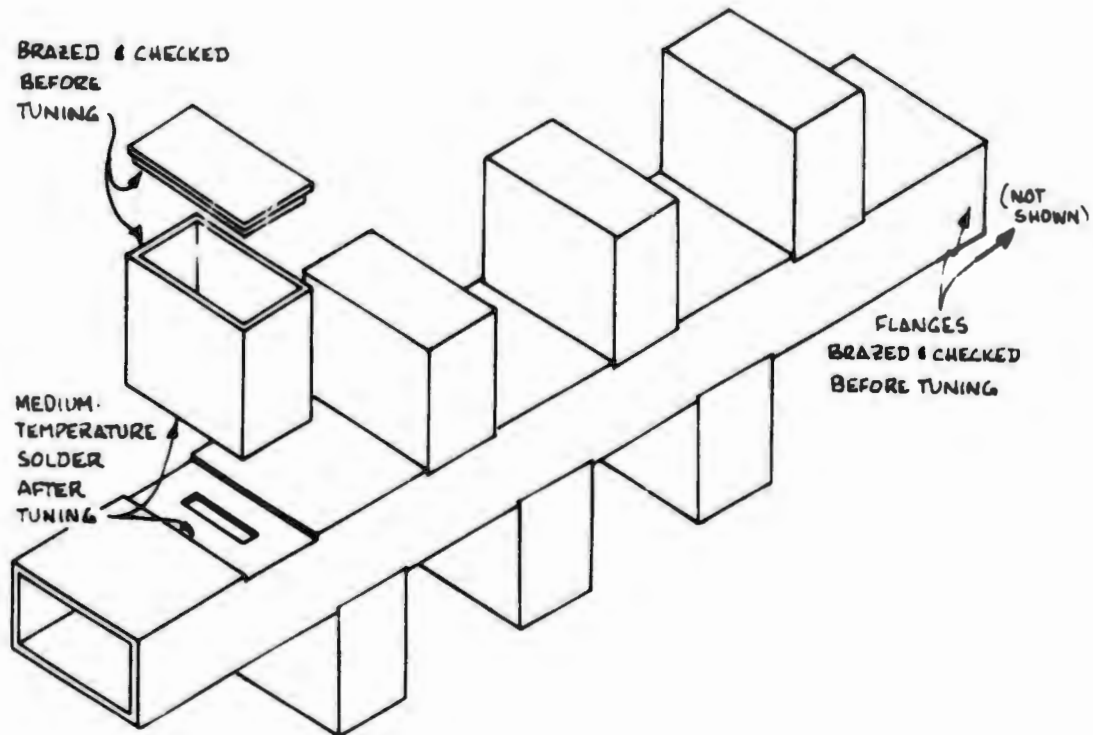


FIGURE 5.3-10  
BANDSTOP FILTER



September 6 a residual intermod was observed at the quiet end of the filter. As the days progressed the intermod level grew as shown in Figure 5.3-11, until the level approach -90 dBm about 6 weeks after the fabrication date. Unfortunately, the cause of this degradation was never learned, since no defects or evidence of voids could be seen when the filter was disassembled.

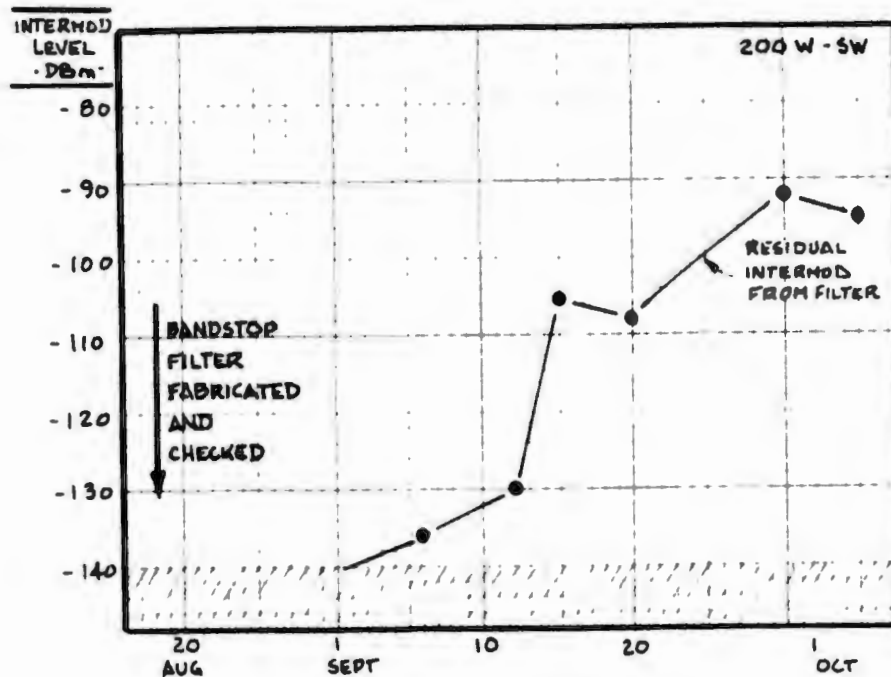


FIGURE 5.3-11  
DEGRADATION OF THE BANDSTOP FILTER

The filter non-linearity is assumed to be related to stresses set up in the solder as it cools, leaving microcracks or fractures along the joint. Each time the waveguide was stressed by other components and handled, these cracks probably grew and encouraged microdischarge, oxidation or other non-linear sources. Also, the cavities were resonant at the transmit frequency so current densities at the sources were many times higher than in normal waveguides, and intermod levels from secondary sources may have become significant.

5.4      Feed Assembly Tests

The Heavy Terminal Feed described in Paragraph 4.3 was examined further during this second phase to isolate and temporarily eliminate the sources of intermods. The areas examined and corrected were the large circular flange, the polarizer assembly, the casting voids and defects, and various flange connections. Ultimately the feed was quieted to below -140 dbm at 6000 watts as described in the following paragraphs.

#### 5.4.1 Circular Flange Gasket Tests

The lack of adequate pressure density around the waveguide walls of standard flanges was also apparent at the large circular flange of the horn where pressures of less than 1600 psi were applied. Here a gasket was installed with raised edges as shown below to increase elasticity of the material and provide repeatable blending of contacting surfaces without exceeding the yield point of the aluminum. However, the bolt holes were too close to the outer lip and pressure on the inner surfaces, although twice the bare flange pressure, was insufficient even when tightening the 1/4-28 screws to their recommended torque of 75 in/lbs. Under this torque, contacting surfaces produced an average pressure of about 4000 psi as indicated below (although pressure near the bolt areas was probably much higher, and pressure away from the bolt holes considerably lower). The effect of this light contact pressure is illustrated on the following page.

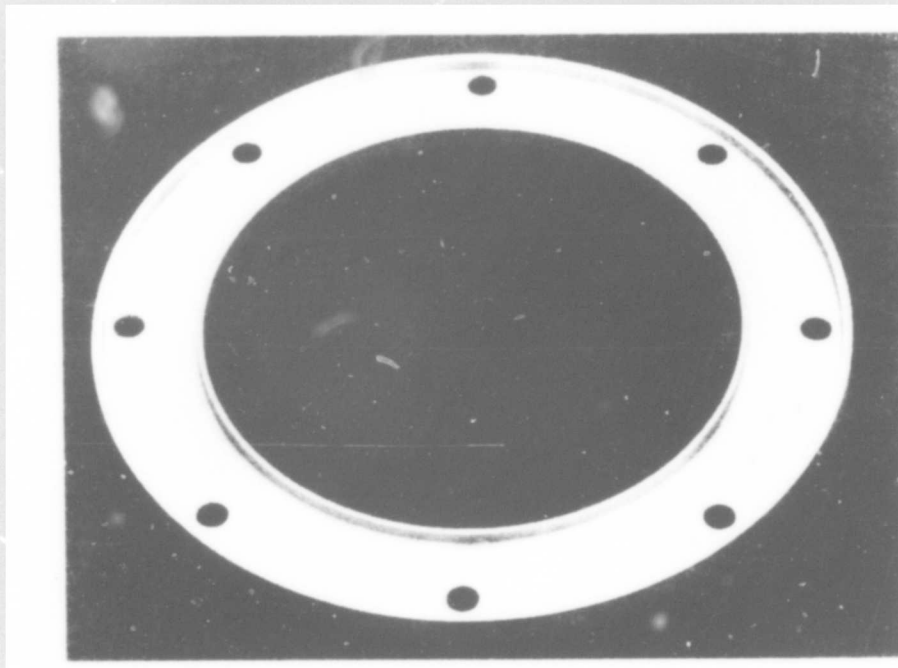
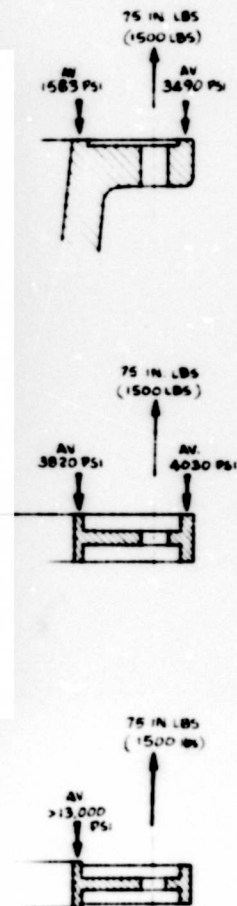


FIGURE 5.4-1  
CIRCULAR FLANGE GASKET



The flange and light pressures described on the previous page added significantly to the horn intermod level as shown in the graph below. The major source of the intermod was isolated to the large flange by inserting a load into the mouth of the horn and observing a significant change in the IM level as the load passed the suspected flange. By removing material from the outer edge of the gasket so the entire bolt force was borne by the inner edge, average pressure was raised to over 13,000 psi and the flange was no longer the major producer of intermods. (Copper gaskets with inner raised lips shown earlier were equally effective providing pressures around the flange were as high.)

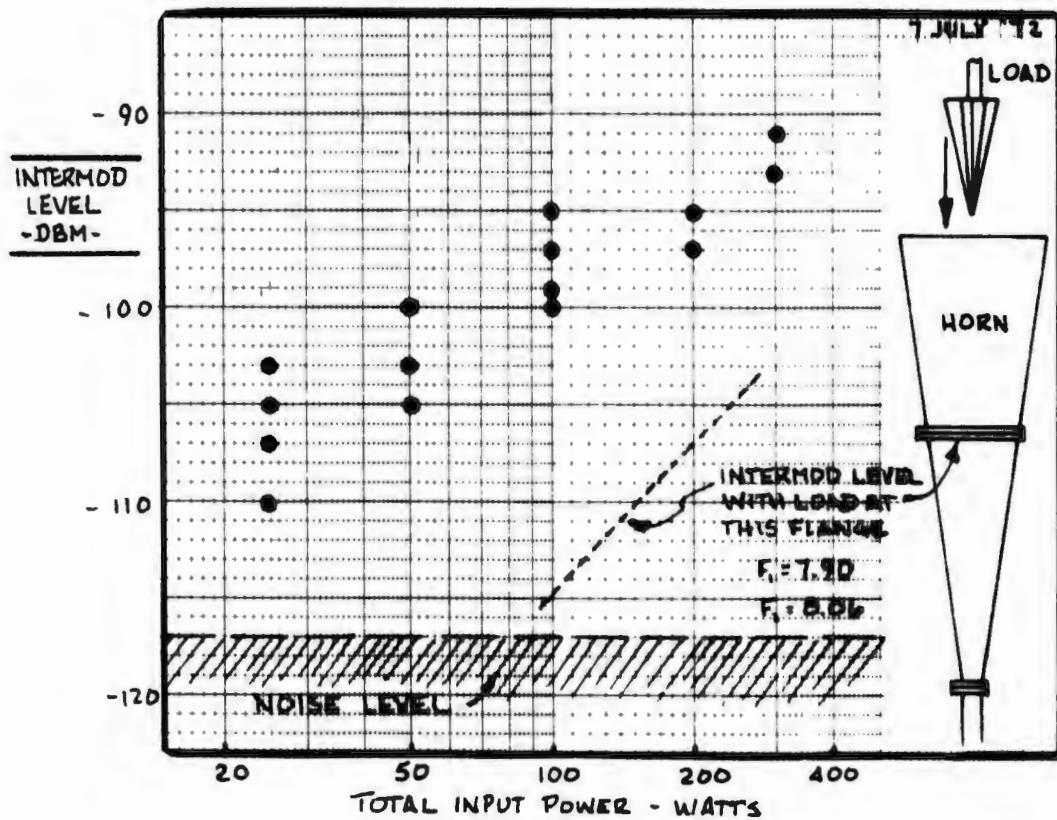


FIGURE 5.4-2  
LEVELS OF IM FROM CIRCULAR FLANGE

5.4.2 Polarizer Seam Effects - The best example (or worst, depending on one's point of view) of soldered seams is the septum polarizer used as the primary transmit/receive separating mechanism. The polarizer is constructed of a vane or septum sandwiched between two machined halves as shown in Figure 5.4-3. Four seams with eight contacting surfaces are involved and all must be bonded together to form an integral unit.

During the study, intermod levels of about -100 dBm at 150 watts (standing wave) were isolated to the polarizer. Applying pressure along the defective edge caused the intermod level to vary about 10 dB. The device was originally x-rayed to see if solder defects could be observed; however, the thickness of the brass compared to the solder was too great to obtain sufficient contrast. Hence, the polarizer was disassembled.

From the photograph, two points are evident: (1) cracks do not have to be perpendicular to wave propagation, as longitudinal seams are equally sensitive to radial current flow; and (2) cracks do not have to extend through the material or be significantly deep with respect to wave length to produce intermods. It was not determined from the seam whether the oxidized crack existed at the time of assembly or whether the crack grew from trapped flux remnants and applied (external) stress; although the former choice is favored.

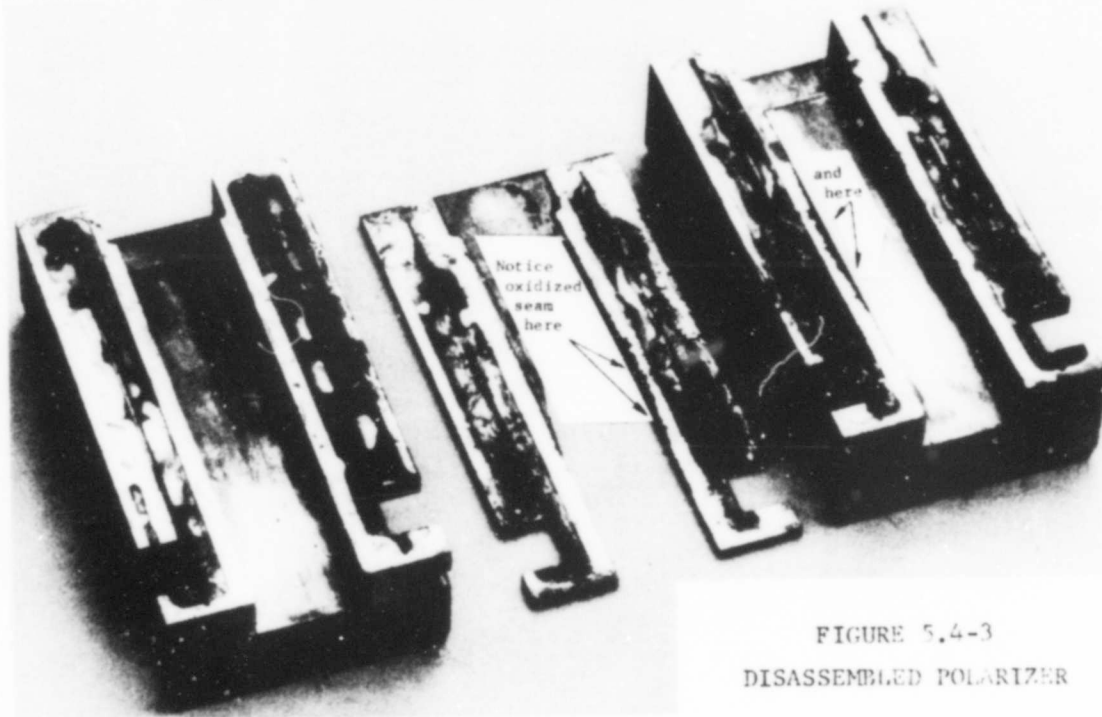


FIGURE 5.4-3  
DISASSEMBLED POLARIZER

### 5.4.3 Other Polarizer Design Defects

In addition to the seam problems, four other design areas of the polarizer encouraged intermod production. These are as illustrated below: (1) One step of a quarterwave transformer was designed as part of the flange and produces high current densities which accentuate non-linearities. (2) A bifurcation at the input flange junction lacked sufficient contact pressure because of its distance from bolt holes in conjunction with normal flange distortion. (3) On both input and output flanges, the four bolts provided insufficient pressure to yield the copper gasket. (4) The polarizer output is so close to cutoff that intermodulation products were more susceptible to small misalignments than on standard flanges. Unfortunately, the defects were noted by gross effect of pressure and misalignment, and no individual data is available to relate magnitude of IM to a particular point.

Nevertheless, these items are presented here as typically accepted microwave practice which is no longer suitable for multicarrier X-band operation.

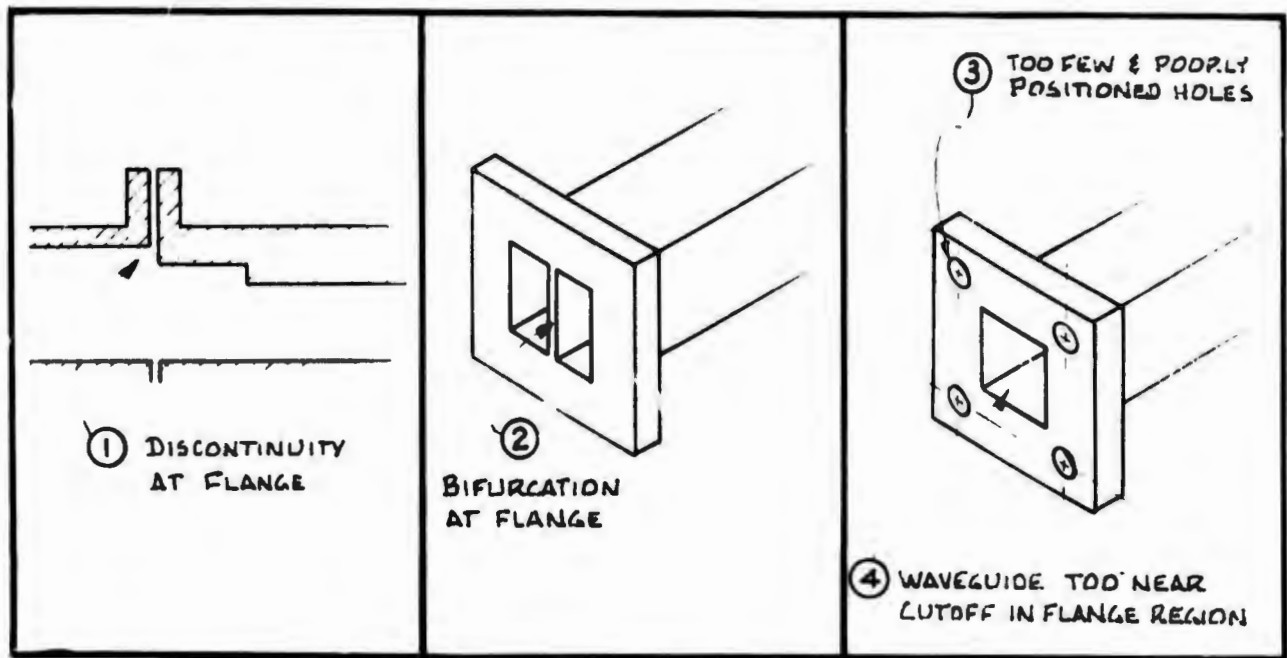


FIGURE 5.4-4  
POLARIZER DESIGN DEFECTS



#### 5.4.4. Effects of Dipbrazing

A three-foot test horn was built from sheet aluminum and dipbrazed to check the effects of brazing operations on intermod level. Tests with this device show no discernable intermods to -140 dBm for 6,000 watts of total applied power. An inspection of the horn showed fillets at all seams and no cracks or visible voids. Hence, dipbrazing if carefully done is acceptable. Later experiments, however, demonstrate that brazing is not always "carefully done" at standard commercial brazing houses. Subsequent attempts to successfully braze aluminum filters failed, as described in paragraph 6.3.2.2.

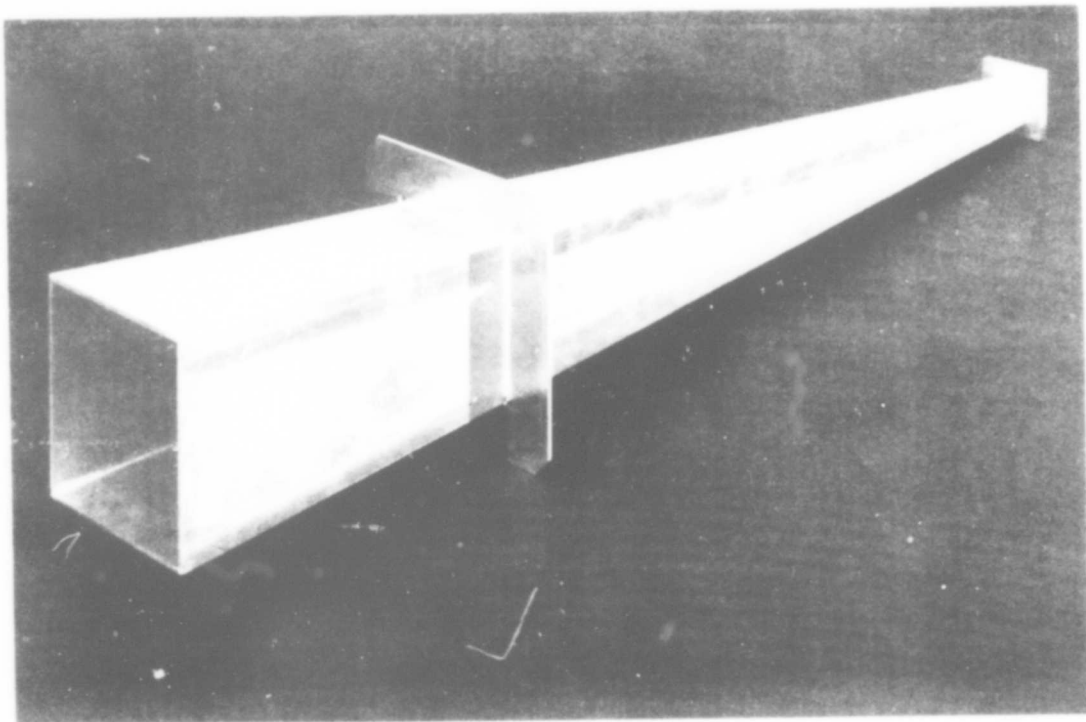


FIGURE 5.4-5  
SAMPLE DIPBRAZED HORN



#### 5.4.5 Temporarily Quieting the HT Feed

From a program point-of-view, it was desirable to apply the principles learned during this study to an HT feed and, at least temporarily, quiet the feed. So, after the solder seam defect was located in the polarizer/OMT assembly, the unit and accompanying waveguide were completely disassembled, thoroughly cleaned, tinned, and oven-heated for uniform flow of solder. Simultaneously the flanges forming the step transformer and bifurcation junction were similarly soldered together. In the meantime the horn casting had all pores in the vicinity of the flanges welded and refinished, and the flanges were lapped and blended to mating waveguide. The total feed was assembled using new soft copper gaskets (with raised inner contacting area) between all flanges, and tested. No intermods were initially present at -140 dBm for a total input power of 6000 watts.

Immediately before assembling each flange for the above test, it was lapped and cleaned thoroughly with acetone so a minimum of oxide was present on contacting surfaces. After being sealed up, the unit was "age-tested" for three days. During this time, no change in the performance was observed. However, when the horn was removed from the feed, aluminum oxide was present around the outer edges of the copper/aluminum interface. No corrosion was observed on the actual contacting surface, although oxygen migration over a sustained period is expected.

(During the feed tests, a reference intermod level was produced by attaching two loose stainless steel washers to a broom handle and placing them in the radiate field. Intermods generated by this method are extremely strong and have shown the non-linearity of contacting steel in RF fields.)

## 5.5 OTHER FEED SYSTEM TESTS

### 5.5.1 MSC-46 Feed Tests

As part of the Intermodulation Study, an MSC-46 (multimode dielectric) feed was examined for intermod levels. In order to test the unit with the dielectric installed, an enclosure lined with absorbing material was fabricated as shown below in Figure 5.5-1. (The rope webbing appearing in the picture was used to support a floor of absorbing material.) All energy radiated below the horizon was intercepted in this manner to prevent possible coupling to intermod generating structures near the test facility. After concluding the scattering test, the dielectric/subreflector was removed and the horn permitted to radiate toward the open sky. Hence, effects of the dielectric itself, if significant, could be observed.

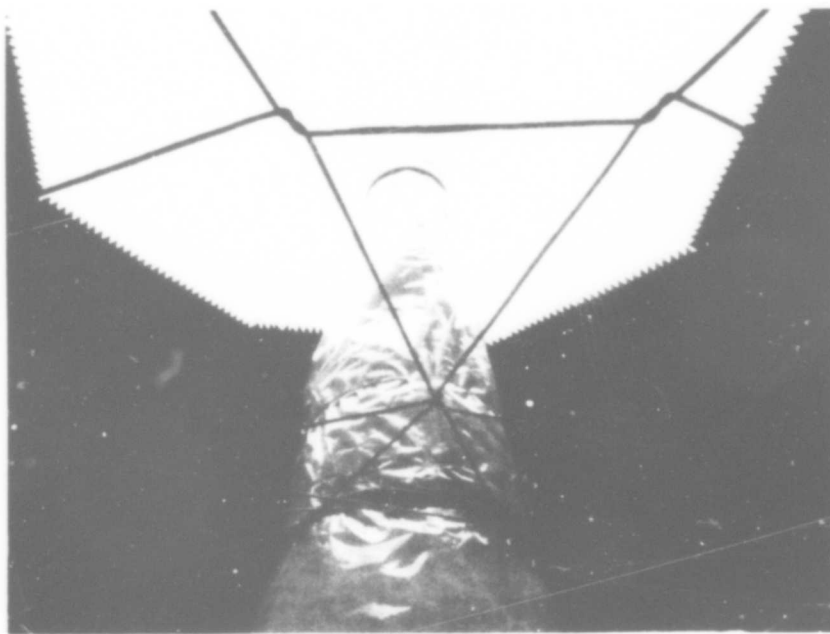
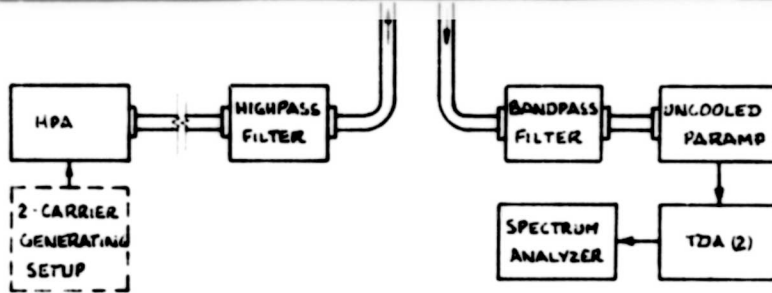


FIGURE 5.5-1  
MSC-46 FEED



The result of the dielguide tests are shown in Figure 5.5-2. With the dielguide in place, intermod levels are extremely high at the beginning of the tests, some 20 dB higher than normally expected for the given power levels. However, after the initial applied power reached 50 watts, the intermod level becomes independent of power until 200 watts is exceeded. After this, the intermod level at all powers from 5 to 1000 watts stabilizes and follows (approximately) the normal 2.5 dB/dB relationship. Tests with the dielguide removed produce a more stable intermod level as indicated by the dashed line of Figure 5.5-2. In both cases, the intermod level at 1000 watts is about -85 dBm.

There is no explanation offered for the instability in dielguide measurements other than the supposition that 1) moisture may have existed in the dielguide and was driven out as the power passed 50 watts; or 2) there was a sensitive non-linearity within the dielguide, subreflector or attaching mechanism that was destroyed above the 50 watt level.

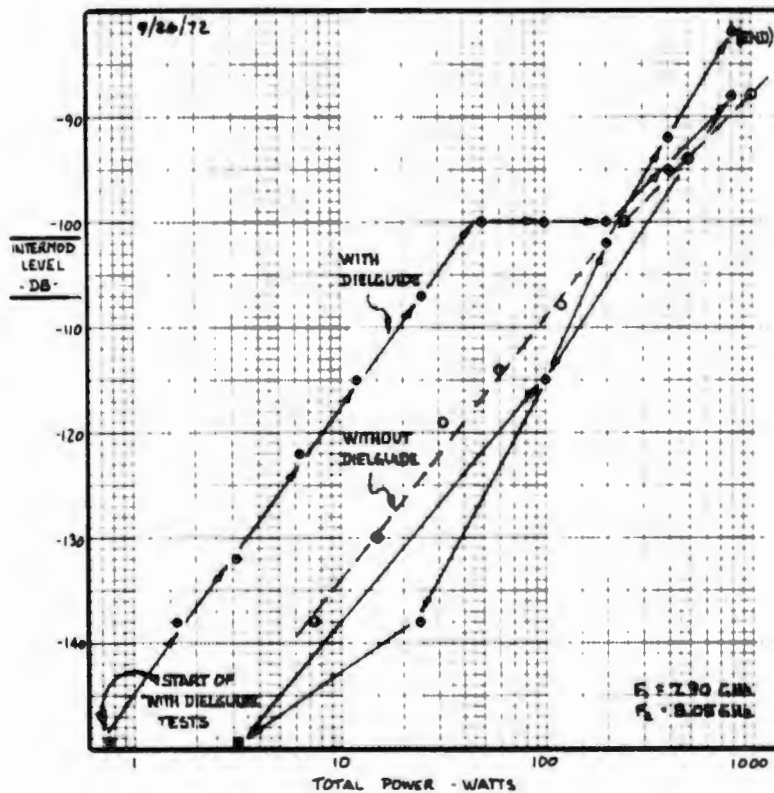


FIGURE 5.5-2  
LEVELS OF IM  
FROM CIRCULAR FLANGE

While the MSC-46 feed was under test, the levels of higher order intermodulation products were observed at 1000 watts of total carrier power. The results are presented in Figure 5.5-3, where the higher orders decrease at about 16 dB/order for the indicated input conditions. Orders higher than the seventh were not found.

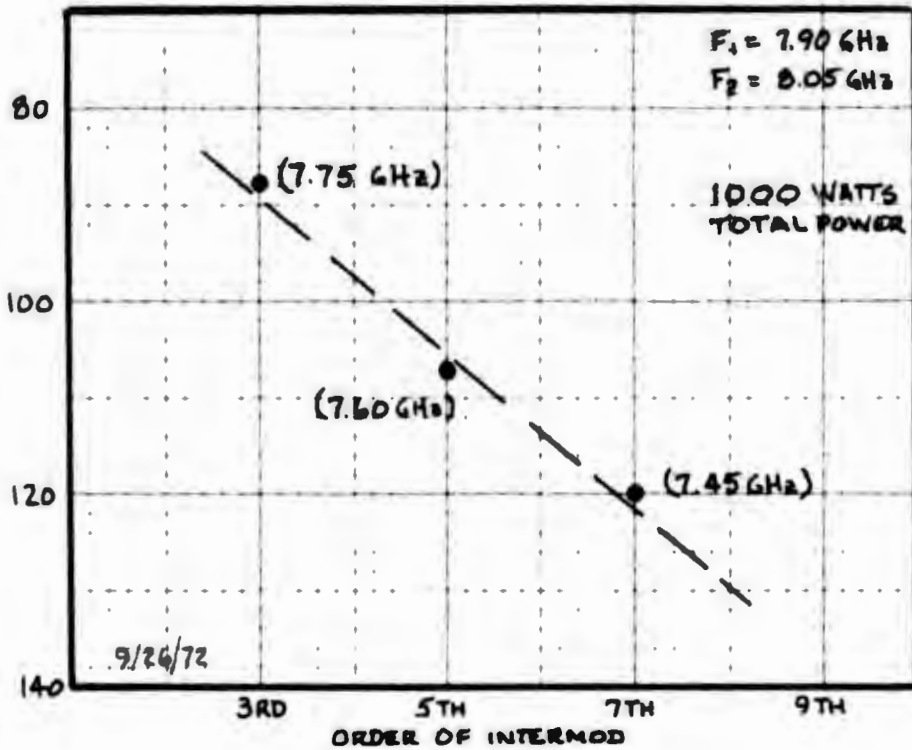


FIGURE 5.5-3  
HIGHER ORDER IM'S FROM MSC-46 FEED

### 5.5.2 HT Terminal Tests

Intermod levels for the HT Antenna were measured to compare with the MSC-46 Feed. The results of these tests are shown in Figure 5.5-4 where the intermod level again follows the 2.5 dB/dB slope and in magnitude is almost identical to MSC-46 levels. The similarity of data in these two cases to the collected data summarized in Figure 4.6.1 is interesting in that the feed data is within 10 dB of the mean value of other travelling-wave data taken during the first phase of the IM Study. This similarity again shows that there is some basic mechanism at work in a waveguide junction that has definite thresholds and is reasonably well-defined in terms of applied current density.

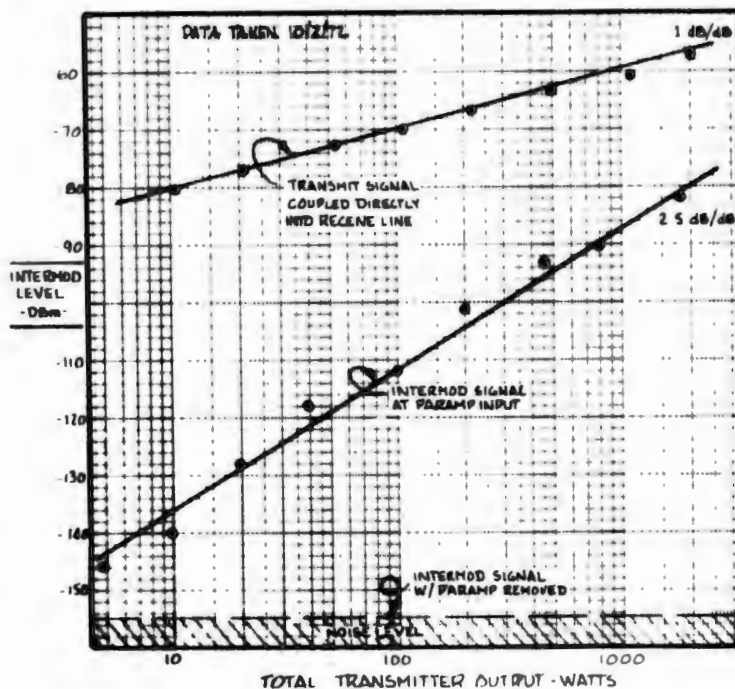


FIGURE 5.5-4  
IM LEVEL OF HT ANTENNA

While the above tests were in progress, transmit/receive line coupling was measured to insure that a quieted feed would not be overshadowed by direct intermod coupling from RFI. The outcome here is shown by the upper line in Figure 3.2-2; where the net coupling level is -120 dB (i.e., 1000 watts or +60 dBm produced a receive line signal of -60 dBm). Although this level is 20 dB higher than the minimum receive line sensitivity (-140 dBm, plus 60 dBm of low noise amplification) it is insufficiently strong either to produce a noticeable intermod or to saturate the down-converter.

Finally, the coupling between HT sum horn and error horns was measured to determine what level returns from the subreflector and what preventative measures are required to quiet tracking channel intermod contributions. The total returned level was -40 dBm, or 1 watt per 10,000 watts radiated power. This data will be used for later feed design recommendations.

## 5.6 Dielectric Separation Tests

The effect of separating two contacting surfaces was studied by inserting a thin (0.0005") sheet of dielectric film between flanges. For this test a pair of flanges having surface finishes of 8 microinches or better were mated, and the intermod level observed as the bolts were tightened. Subsequently, the dielectric film (Kapton) was inserted and the procedure was repeated.

Intermod levels for the bare flange varied considerably in the 0 to 15 in-lb torque range and levelled off above 20 in-lb as shown in Figure 5.6-1. The high initial intermod levels are attributed to gross curvature or waviness of the flange which is removed by tightening the bolts. However, once the flat surfaces are snugly mated there is insufficient pressure, even if bolts

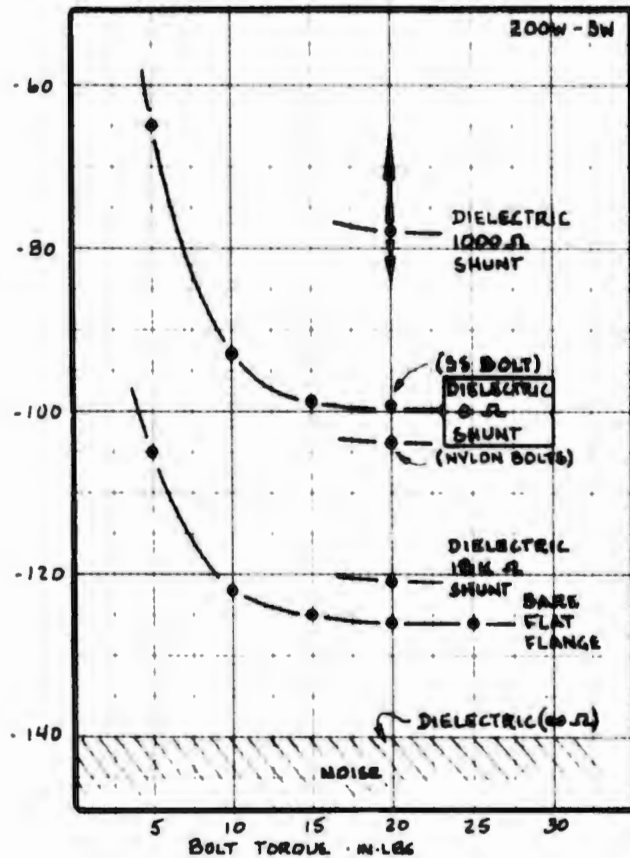


FIGURE 5.6-1  
DIELECTRIC SEPARATION EFFECTS

are tightened to the stripping point, to break down oxide layers or otherwise deform the surface because of the low average pressure ( $\approx 1000$  psi) over the broad face.

With the dielectric inserted and stainless steel bolts holding the flanges together (hence 0 ohm between flanges) the intermod variation with flange pressure has the same form as the bare flanges, except the dielectric level was about 12 dB higher. This occurrence suggested that there may have been coupling of the waveguide fields to the bolts, which became the source of intermods rather than the dielectric or flange surfaces themselves.



When nylon bolts were added the intermod level dropped below the noise level whenever the resistance between flanges was essentially infinite. However, as the flanges were tightened to the point of spot breakthrough where the resistance was about 18,000 ohms, an intermod appeared at the -120 dBm level. Further tightening reduced the resistance to 1000 ohms and raised the intermod to above -80 dBm. At this point, both resistance and intermod levels were unstable. (Note: Bolt torque has little meaning for nylon screws which readily stretch as they are tightened; nevertheless, an equivalent torque of 20 in-lb has been arbitrarily assigned.)

The addition of a D.C. bias had little effect until about 20 volts at which level a current surge dropped the resistance to a very low value and the intermod decreased by about 25 dB. This effect implied that a diode or tunnelling mechanism was set up during spot breakthrough, which was destroyed by the D.C. bias.

Materials Tests

Several sets of waveguide sections were fabricated and plated to determine the effects of different materials on IM's. The units consisted of brass flanges (with raised contacting surfaces) brazed to OFHC copper waveguides and plated with gold, silver, cadmium, nickel and copper as shown below. The raised areas near the edges of the flanges were recessed about 0.08" below the inner surfaces so the entire combined bolt force was applied to the waveguide area. The results are presented on subsequent pages.

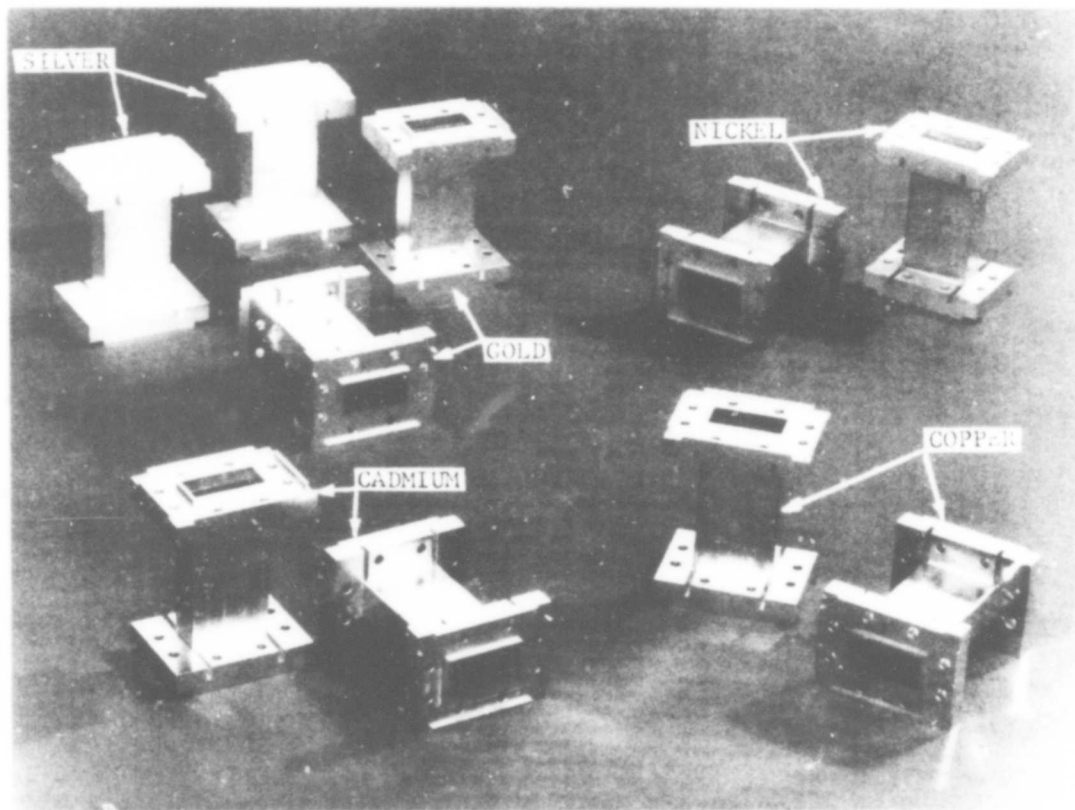


FIGURE 5.7-1  
SAMPLE WAVEGUIDES

Some testing was done with gold-plated flanges. For extremely light contact intermodulation products were noted at levels greater than -60 dBm, typical of discharge phenomena that is noticed with all very loose contacting surfaces. However, when tightened, the gold flanges quieted with pressures barely beyond finger-tight (much less than the 10 inch-pounds minimum measurement capability). The impressions left on the gold surfaces from mating flanges are well defined, confirming that virgin gold plate behaves like putty under pressure and provides continuous metallic contact. This test demonstrated that for a one-time connection, gold plating is equivalent to a soft gasket.

Stainless steel flanges of two types have been fabricated as shown in Figure 5.7-2. The first set have raised bosses, and will be used to measure intermod levels produced by steel-to-steel contact and as a hardened base for future gold tunnelling tests. The second set have grooves around the waveguide area in which a gold or copper ring will be set and crushed under the combined force of all the bolts.

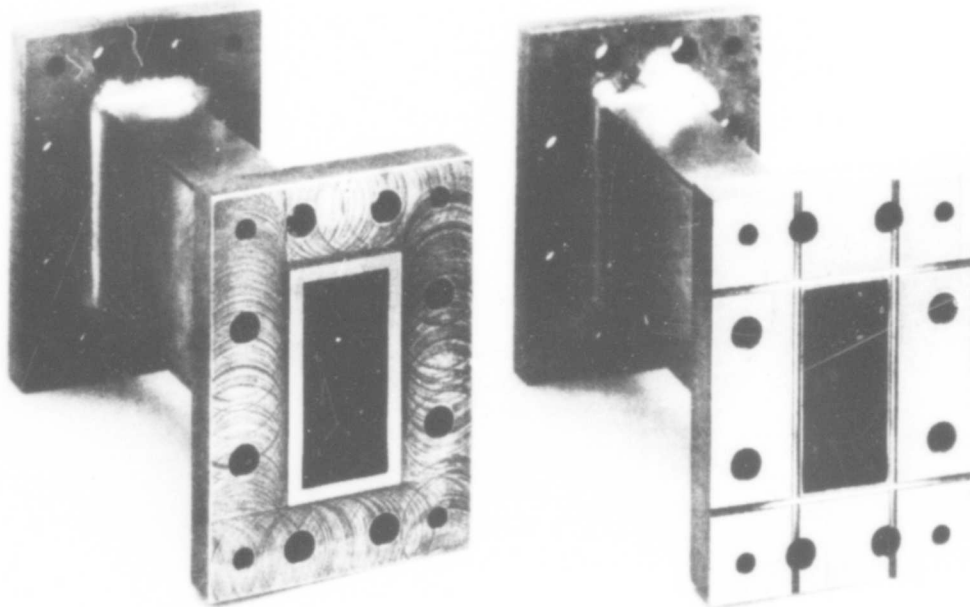


FIGURE 5.7-2  
STAINLESS STEEL FLANGE SAMPLES

SECTION 6.0

TESTING PROGRAM - PHASE III

(As Performed October 1972 - May 1973)

6.1 SCOPE - PHASE III

The third portion of the Intermodulation Study continued the experimentation with filters by examining various types of bandpass and low pass designs, and various methods of fabrication such as electroforming, ovenbrazing, dip-brazing, and milling. New methods of tuning were devised, and were proven linear and repeatable. Acceptable flanges were defined and proven quiet. All other tasks required of the Intermodulation Study were completed.

## 6.2 Test Facilities

The DTF facilities described in Paragraph 5.1 were used for Phase III testing, except a two-stage tunnel diode amplifier replaced the uncooled paramp as shown in Figure 6.2-1. Even though the system noise figure increased by 3 dB, sensitivity remained at -140 dBm by decreasing the predetection bandwidth and scan rate of the spectrum analyzer. All readings taken in this section were obtained with a 300 Hz bandwidth, a 5000 Hz scan width and scan rates compatible with calibration requirements.

Tests were made with the screen room standing wave setup, thereby constraining power levels to the rating of the HPA output circulator. Most experiments were made with power levels of 400 watts or less, although occasional short term tests were made at levels approaching 800 watts. By phasing both carrier frequencies as described in paragraph 4.2.1, an equivalent current density of 1600 to 3200 watts was produced at a flange or similar (potential) IM source. Furthermore, any resulting IM propagated directly into the receiving system without the 3 dB loss associated with a randomly polarized wave in a horn/OMT region. The power/sensitivity relationship then simulated an operational situation quite closely.

Total carrier power remained in the 400 watt range during filter tests, even though exposure is considerably less in a real feed. With an OMT/polarizer isolation of 23 dB, the receive arm filter sees only 50 watts of a 10 kw transmit signal, and even less after interfacility lines and other losses reduce the power by 2 or 3 dB. When a filter is described as quiet in subsequent sections, it is quiet to a much lower level than indicated.

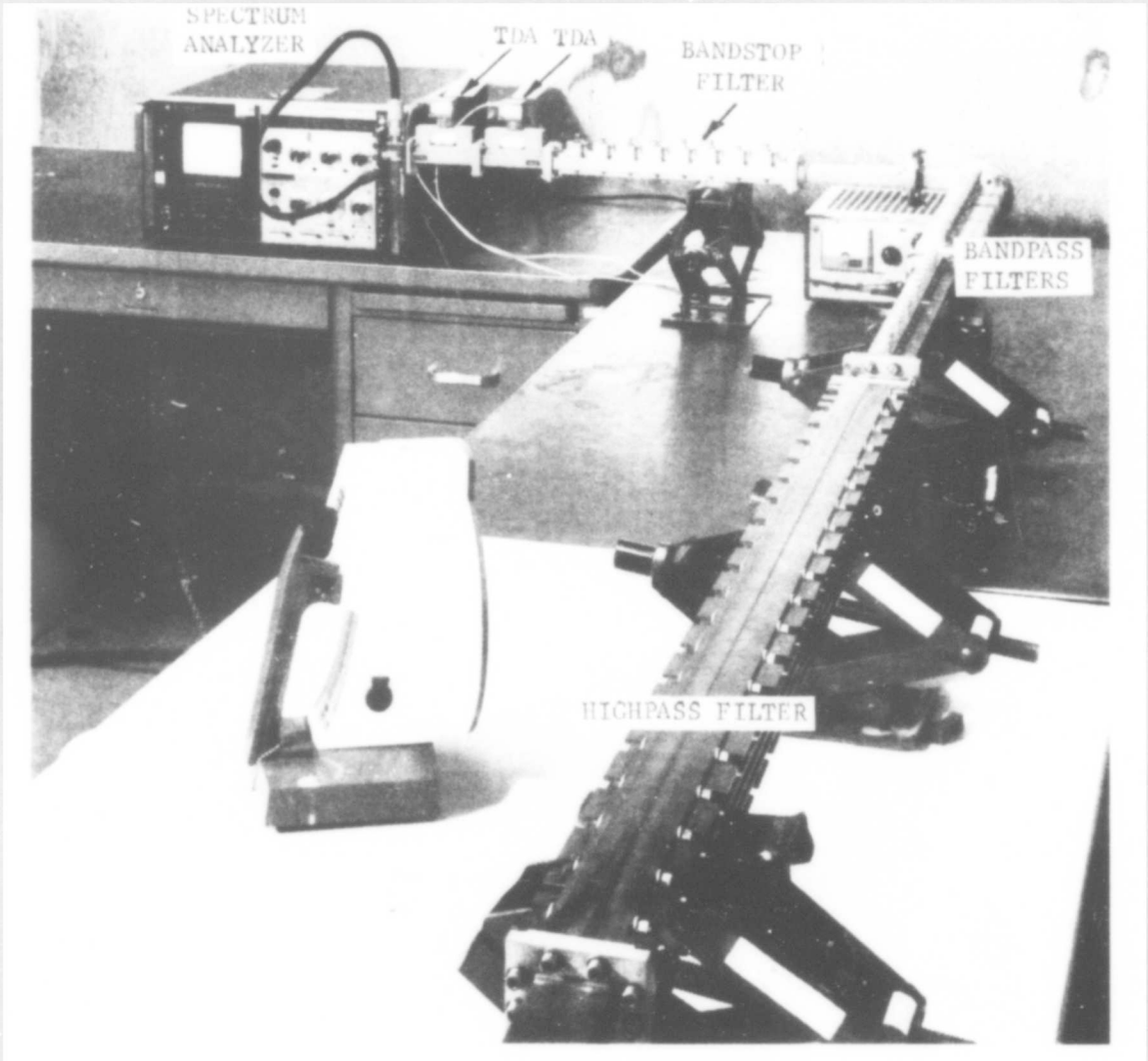


Figure 6.2-1 Typical Test Bench



### 6.3 Filter Experimental Program

In progressing toward an intermodulation-free filter three basic approaches have been pursued, each with several variations: dent tuned bandpass, untuned lowpass, and taper-pin tuned bandpass. This section describes the devices and the results.

#### 6.3.1 Dent-tuned Bandpass Filters

Three bandpass filters were fabricated for dent tuning experiments: an electroformed filter with iris susceptances, an electroformed filter with post susceptances and an oven-brazed (inert gas) filter with iris susceptances. The top and bottom walls of each filter were counterbored between sets of irises to reduce the wall thickness to 0.030", and the tuning bridges added as shown in Figure 6.3-1. Cavities were simultaneously tuned from the top and bottom to reduce stresses within the walls and along the susceptance/wall junctions.

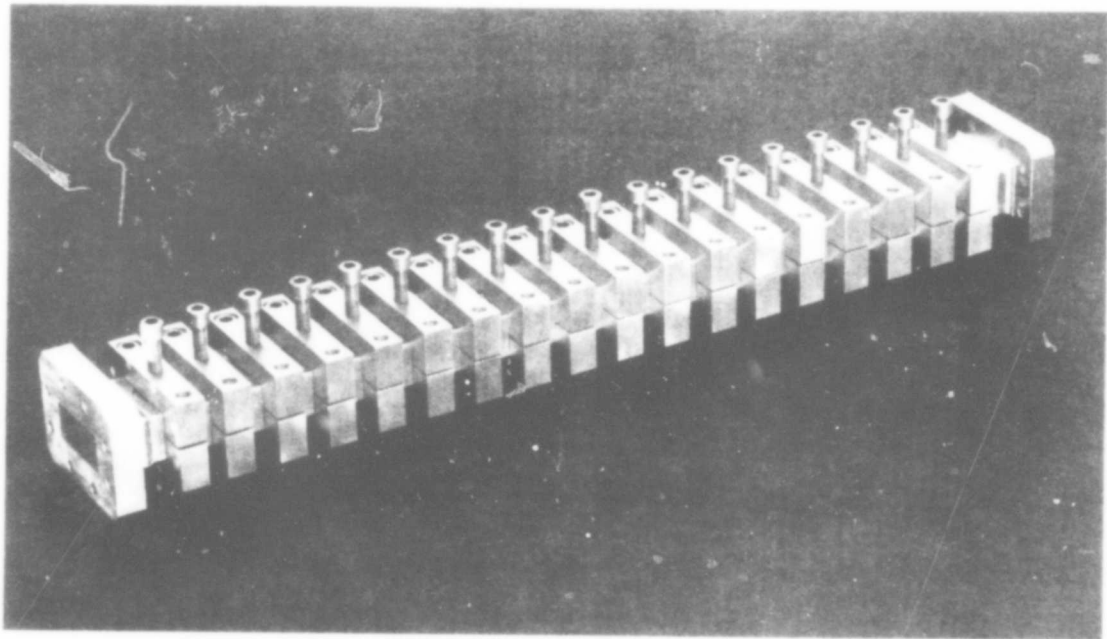


Figure 6.3-1  
Dent Tuned Bandpass

The first bandpass filter was electroformed by inserting precut copper irises into an aluminum mandrel and depositing a heavy copper plate over the assembly, forming a molecular bond between the iris and wall. Unfortunately, the filter neither responded to tuning nor was free of intermodulation products. Figure 6.3-2 illustrates quite clearly why this was so; the vendor had inadvertently left traces of mandrel material, and the residue in three cavities upset the electrical characteristics.

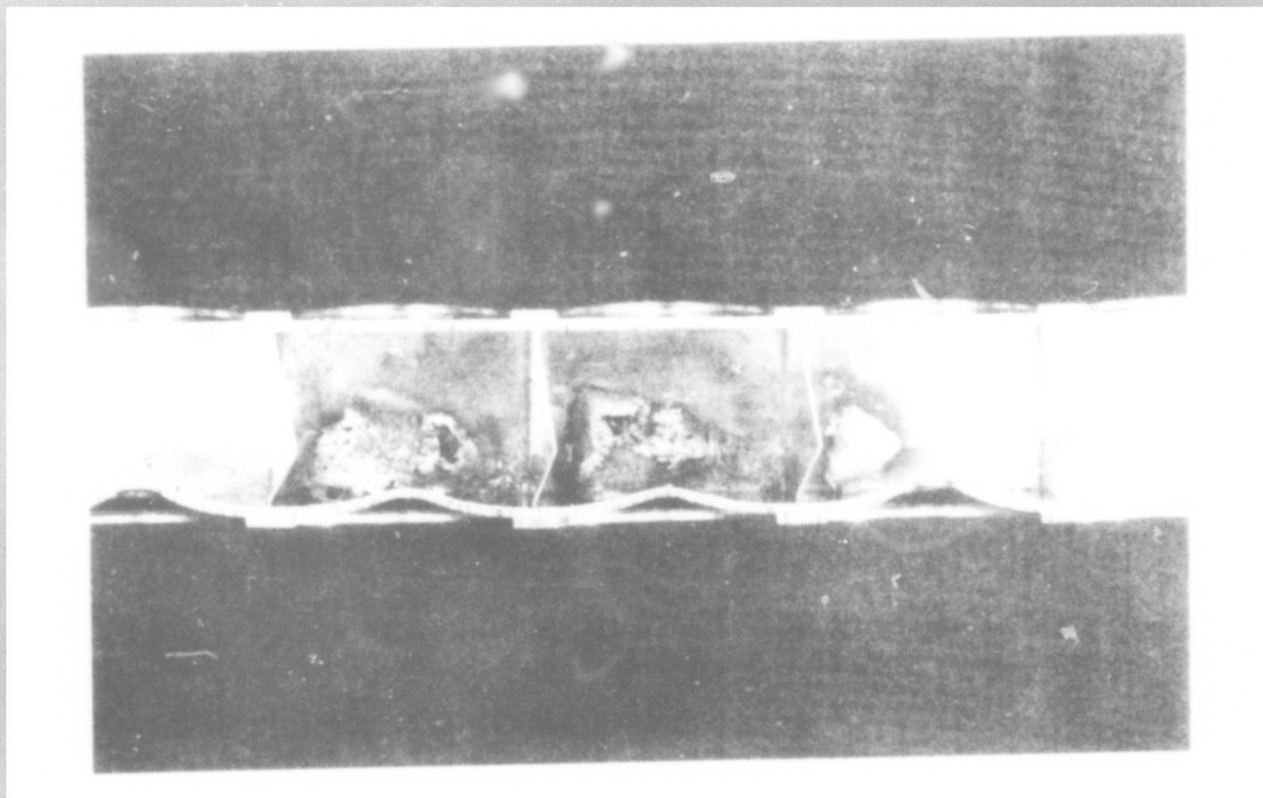


FIGURE 6.3-2  
MANDREL RESIDUAL

The remaining cavities were tested with a dye-penetrant to see how well the copper had bonded to the mandrel inserts. The dye revealed several apparent cracks as shown in Figure 6.3-3. However, the vendor suggested that the dye simply exposed shallow creases in the bond, rather than cracks per se. The inserts had been extended beyond the mandrel and as the plating began no electric fields extended into the corners and a void or crease results. Even though the void is not a fracture, it does concentrate stresses and is likely to produce a fault in an operational system. Later samples built by another electroforming company showed no evidence of voids at similar junctions, so dye penetrant tests are now considered mandatory for electroformed parts used in multicarrier systems.

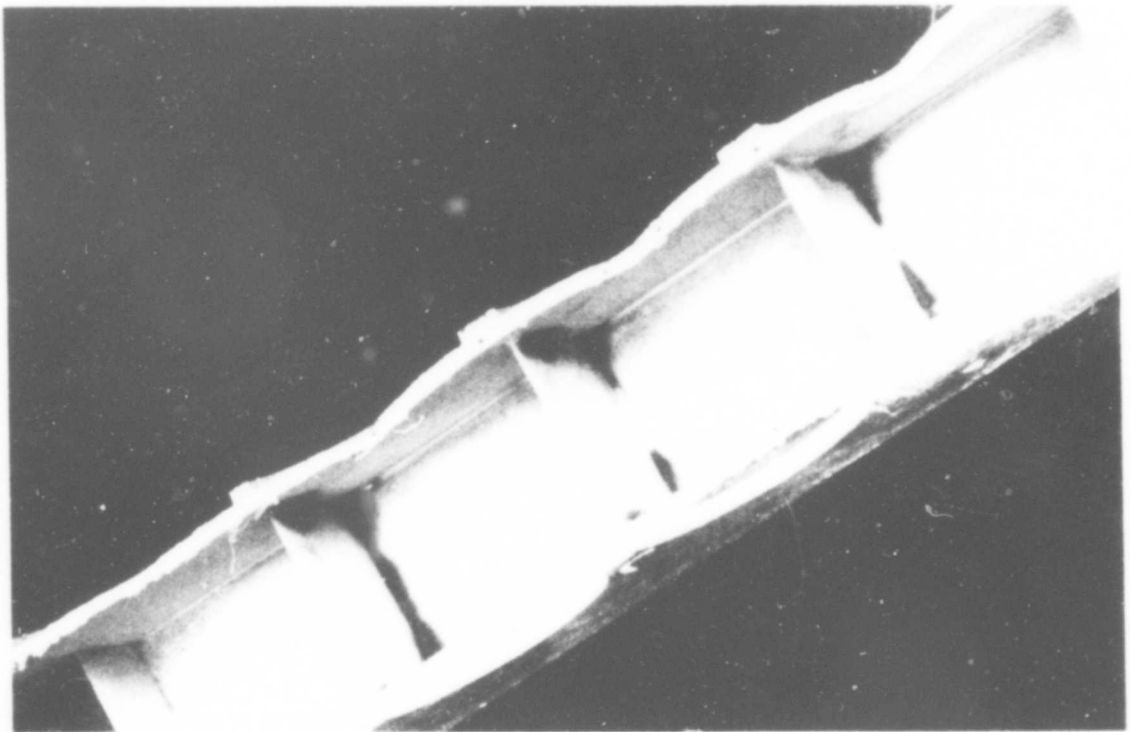


Figure 6.3-3  
Result of Dye-Penetrant Test  
(Electroformed Filter)

The second test filter was also built by the first vendor, but this unit used posts for susceptances rather than irises. The tuning method and external appearance was identical to the first filter. Intermods were present at the -119 dBm level for 400 watts of power, even though the dent tuning was applied in several stages and stress-relieved between each stage. Again, it is assumed that the posts had not bonded ideally to the wall. An attempt was made to fill the recesses by plating the filter with a heavy coating of chemically deposited nickel and gold, but the final filter had unstable IM's at 125 dBm for 400 watts, rising to -85 dBm whenever the filter was lightly tapped. Thus, once an item possesses a non-linearity this defect is not readily suppressed or covered by additional plating.

The third filter was fabricated from standard waveguide and shim stock, and oven-brazed in an inert atmosphere. However, the brazing process softened the copper and distorted both waveguide and irises to the point where tuning could not produce the desired bandpass response. Even so, this particular filter was free of intermodulation and was used in the test setup for subsequent measurements. The oven-brazing process was not used again, however, because soft copper is too susceptible to distortion from external stress or pressure, and the response of an 18-cavity filter is too unpredictable.

### 6.3.2 Untuned Lowpass Filter

The image parameter filter, as developed by Cohn<sup>1</sup> and extended by Young<sup>2</sup>, is predominately used in the waffle-iron configuration to suppress harmonics, and nowadays is rarely used to provide isolation between two closely spaced bands because there is no convenient method to tune the passband response. Nevertheless, if Cohn's original equations are used without approximation and adapted for a T-network instead of a  $\Pi$ -network filter, skirt location and rejection are accurately predictable. Hence, such a filter that requires no tuning is ideal for an intermodulation-free feed. Unfortunately passband impedance close to the skirt is not accurately predictable because it is a function of the pole location and impedance of the first (and last) half cavity, and this cavity is influenced by the dimensions of the terminating waveguide. By careful choice (and iteration) of the dimensions of the first cavity, the impedance slope should correspond reasonably well to the impedance slope of an arbitrary input waveguide.

A preliminary look at the corrugated (image parameter) filter reveals that to obtain the required 80 dB of isolation at 7.9 GHz and still have a good match at 7.75 GHz (only 1.9% away) requires combined theoretical and manufacturing accuracy of about 0.3%, which is difficult to hold on a production device where dimensions of slots and teeth are on the order of 0.1 inch. As a direct substitute for the bandpass, then, the image parameter filter is a poor choice.

Philco-Ford continued with the low pass, not as a principal filter, but as a pre-filter; that is, a filter that removes sufficient carrier power so that IM's generated by subsequent filters or components are below the -140 dBm requirement. Here it is not as important that total carrier power be reduced as it is for the resulting intermod to be eliminated.

- 
1. Cohn, S.B., "Analysis of a Wideband Waveguide Filter", Proc. IRE 37, pp. 651-656, June 1949.
  2. Young, L, "Postscript to Two Papers on Waffle-Iron Filters", IEEE Trans. on MTT-11, pp. 555-557, Nov. 1963.

For example, a 7.9 GHz carrier, regardless of how strong, will not produce a 3rd order product in the receive band without a second carrier between 8.05 and 8.40 GHz. The skirt requirements on a pre-filter are therefore considerably less than those for the bandpass filter itself, providing orders higher than the third are substantially weaker.

The actual skirt depends on the total isolation required at 8.05 GHz for a worst case combination of carrier, and the relative levels of the higher order IM's. Figure 6.3-5 compares the skirt of a standard 80 dB bandpass filter (dashed line) with the skirts of 40 dB prefilters designed to suppress higher order IM's with levels decreasing by -10, -15 and -20 dB per order. An additional 100 to 120 MHz separates the prefilter passband from the stop band, and the filter becomes easier to match without separate tuning.

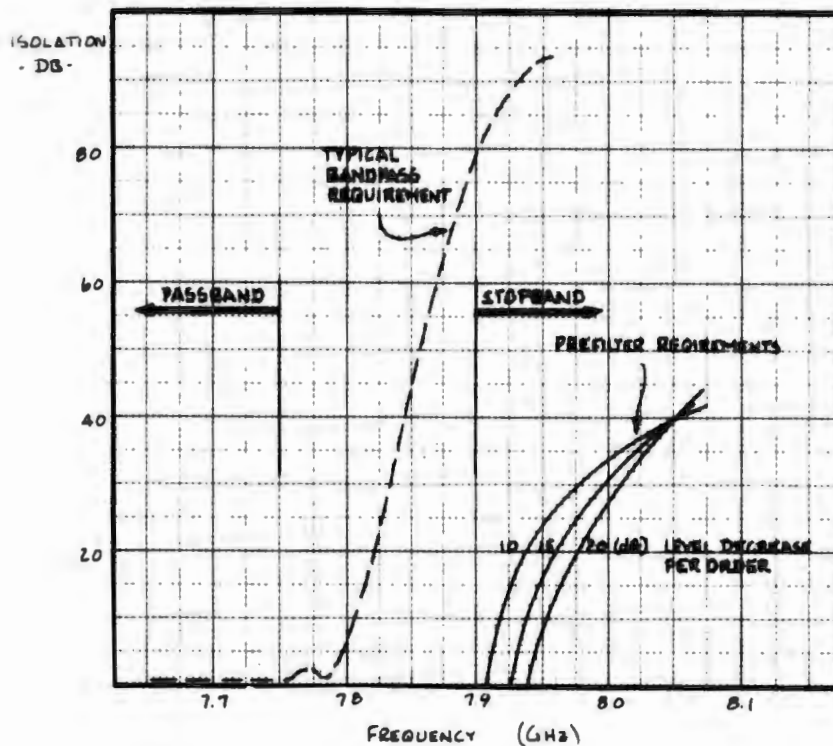


FIGURE 6.3-5 PRE-FILTER SKIRT REQUIREMENTS

[AS A FUNCTION OF HIGHER ORDER IM ROLLOFF (dB/ORDER)]



Using the prefilter concept, three types of units were fabricated: a solid copper machined unit, a segmented aluminum model that was later dipbrazed, and a solid aluminum filter formed by electrical discharge machining (EDM).

6.3.2.1 Solid Copper Lowpass. The solid copper filter shown in Figure 6.3-6 was designed and built solely to demonstrate that the prefilter concept was a viable one. The item was made in two halves after the manner of previous highpass and bandpass filters for longitudinal seams not subjected to orthogonal currents produce no intermods. When first completed on an automatic (tape controlled) milling machine the corners of the transformer sections had a 1/8" radius and produced no IM's. However, when the steps were rough broached to form the square corners shown in Figure 6.3-6 the filter produced its own intermods at the -80 dBm level at 400 watts.

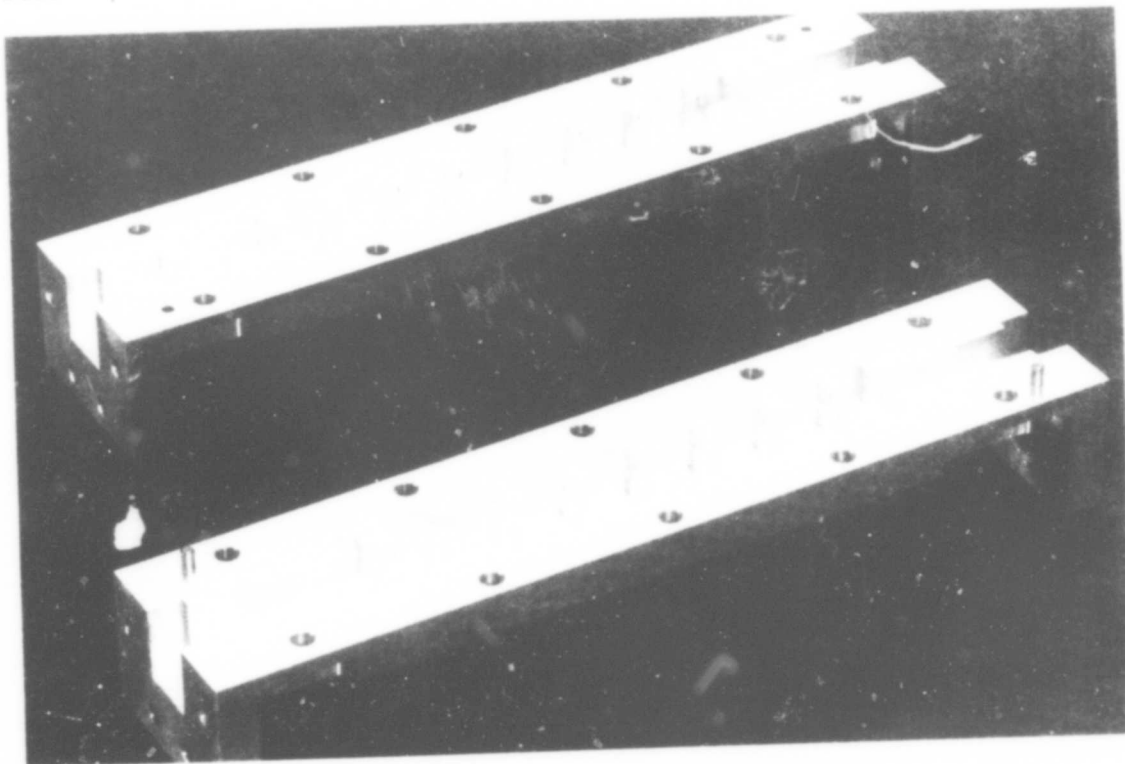


Figure 6.3-6  
Copper Lowpass Filter

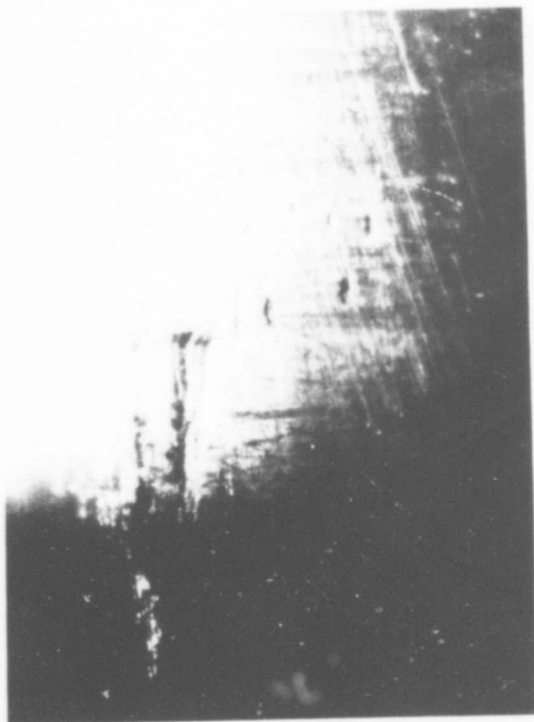
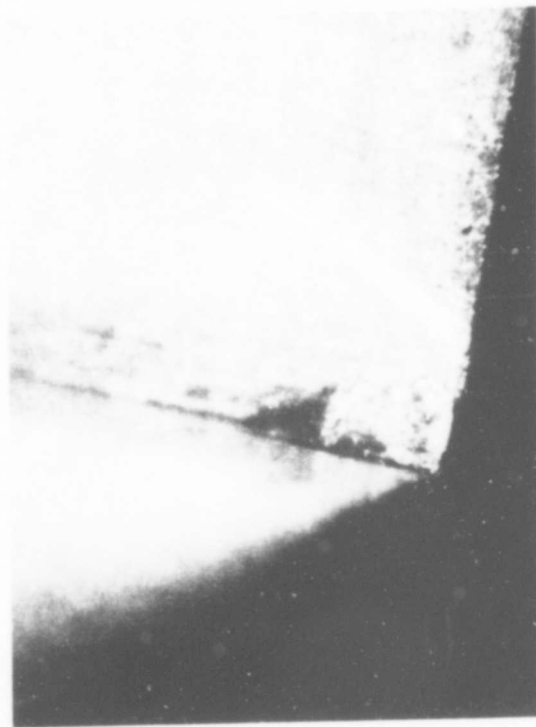


FIGURE 6.3-7  
BROACHED SURFACE TEXTURE

High magnification photographs ( $\times 30$ ) taken of the broached areas reveal not only grooves and scratches, but also small chunks of metal imbedded into copper surfaces. With the broached area in the indicated condition, the intermodulation products were  $-115$  dBm at one end and  $-130$  dBm on the other for 400 watts of power.

Reproduced from  
best available copy.



Thus, intermodulation products are not only produced at obvious seams that surround tuning screws or lie between flanges or parts, but are also produced in solid components wherever the metal is scraped or torn to depths of several skin depths (a skin depth is approximately 25 microinches at 8 GHz). This problem of metal tearing is particularly evident in copper, and appeared earlier as galling on the first press-fit samples (reference paragraph 5.3.2.1).

**6.3.2.2 Aluminum Segmented Filter.** A second lowpass filter was manufactured from aluminum in six separate sections and dipbrazed as shown in Figure 6.3-8. The intent here was two-fold: to simplify the fabrication of a steep skirt (narrow slot) filter, and to verify dipbrazing as a consistently linear method for complex pieces. The first goal was achieved but not the second. As the unit was received from the brazing vendor it produced intermods at the -75 dBm level. Some slag and brazing materials were removed from the cavities by an etching bath and IM's were lowered to -100 dBm; further etching yielded no improvement.

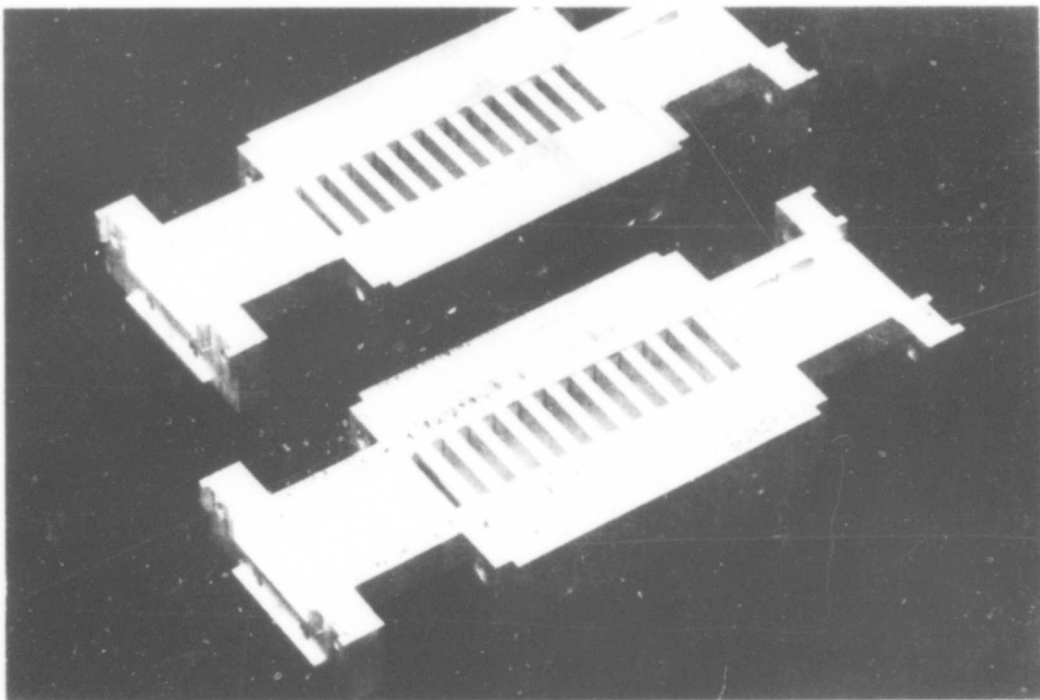


Figure 6.3-8  
Dipbrazed Lowpass Filter

As shown in Figure 6.3-8, the filter was cut in half and examined under a microscope. The end slots contained excess brazing material, and some seams were quite porous as demonstrated in Figure 6.3-9. These results conflict with the satisfactory outcome of the dipbrazed horn tests described in paragraph 5.4.4, partly because of complexity and partly because of the brazing process. It is concluded that success depends upon the cleanliness (or freshness) of the dipbrazing solution and simplicity of the part to be assembled. As an example of the latter, flanges have been dipbrazed and have created no intermods.

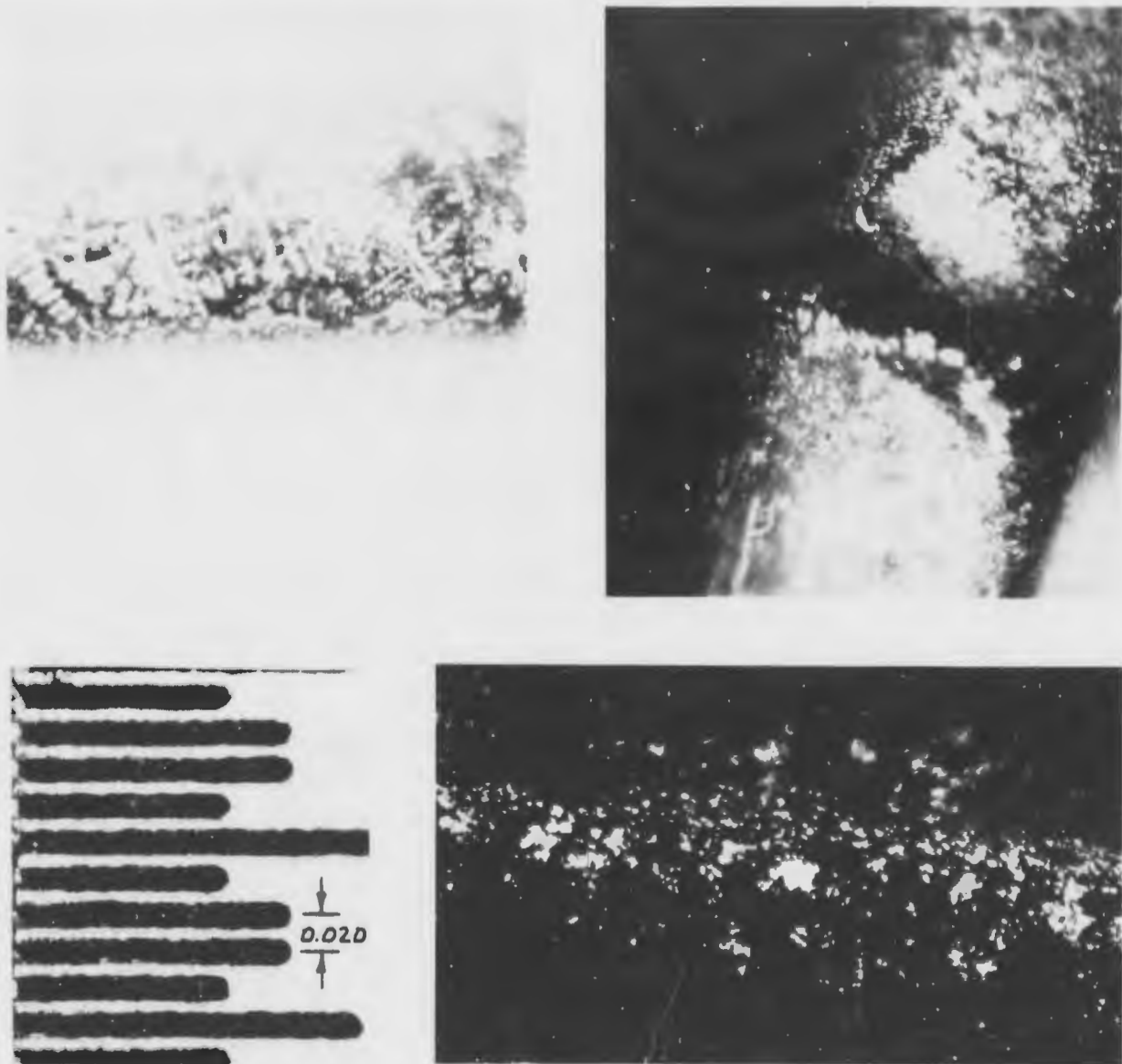
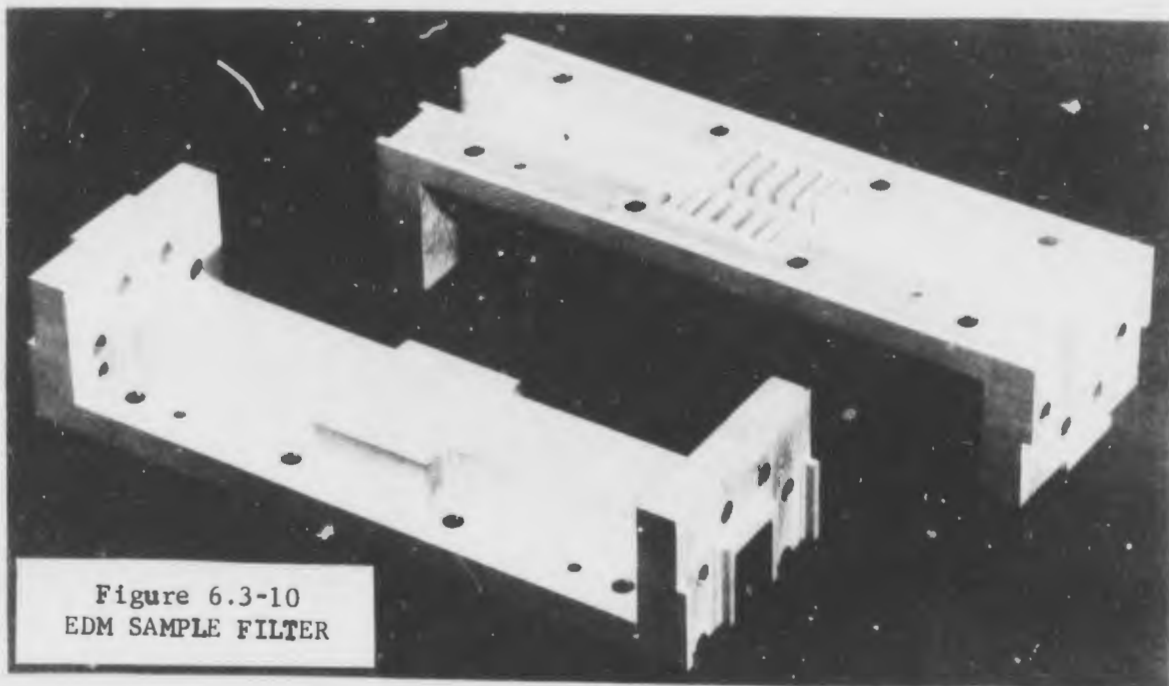


Figure 6.3-9  
Dipbrazing Seams

### 6.3.2.3 EDM Filter

Electrical discharge machining was the third process applied to the low pass filter. Here the device is manufactured from a solid piece of aluminum with the cutting achieved by an electrical discharge or arc. With this process there is no chance of imbedding metal fibres in surrounding material, nor of producing splits or faults in the surface crystalline structure. Furthermore, there are no joints or seams exposed to orthogonal currents (the center seam has no field gradient to excite IM's.) The EDM does, however, leave a matte finish occasionally coated with carbon from interactions between casting, oil and arcs. Tests on the unit shown in Figure 6.3-10 revealed IM's below the 140 dBm for transmit powers to 400 watts, although for these particular tests an IM appeared at about -138 dBm for 600 watts. This small residual is attributed to a particular setup deficiency rather than the EDM process. (The reader should also remember that these filters are typically used in the receive arm, which for any reasonably designed system, is isolated from transmit energy by at least 20 dB. Thus a 10 kw system exposes the receive filter or pre-filter to less than 100 watts of power. If a filter is reliably quiet at this level it will not degrade overall performance. However, if filters of any type are used in the transmit arm other than waveguides below cutoff, full power quieting must be confirmed.)



### 6.3.3 Pin Tuned Filter

The previous exercises with dent-tuned and untuned filters were implemented only because quiet tuning methods were unavailable during the earlier portion of the study. However, since design and manufacturing processes are rarely accurate enough to produce a predictable product and tuning gives the margin of adjustment often required to compensate for inaccuracies, the program to develop linear tuning methods continued. In reviewing previous tuning attempts it was observed that (1) screws often have burrs and coarse surfaces and do not provide continuous full contact with their mating holes; (2) solid press-fit pins create burrs or gall; (3) shrink-fit pins are difficult to remove or reposition and once in place present the same problems as press-fit pins; and (4) collet tuning doubles the potential non-linear sources by adding a second contacting area (but otherwise offers good contact and tuning capability).

To continue the tuning pin analysis and experimentation, three more pin variations were studied: the elastic (hollow) pin, the expanding pin, and the taper pin. The third type had the best theoretical ability to get full contact and was the only one pursued in the experimental phase.

6.3.3.1 The Taper Pin Analysis. Previous flange work and other experimentation indicate that not only must full contact be attempted between mating parts, but that this full contact must have theoretical support in the form of surface pressure/texture relationships described in Paragraph 5.2.4. The problem, then, is one of designing a pin with accurate placement capability, without galling potential, and capable of producing 8000 to 12000 psi over contacting surfaces. The solution is the tapered pin.

For this analysis, a commercial #1 taper pin with a taper of 1/4" per foot was selected and was designed to seat in a tuning hole as shown in Figure 6.3-11. The lower seat is approximately 1/16" long and has a slope of 0.0104 (or  $L/s$  ratio of 96:1). It is assumed that the coefficient of friction is 0.3 (equal to sliding coefficient) because the pin is inserted with impulse forces. Then, as shown in Figure 6.3-11,  $P/2 \approx .3 F$  and the total pressure between seat and pin is

$$S \approx 2F/A = P/.2A = P/.0083$$

and 12,000 psi can be achieved in the limit wher ever impulse forces exceed 100 lbs. are applied (i.e., under these conditions the friction force is overcome and elastic forces are effective).

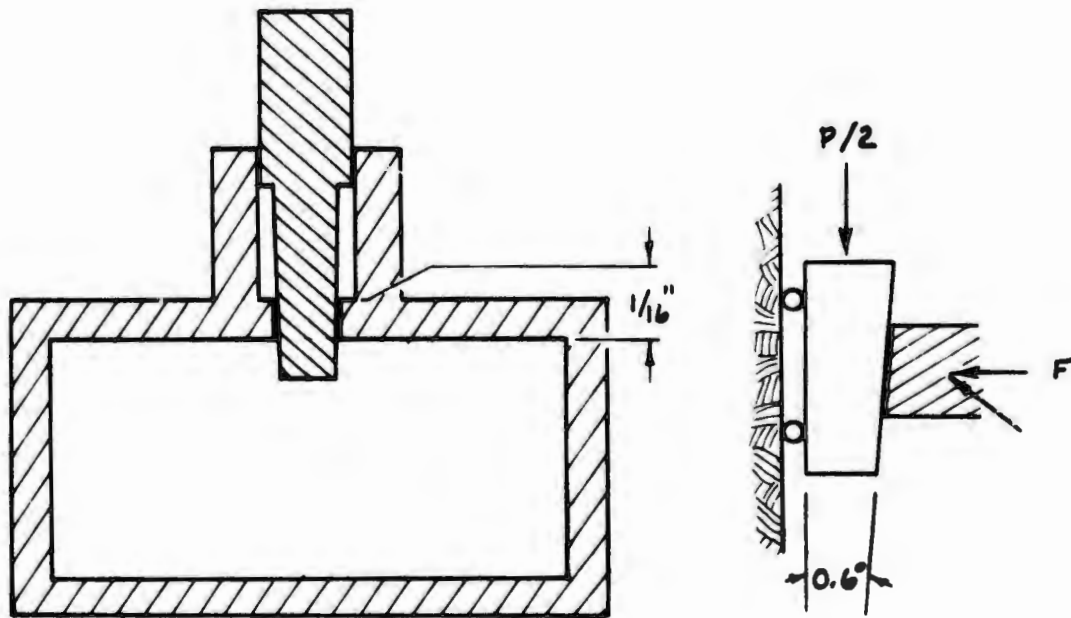


Figure 6.3-11  
Taper Pin Geometry

In order to make the amount of tuning accurately predictable, we need to determine how much wall deflection occurs under 12,000 psi. Assuming the modulus of elasticity of brass or copper to be  $17 \times 10^6$  in./in.<sup>2</sup> then the deflection is given by

$$\Delta = \frac{2rP}{E} = \frac{.141 \times 12 \times 10^3}{17 \times 10^6}$$

$$\Delta = 0.1 \times 10^{-3} \text{ in.}$$

Thus, for a slope of 1:96, the pin must be driven in  $96 \times 0.1 \times 10^{-3}$  or  $9.6 \times 10^{-3}$  beyond its free contact point to achieve the desired pressure. With this knowledge, the filter can be pretuned with free sliding split pins and the sliding pins replaced one-by-one with accurately cut taper pins.

6.3.3.2 Taper Pin Experimentation. To confirm that taper pins could be inserted according to calculations, three waveguide models were fabricated with one, three, and five holes, respectively, as shown in Figure 6.3-12. Strong intermodulation products ( -80 dBm for 200 w) were observed when the pins were inserted lightly, but in general these products vanished when the pins were rapped. Occasionally the IM remained after the pin was securely in place, but for these cases burrs or similar particles were the cause. Sometimes the intermodulation product could actually be "blown out" by blowing into an adjacent (open) hole, which suggests that particular types of free particles in certain areas of the waveguide can cause intermodulation. On two or three occasions a brilliant sustained glow appeared at about 300 watts, behaving like a corona rather than an arc. The glow neither travelled nor affected the power amplifier, left no trace of discharge on the waveguide, but produced the smell of ozone. This phenomena was also attributed to burrs or metallic particles.

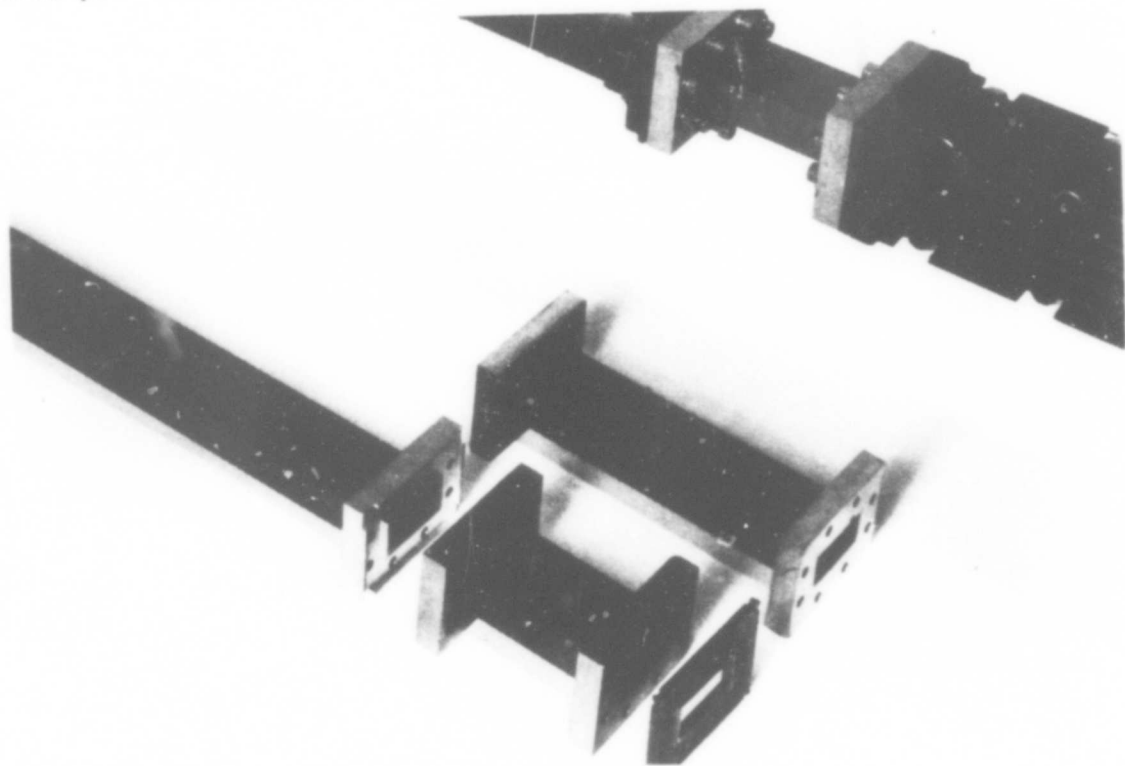


Figure 6.3-12  
Waveguide Taper Pin Models

These pins also demonstrated that 12,000 psi pressure is not always required to quiet a junction if the holes and pins are round to a few micro-inches. This observation is consistent with the conclusions of Paragraph 5.2.4 that a pressure of 546 psi per microinch of surface deviation is required for complete contact, rather than an absolute value. The standard commercial taper pin, shown (in part) in Figure 6.3-13, has a peak-to-peak surface roughness of nearly 0.002 inch with an ellipticity of about the same amount. Under light insertion pressure the commercial pin was not readily quieted, so new pins with 16 microinch or better finishes were fabricated. Original pins were stainless steel with a 500 microinch copper plate on the surface. Later pins were made directly from OFHC copper (not annealed). Once the test waveguide and pins were consistently quiet, the program continued with the actual filter.

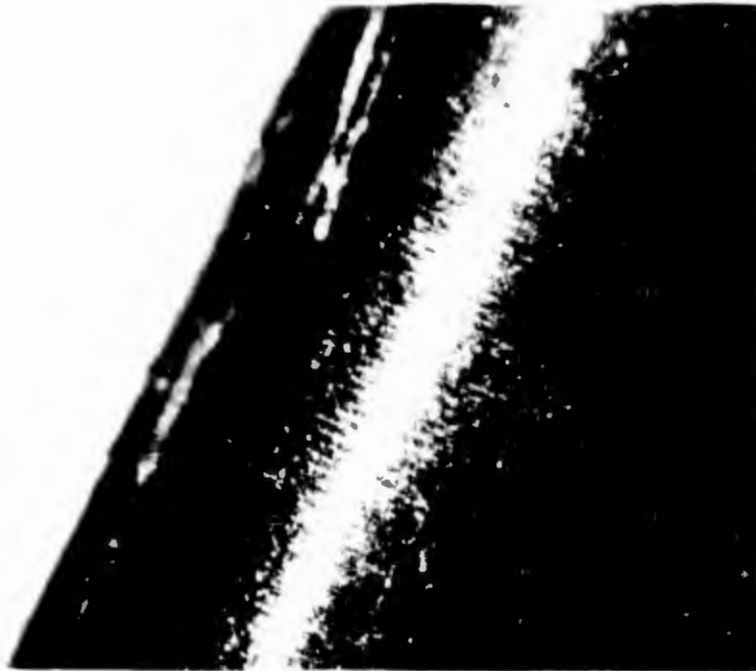


Figure 6.3-13  
Standard Taper Pin Surface Texture



6.3.3.3 Tuning with Taper Pins. Precision taper pins cannot be used alone to tune a bandpass filter because of their limited maneuverability; hence a pre-tuning method was devised. For the 18-cavity filter a corresponding number of split pins were fabricated with locking collars as shown in the foreground of Figure 6.3-14. The pins were slip-fit with sufficient spring action to provide good contact with the tuning hole. The split pins were inserted into the filter and their collars adjusted for normal passband/rejectband response. The lengths of the preliminary tuning pins were then measured and replaced with taper pins of a corresponding length (less approximately 0.015" to allow for seat pressure buildup). The filter with the precision pins in place is shown in the background of Figure 6.3-14. The correct "press-fit" position was achieved with a two-ounce weight dropped from a height of four inches about four times. This tool lies immediately behind the split pins shown in the preceding figure.

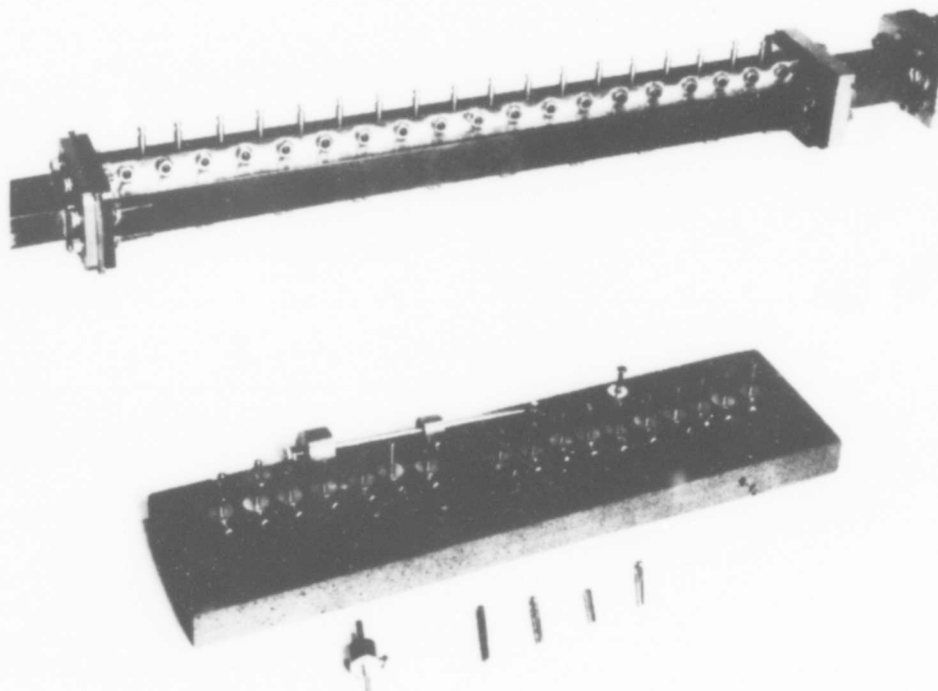


Figure 6.3-14  
Taper Pin Tuning Model

The taper pin proved to be both a reliable and quiet tuning method, with the final filter response as good as or better than could be achieved with conventional screws. Removing and replacing the pins several times did not affect either the tuning response or the linearity, which confirmed that all stresses remained within the elastic limit of the materials. It was further observed that when the filter was properly tuned, pins six or seven cavities from each end had no measurable effect on intermodulation levels for powers up to 600 watts. This observation is consistent with anticipated attenuation of about 5 dB per cavity for the bandpass filter.

The taper pin method appears also to have long term stability in that the filter described above was used in several test setups, both inside and outside, and appears to remain quiet even when left outside for several weeks without the protection of sealed waveguide or coatings. (Although the reader should remember that the Palo Alto climate is mild in terms of corrosive capability and any operating filter or feed should be pressurized with dry air, nitrogen, or other inert gas.)

#### 6.4 Material Tests (continued from Para. 5.7)

The waveguide sections described in paragraph 5.7 were not examined at the time of fabrication because of continuing filter problems. With the reliable taper-pin filter, complete testing resumed.

The waveguide sections were installed in the setup with an accumulated oxide layer equivalent to six months of aging in an air-conditioned/heated environment. Contacting surfaces were wiped lightly with acetone to remove dust and oils, but there was no attempt to remove oxides or polish surfaces. In this condition there were no IMP's observable with the silver, gold, brass, aluminum, cadmium and copper flanges for 400 watts of power and 15-inch pounds of bolt torque. However, the nickel and stainless steel flanges did produce IMP's about -110 dBm at 400 W. A light polishing of the nickel flange removed the intermod but a similar treatment of the stainless flange made no change.

The nickel plated flanges had a coarse (matte) surface, and it is believed that the smoothing or flattening of this surface lowered the IMP, rather than the removal of oxide film. All plated waveguide sections were then polished and checked; again no intermods were recorded. The flanges were exposed to the interior environment for 24 hours (to accumulate angstrom layers of oxide) and again tested; no observed intermods.

For various combinations of materials (i.e., dissimilar junctions) there were also no observed intermods, except in the case of stainless steel. Although steel flanges by themselves or in contact with other metals (e.g., copper) do not always behave non-linearly, there appears to be a greater tendency toward intermodulation production. This susceptibility was noticed both in flanges and timing pin experiments of paragraph 6.3.3.2.

#### 6.5 Additional Higher Order Observations

During the execution of the program, Philco-Ford has occasionally observed and noted levels of higher order intermodulation products beyond the third, even though no specific effort was directed toward that end. The observations

are presented here so the reader is as knowledgeable as Philco-Ford in this area, even though the data is neither consistent nor of sufficient quantity to establish a definite behavior for the higher orders.

The first higher order IM data was taken during the vacuum tests of 24 May 1972, and is recorded in Figure 4.4-3. Since only 10 watts of power were available, a poor flange connection was purposely made to accentuate the IM levels. For the data shown the average change in level is about 13 dB per order.

The next sampling of the higher orders taken from the MSC-46 feed is shown in Figure 6.5-1 where the average rolloff is 16 dB per order through the 7th. Since the 9th order could not be found, it is normally assumed that its level is near the residual noise level of -140 dBm. However, because generator instabilities are multiplied by at least five (9th order consists of a beat between  $5 \times f_a$  and  $4 \times f_b$ ) the signal is harder to find, even though it may be as much as 10 or 15 dB above noise. Since 9th order was observed directly just once, subsequent levels were only implied by its absence.

In comparing Figures 4.4-3 and 6.5-1 it is apparent that a poorly assembled flange subjected to less than 10 watts of power can produce IM's through the 9th order at comparable levels to a well-assembled feed subject to 1000 watts; hence, one must exercise considerable care in feed design and fabrication.

The general rolloff trend continues with tests made on aged bandpass filters utilizing Johansson-type tuning screws. Here there is a 40 to 60 dB decrease between the 3rd and 5th orders and virtually no change between the 5th and 7th orders, as shown in Figure 6.5-2. Again the 9th was not observed. Notice that the slope of the IM level with power is the greatest for the 5th rather than the 7th. The reason for this effect has not been explained yet. The only remaining information about the higher orders is taken from the 5th and is presented here solely as additional data which may permit a better extrapolation of some (as yet undefined) theory. Figure 6.5-3 shows the relative power/IM relationships for the 3rd and 5th orders as taken from an

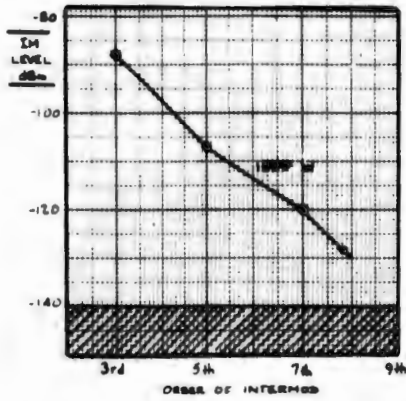


FIGURE 6.5-1 HIGH POWER DATA (MSC 46 FEED)

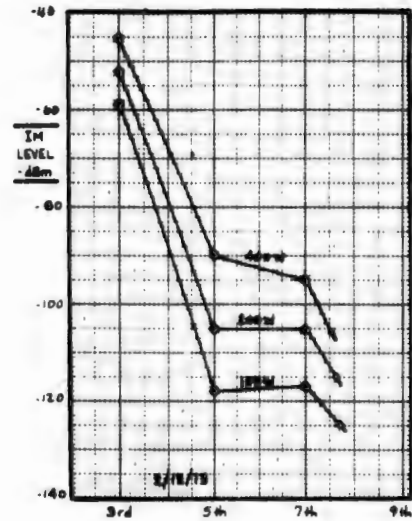


FIGURE 6.5-2 TUNED FILTER LEVELS (HIGHER ORDERS IN AGED FILTER W/CONVENTIONAL SCREWS)

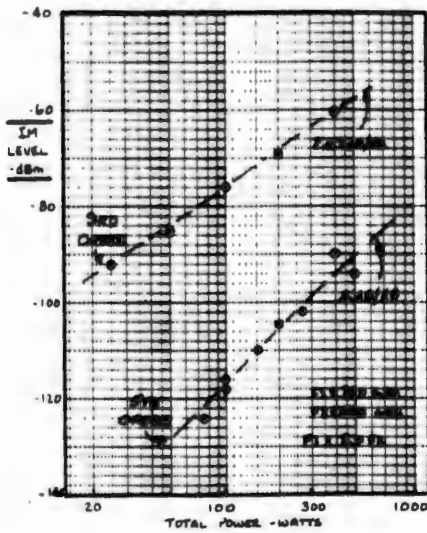


FIGURE 6.5-3 SLOPE OF 3RD & 5TH ORDERS (AGED FILTER W/CONVENTIONAL TUNING SCREWS & LOCK NUTS)

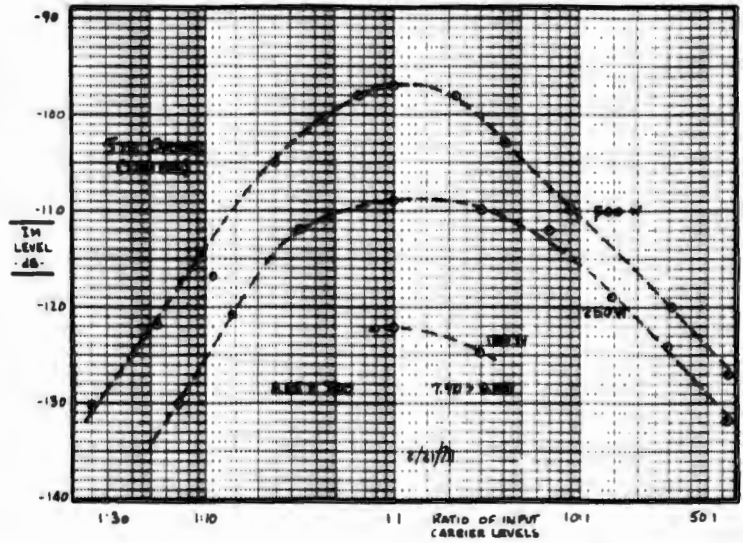


FIGURE 6.5-4 EFFECT OF POWER DISTRIBUTION

Reproduced from best available copy.

aged, conventionally tuned, filter. Figure 6.5-4 illustrates that carrier power distributions of about 1.1 produce the strongest 5th order level, and that previous tests are typically worst case situations.

The foregoing is the total data presently available, and the reader can draw whatever conclusions he feels are reasonable. However, Philco-Ford feels that the extent of testing is insufficient to conclude that the 9th or higher orders are of no consequence to an arbitrary feed system, especially when possible influences of the environment are included. Degradation with time and exposure cannot be estimated for the higher orders when predictions for the 3rd order have not yet been made. The reader should note also that trends established here definitely do not hold in general or JPL would not have been able to observe the 31st order in their reflector tests.\*

---

\* Bathker, D.A., and Brown D.W., "Dual Carrier Preparations for Viking", JPL Technical Report 32-1526, Vol. XIV, pp. 178-199.

SECTION 7.0

INTERMODULATION PRODUCT FREE WAVEGUIDE FLANGE

## 7.0 INTERMODULATION PRODUCT FREE WAVEGUIDE FLANGE

### 7.1 Summary

This section presents the assumptions, design analysis, and test results of a waveguide flange joint that is intermodulation-free to -140 dBm with 2400 watts equivalent power (current maximum) at the flange joint. Models were made of this flange design in copper to copper and in copper to aluminum pairs. The copper to aluminum pair showed no IMP, inert gas leakage, or corrosion of functional surfaces during more than 400 hours of exposure to the standard salt fog corrosion tests.

### 7.2 Assumptions

Tests described in previous sections imply that IMP's are caused by a sharply rough surface, a burr, a crack (negative burr), a poorly (perhaps non-linear E/I) conducting joint, or a combination of the preceding R.F. measurements; have shown that standard flange connections having a surface finish of 60 to 120 microinches and a flatness of one-half thousandth of an inch will produce IMP's of approximately -80 dBm at 5 KW dual carrier input; thereby suggesting a relationship between the order of surface roughness to the R.F. current skin depth (30 microinches in copper for 8 GHz). Since most of the R.F. surface current is in the first 100 microinches of the surface, this value provides one dimensional criteria for R.F. surface roughness and discontinuity that should not be exceeded.

A second assumption is that the waveguide joint be so made that the R.F. skin current will have constant conductivity through the joint as though it were passing through solid copper. This can be achieved by providing a metal to metal pressure at the skin junction that is equivalent to the loading strength of a good conducting metal.

A third assumption is that the conducting surface joint must have full area contact. Because surfaces are not perfectly flat they contact on the high points. To insure full area contact the flange bolt clamping force, the peak to valley waviness of the mating surfaces and the loaded joint areas must be chosen so that all gaps are closed and are under adequate pressure to give "unity" conductance. This defines the surface finish and waviness dimensional constraint.



The fourth assumption is that the loaded joint must retain its IMP-free performance for a long period of time under real life conditions of fabrication; assembly/testing handling; shipping and field environment of acceleration loadings, temperature variations and corrosion elements.

To meet these endurance requirements a design philosophy used in aircraft and structures is employed. A safety factor of  $\approx 4X$  is applied to stress loadings of the flange joint and the clamp bolts to provide for abuse. Additionally, the long term loadings are maintained below the "endurance (fatigue) limit".\* The endurance limit specified the number of cycles of complete reversal of a stress to failure. For copper and aluminum a loading of one-third of yield stress will permit over one billion cycles of flexing without failure. If the waveguide flange joint is made of unannealed metal (copper or aluminum), the loading may safely be 15K psi. This creep of metal with time is of concern because if the waveguide joint loading decreases with time, IMP's are likely to return. It follows that a soft metal gasket that is squeezed in a flange joint so it cold flows to produce full area contact, will be IMP-free at the time of installation. Because its stress loading is at the full yield stress, there is no creep allowance. The metal is critically loaded and there is a high expectation that an IMP can reoccur with time.

The assumptions are summarized as follows:

- (1) A smooth, flat surface is required in order to achieve full area contact, the smoothness to be within 30 microinches, and the flatness to be within 100 microinches.
- (2) The material stress at the pressure-loaded surface should be within the elastic range to provide for long life and abuse. A stress maximum of 15K to 20K is indicated.
- (3) The surface loading must be high enough to achieve equivalent solid metal conductance at the surface current junction. Average loadings of 7K psi to 12K psi are indicated.

---

\* Marks Handbook, 7th edition, pp 5-11, Figure 15 and Table 7.

### 7.3 DESIGN APPROACH

A flange face is a fabricated surface. It never is "perfectly" smooth or flat. When two surfaces are brought into face to face contact they initially touch on high points. A considerable portion of the interfacing area is not in metal to metal contact. If external pressure is applied to force the surfaces together, the contact area will increase following the rules of elastic/compressive behavior. Full area contact may occur if the "bumps" are not too high and if loading can be applied uniformly to the entire area. When the "bumps", peak-to-valley, are too high for elastic range<sup>3</sup> full contact, further loading will result in "cold flow" and full area contact may occur if the metals of the flange are sufficiently plastic; otherwise, the metal surface will break, probably in shear.

A concept of material behavior in real flange faces is developed. The bumps are considered in two size classes:

- (1) Surface roughness in the microinch scale ( $\mu$ ").
- (2) Surface waviness and flatness.

Surface roughness of fine machining has rms height values of 60 to 8 micro-inches. The pitch or spacing of the peaks is correspondingly small and in the region of 100 to 10,000 microinches. These irregularities are essentially scratches.

Waviness typically has peak to valley values of approximately 100 to 5000 micro-inches and the pitch will be typically one-half wave per flange face dimension. Figure 7.3-1, "Curved Flange Face", shows the concave configuration that results from certain machine operations and from release of clamp loads after machining, welding, or heat treating. The convex surface, opposite to that pictured, results from poor lapping and from excessive torque loads at joint while installed.

Figure 7.3-2, "Mating Surface Geometry", shows the general case of surfaces bearing on each other. Figure 7.3-2(A) with peaks in contact would require the most load to make valleys contact. Figure 7.3-2(C), having amplitudes

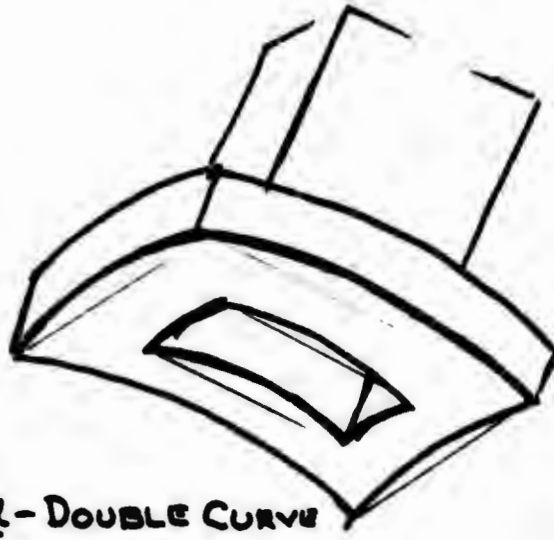
match and positions opposite, has full face contact at initial "zero" load, and is most desirable, but most unlikely. Figure 7.3-2(B) is the in-between case. Figure 7.3-2(D) is an analytical model of Figure 1(A), having same loads and deflections per surface.

Applying the Figure 7.3-2(D) to the surface roughness model, the P/V value is small and the pitch is short. The slope of the "scratch" can be high and orthogonal flow of material may occur. Figure 7.3-3, "Rough Surface Contact", shows types of surface profiles with micro "bumps". Figure 7.3-3(C) represents a worst case and is used for analysis. The area ABD is moved down when the flat plate moves from "start" to "land" position. The volume represented by ABD reappears at AEF, except for a portion lost to compressibility.\* The compressibility of the metal requires that the flange deflects about 10% more to full seating. If the P/V roughness is 20 micro-inches, seating will occur at  $\cong 11$  microinches deflection, per Figure 7.3-3(C).

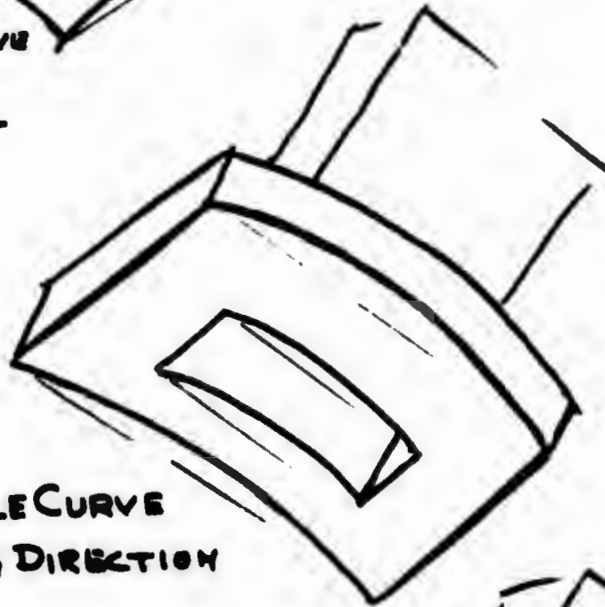
The unit load on surface FD due to Load P is represented by the ratio of the area ABD to area BDFG, and is  $.25 K_1 \times \Delta S$ , where  $K_1$  is the spring constant of the flange load bearing surface and  $\Delta S$  is the deflection. In this flange face design the elastic length of the spring is chosen as 0.10". It follows that the flange spring constant  $K_1$  in copper is  $170 \times 10^6 \times K_1 = 1870$  psi; and the average area stress on surface FD is  $0.25 \times 1870 = 467.5$  psi. The significance of these small loadings is that, if the roughness is small compared to the waviness amplitude, the waviness will determine the loading required to make full area contact. A second implication is that in the waviness analysis the orthogonal material flow will not occur appreciably. An analysis model is developed for the condition of "waviness" in Figure 7.3-4, "Waviness Surface Load Model". Figure 7.3-4(A) shows an element area treated as a linear spring with a constant of  $K_1$ . Figure 7.3-4(B) shows the apparent loading to be a function of one-half times the P/V,  $\Delta h_1$ , when the waviness is a continuous ridge. If the waviness were pyramidal (or conical), the apparent loading (to full area contact) would be a function of one-third (or less) of the deflection. The continuous ridge shape of waviness will be used because its higher apparent loading to seating is a worst case. Figure 7.3-4(C) develops the conditions of maximum unit loading,

---

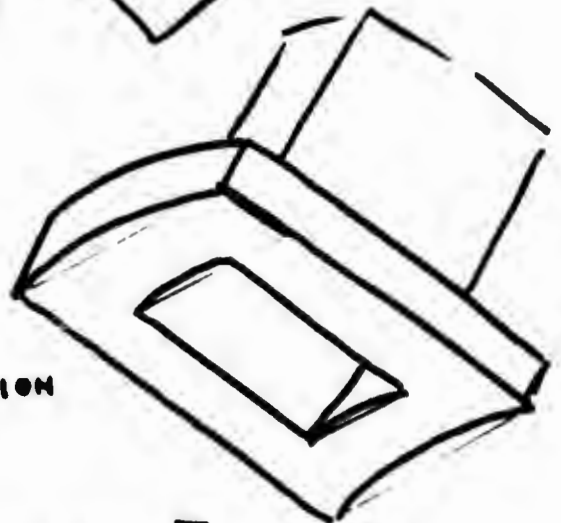
\* Poissons ratio ( $\mu$ ) of Cu. is 0.355 per Mark's Handbook VII, p.5-6, and Volume of AEF  $\cong 2$  ABD  $\cong .71$  ABD.



Q - DOUBLE CURVE  
OR  
SPHERICAL

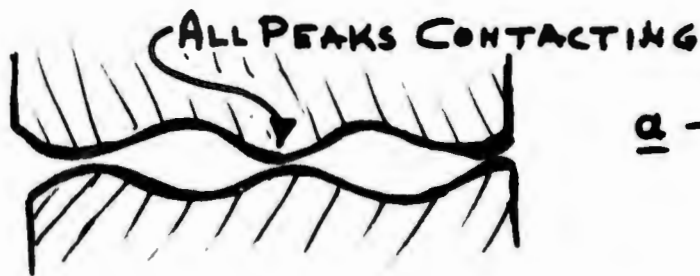


b - SINGLE CURVE  
IN LONG DIRECTION



C - SINGLE CURVE  
IN SHORT DIRECTION

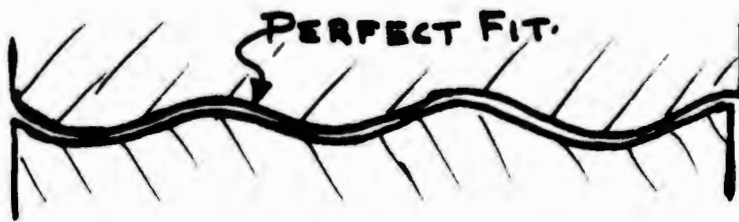
FIG 7.3-1 - W/G FLANGE FACES  
CURVED



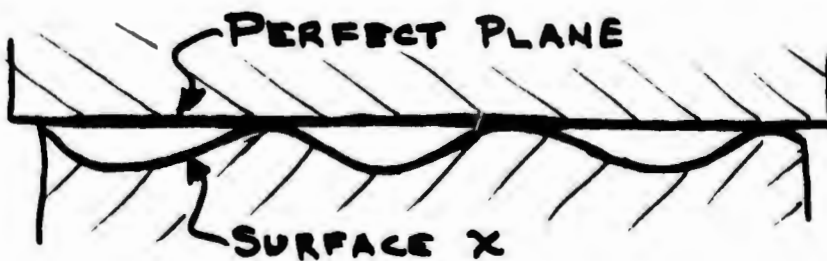
a - SAME PITCH  
OUT OF PHASE  
WORST CASE DEFLECTION



b - DIFFERENT PITCH  
DIFF. PHASE  
MEDIUM CASE DEFL.



c - SAME PITCH  
180° PHASE  
LEAST DEFL.



d - ANY PITCH AGAINST  
FLAT.  
EQUIV. TO CASE "a".  
USE THIS FOR  
LOAD ANALYSIS.

FIG. 7.3-2 - MATING SURFACE GEOMETRY.

IMPfree  
W<sub>y</sub> FL



a. REGULAR SURFACE



b. RANDOM SURFACE

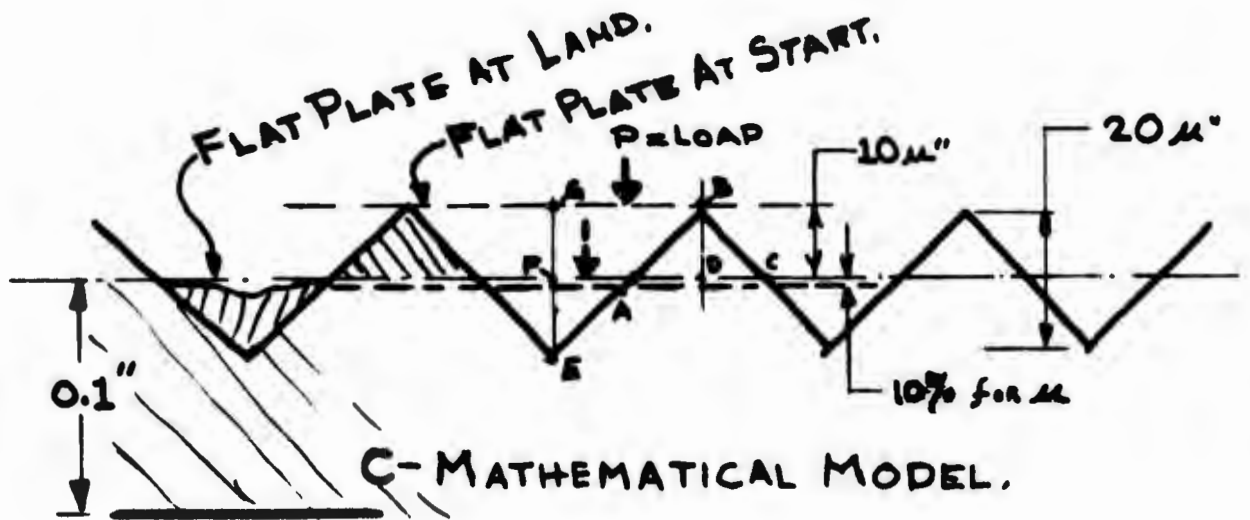


FIG. 7.3-3 ROUGH SURFACE ELASTIC BEHAVIOR

$$S_{\max} = K_1/A (\Delta h_1 + \Delta h_2)$$

Equation 1

occurring at the peak of the surface wave; and the minimum unit loading,

$$S_{\min} = K_1/A \Delta h_2$$

Equation 2

occurring at the low point of the surface. The average Unit Loading is

$$P_2/A = S_{\text{av}} = K_1/A (\frac{1}{2} \Delta h_{1(\max)} + \Delta h_2)$$

These three equations show that the lower the spring constant "K" of the flange seat the greater is the surface irregularity that will contact metal to metal for a given compressive loading. The geometric configuration of the flange seat profile should be such that the "K" is reduced to a practical tradeoff with area, loading, bolt configuration and fabrication feasibility.

Now consider the prevailing flange of MIL-F-3922/52 shown in Figure 7.3-5. If the full face contact is used, the area is

$$\begin{aligned} A &= (2.69 \times 1.94) - (1.372 \times .622) - 8 \text{ holes \& corner R} \\ &= 4.08 \text{ square inches} \end{aligned}$$

Assuming a minimum face loading of 7K psi, the load per bolt (there are 8 - #10-32 bolts) is:

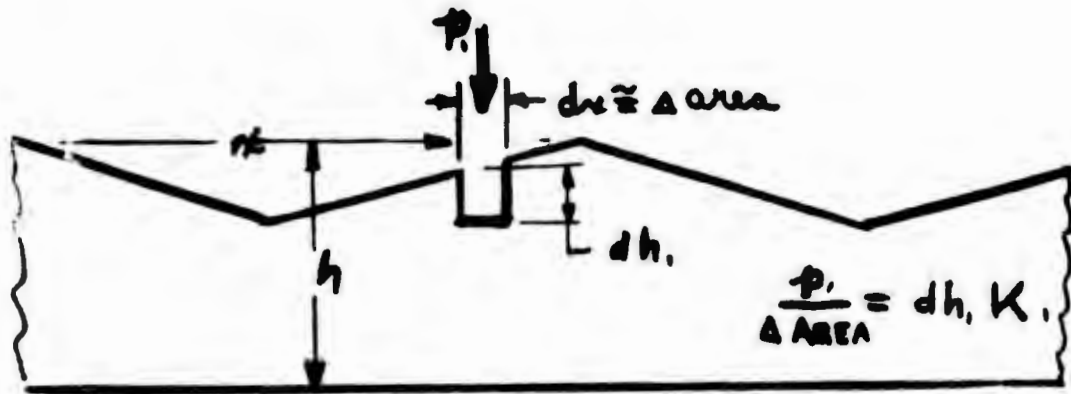
$$L = P \times A \times 1/N = 7K \text{ psi} \times 4.08 \times 1/8 = 3570\#$$

and bolt stress is  $P/A = 3570/.02 = 178,500 \text{ psi}$ .

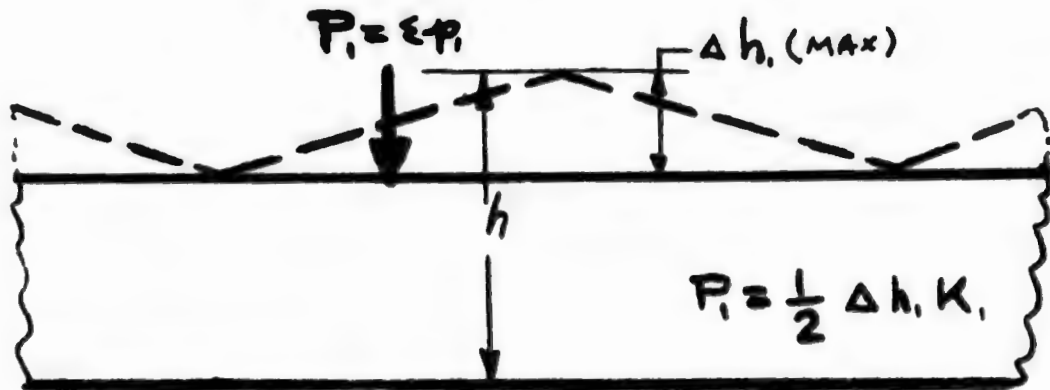
The 178K psi stress is over 4 times greater than desired. The SAE #5 grade bolt has a proof load stress of 85K psi. The preload for the bolt should be half or less of proof stress so that there is a safety factor of more than two and a structural integrity safety factor of  $\cong 4 \times$  against the 120K psi tensile strength.

In order to reduce the loading on the bolts, the flange seat area may be reduced to a narrow seat (0.1" wide) about the R.F. aperture and an equal load balancing area about the flange face periphery, as shown in Figure 7.3-5, as "Optional Raised Seat".

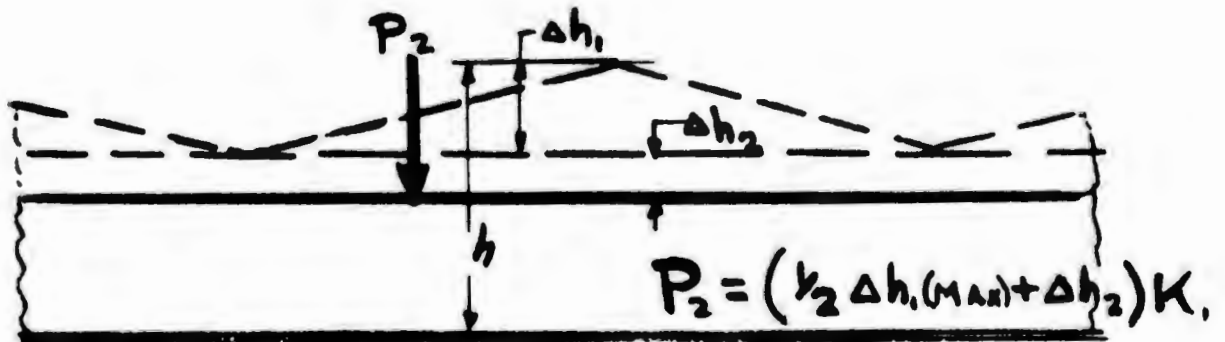




**A - AN ELEMENT LOAD.**



**B - LOAD FOR TOTAL SURFACE CONTACT.**



**C - LOAD FOR TOTAL SURFACE CONTACT WITH HIGH PRESSURE.**

**FIG 7.3-4 WAVINESS SURFACE LOAD MODEL.**



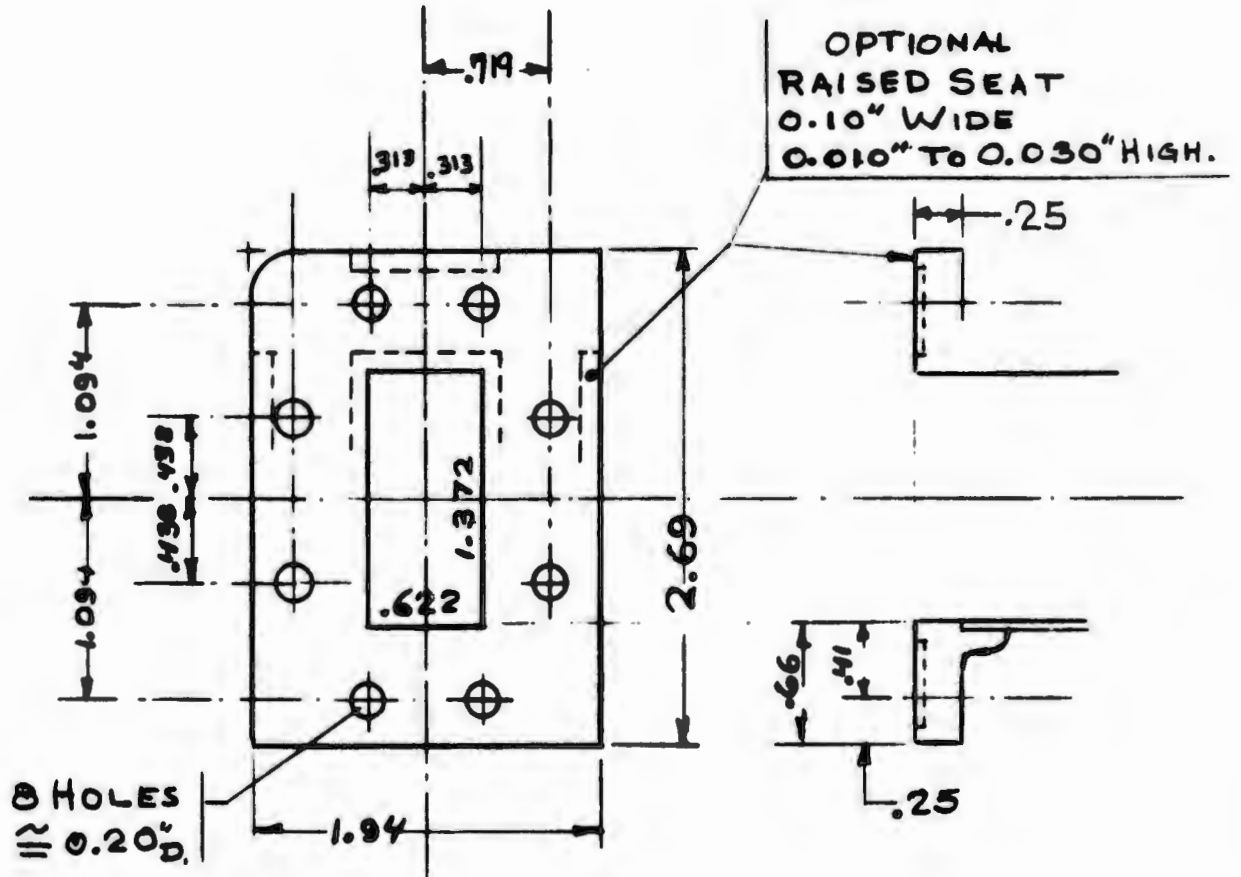


FIG 7.3-5 - FLANGE GEOMETRY  
 (PER MIL F 3922/52 WR 137 SIZE.  
 FLAT FACE - ALSO RAISED SEAT)

AREA OF FULL FACE = 4.08  $\square$

AREA OF RAISED SEAT = 3.88  $\square$

Now, if the flange seat loading is raised to its maximum capability of 50K psi, as might occur momentarily in a field condition, the bolt stress would be a calculated 275K psi (See Appendix I), which is over 2 times of the 120K psi listed for SAE Grade 5 bolts. Appendix I then shows that the flange stress in the net section between bolts becomes a calculated 96K psi, which is  $\cong 2$  X of the 50K psi for unannealed electroformed copper (or the  $\cong 60$ K psi for unannealed brass). Since most brass flanges are "silver soldered" to the waveguide, the yield point of the flange is reduced to the region of 10K psi, or "dead-soft". (This accounts for the many convex flanges discovered after disassembly.)

Appendix I, Figure I(A) and Figure 7.3-5, show that the bolt load is distributed unevenly between the R.F. seat and the outer seat. 64% (.36/.56) of bolt force goes to the outer seat and 36% (0.2/.56) is on the inner seat. This is unfortunate because the inner seat that is R.F. functional needs the pressure.

#### 7.4 DESIGN ANALYSIS

This structural/functional analysis showed that the MIL-F-3922/52 - WR-137 flange has the following shortcomings if it is used in the USASCA HT/MT low IMP system:

- (1) The flange plate is too thin, and when heated during brazing it is further weakened so that high mechanical pressures cannot be attained at R.F. junction. The net section and the metal hardness are inadequate.
- (2) This lack of pressure capability makes it unlikely that existing flange seat waviness can be seated elastically to produce mating flange metal to metal contact.
- (3) The bolt loads are excessive.
- (4) The flange profile is such that bolt holes are placed too near the outer periphery, causing the bolt clamp load to go predominantly to the outer--non R.F.-- seat of the flange.

- (5) Three dimensionally critical parameters are not adequately specified.
- (a) The flange face finish and waviness.
  - (b) The waveguide aperture tolerance that permits a step joint.
  - (c) Waveguide aperture alignment by some mechanical means to reduce step joint.

An improved flange concept is shown in Figure 7.4-1. It attempts to reduce the above shortcomings:

#### 7.4.1 Flange Thickness

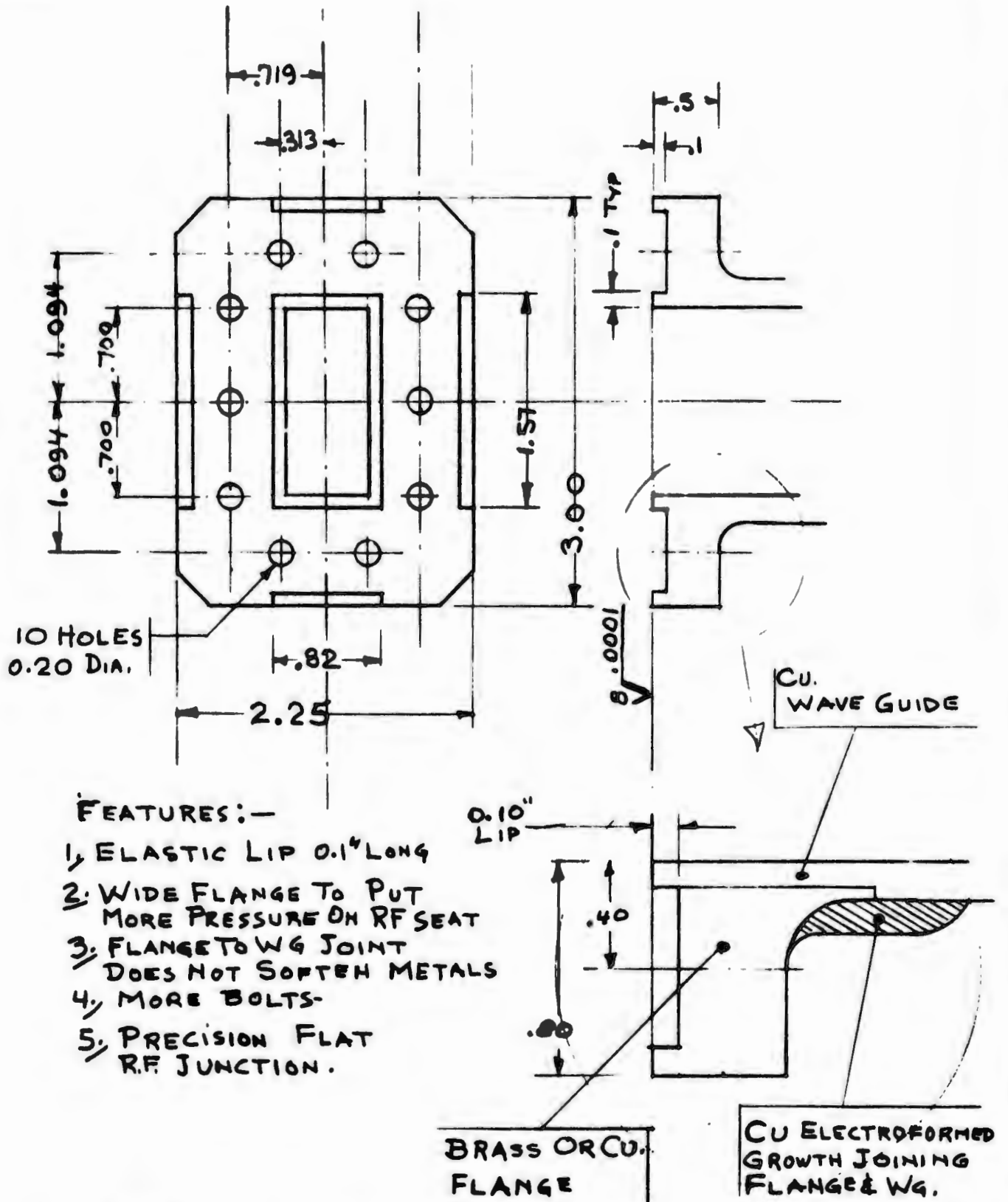
Flange thickness is increased from 0.25" to 0.50". The stress in flange net section with maximum compressive load on R.F. seat is  $\cong 63K$  psi (See Appendix II). This is satisfactory and matches the  $S_y$  of flange brass material of 60K psi if the flange is not softened by brazing. Figure 7.4-1, Section A, shows a machined flange joined to high strength (50K psi minimum) copper waveguide. No brazing temperatures are applied that would soften and weaken copper alloys. Design values of 50K psi for copper electroformed high-conductivity material can be used. In brass the design  $S_y$  can be 60K psi or higher.

In aluminum, if 6061 alloy is used, the joint may be brazed and the assembly heat treated to an  $S_y$  of 40K psi.

With the 0.4" thick flange and the electroformed joint of flange to waveguide, the flange net load capacity can provide 50K psi to the R.F. seat and a 2X loading to the ten clamp bolts (Appendix II).

#### 7.4.2 Surface Pressure and Flatness

Pressure capability to produce metal to metal contact, the following flange seat configuration is used. (See Figure 7.4-1). The 0.10" wide seat, having an area of 0.88 square inches is made as a column 0.10" high, so this column length provides elastic deflection to permit metal to metal seating. Figure 7.3-4(B) provides the loading equation



FEATURES:-

1. ELASTIC LIP 0.1" LONG
2. WIDE FLANGE TO PUT MORE PRESSURE ON RF SEAT
3. FLANGE TO WG JOINT DOES NOT SOFTEN METALS
4. MORE BOLTS
5. PRECISION FLAT R.F. JUNCTION.

FIG. 7.4-1 - IMP-FREE WG. FLANGE (WR-137 SIZE)

$$P = \frac{1}{2} \Delta h_1(\max) \times K_1$$

to produce valley seating.

With the 0.1" high seat and an area of 0.88" in copper or brass, the  $K_1$ , spring constant of seat, will be

$$K_1 = E \times \text{Area} \times 1/\text{length}$$

$$K_1 = 17 \times 10^6 \times 0.88 \times 1/0.1 = 1.496 \times 10^8 \text{ \#/inch}$$

Now assume the waviness to be 0.0001" =  $\Delta h_1$

$$P_1 = \frac{1}{2} \times .0001 \times 1.496 \times 10^8 = 7480\#$$

Stress =  $P/A = 7480/.88 = 8500\#/\text{square inch}$  - average loading

peak stress - 17,000 psi

minimum stress = 0

These loadings are well within the elastic limit of brass (60K psi minimum) that the flange peripheral seat is made of. By applying a 3K psi added force, the minimum clamp force is 3K psi and maximum is 20K psi.

The principal features of the new flange design are:

- (1) The elastic lip concept
- (2) The structural joining of the flange and waveguide in copper (alloys) without application of heat.
- (3) The precision lapping of the R.F. seat

This precision lapping provides a very smooth finish, better than 8 micro-inches, and an extremely flat surface well under 100 microinches. A surface that is machined with a mill cutter or by a fly cutter may be very free of waviness, but it is not sufficiently smooth. A ground surface has ripples and roughness. A surface "lapped" flat using emery paper over a smooth flat plate has rounded edges because of the elasticity of the paper backing and because of the rolling action of grit particles.

The "lapping" used here is the true mechanical lapping wherein a very flat cast iron or marble surface is the lap. The cutting is done by very small particles of the order of 10 microinches. These may be levigated alumina, perhaps 12 microinches ( $0.3\mu$ ) in size; rouge (iron oxide); synthetic

sapphire; etc. For soft metals such as copper and aluminum alloys a friable grit is used, suspended in a water or kerosene solution. The technique of lens polishing is employed wherein the abrasive breaks down with use and solvent only is added to thin the cutting mixture.

Because a polished surface is produced on the 0.10" wide lands, visual inspection with simple lighting reveals untouched surface areas and edge rounding. A surface appearing essentially scratch-free to the eye must have its largest irregularities, or scratches, considerably smaller than one-half wavelength of visible light ( 20 microinches).

If cast iron lapping plates are brought to a flatness of better than 0.0001" in sets of three, and they are about 1½X or 2X the size of the flange, the plates can be lapped against each other in the proper sequence to improve the flatness and to retain flatness with use.

A natural consequence of the metal to metal seat contact is that if it is IMP-free it must also be sealed to gas leakage. The gas holding capability will be 3000 psig if the R.F. surface has a minimum pressure of 3K psi. The flange is at  $\approx 25\%$  (11.5/50.0) of its yield capability.

#### 7.4.3 Bolt Loading

The bolt loads are excessive. By reducing the seat area to 0.88 square inches and the flatness to under 0.0001" and the minimum seat loading to 3K psi. The total bolt load is:

$$\begin{aligned} L &= \text{stress} \times \text{area} \times 1/N & N &= 10 \text{ bolts} \\ &= 11.5K \times .88 \times 1/10 = 1012\#/ \text{bolt} & A &= 0.88 \text{ sq. in.} \\ \text{Stress} &= L/A = 1012/.02 = 50,600 \text{ psi} \end{aligned}$$

This is under the 75% of 85K psi, and is less than ½X of the 120K psi ultimate for the bolt.

#### 7.4.4 Flange Profile

The flange profile with major seat pressure loading on outer non-R.F. seat-- the flange profile has been increased to 2.25 x 3.00 inches so the bolts

are located midway between the inner and outer seat (See Figure 7.4-1). The loading is uniform, the joint moment strength has been increased, and the safety factor improved.

Moment Load Capability of Joint. Materials at Yield -

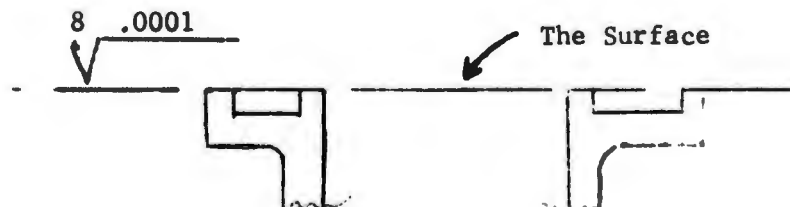
<u>M-Axis</u>	<u>Raised Seat</u>	<u>10 Bolts</u>	<u>Waveguide - Copper</u>	
			<u>.062 Wall</u>	<u>.150 Wall</u>
X X	1480 ft. #	876 ft. #	417 ft. #	1122 ft. #
Y Y	906 ft. #	495 ft. #	273 ft. #	738 ft. #

Perhaps it is preferred that the bolts, rather than the flange, go into failure in case of large overloads, so as to spare the more expensive component.

7.4.5 Three Dimensionally Critical parameters:

(5a) Surface finish and waviness

The drawing will be made to specify a surface finish of better than 8 micro-inches and a waviness of better than 100 microinches by using the ASA B46.1-1962 Surface Texture symbol:



Experience to date with lapping has shown that these tolerances are practical and that uninitiated personnel can be trained to perform the operation. The laps and the process have been chosen so that flange lapping can be done in the field.

(5b) Waveguide Aperture Tolerance relative to step mismatch:

This area has not been adequately studied. Even though intended offsets of about 0.005" have produced no measurable deterioration of IMP level. It is suggested that where machined flanges or electroformed waveguide parts contain the flange-face matching apertures, that the tolerance be reduced from  $\pm .003"$  to  $\pm .001"$ .

Future work should include experimentation with cold-press sizing of the aperture with a combination tool that will include provisions for producing the aligning means for item 5c.

(5c) Mechanical Aligning Means

A pair of pins passing through the joining flanges is simple. Taper pins would be more precise.

7.5 Experimental Results

Models of the "Hi Pressure-Elastic-Full Area Contact" flange were made to the dimensions shown in Figure 7.4-1. Two were made of electroform copper and brass flanges, and one was made of 6061-T6 aluminum as pictured in Figure 7.5-1, "Three Models of IMP-Free Flange". The extreme right and left models have the new flange design facing forward. The center model has the standard flange showing. The models were made with a standard flange on one end so they could be installed into the IMP measuring R.F. test. The polished contact surface is apparent in the two models. Figure 7.5-2, "IMP-Free Cu Flange", is a close-up view of the new flange.

Figure 7.5-3, "X-Band IMP Measuring Test Setup", shows only that portion of the waveguide run in the test setup that would contain the test specimen. To the extreme left is an IMP-free bandpass filter. To the extreme right is a finned highpass filter that is IMP-free. The specimen in this picture is a pin-tuning bandpass filter having a short section of waveguide to its right. The hole in the waveguide permits inserting a point disturbance into the R.F. passage to deliberately produce an IMP to verify system operation and tuning when it is "quiet".

Figure 7.5-4, "IMP Flange Junction of Cu & Alum During Salt Fog Test", shows a flange pair model, and companion control models, in the chamber. Figure 7.5-5 shows the model just removed from the chamber. The center R.F. joint--the new IMP free flange--is never disassembled during the 418 hours of salt spray. The outer flanges are sealed with a rubber gasket and the cover plates contain brass petcocks to charge the assembly with dry nitrogen gas to a pressure of 1.5 psig. At intervals of one, six and seventeen days



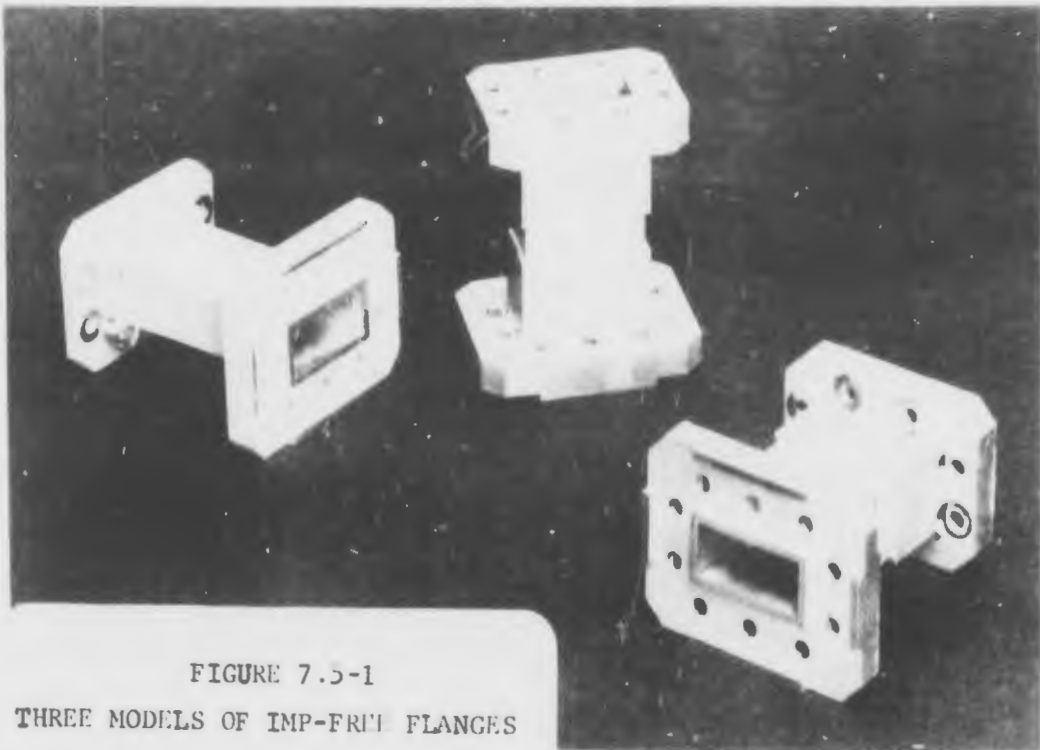


FIGURE 7.5-1  
THREE MODELS OF IMP-FREE FLANGES

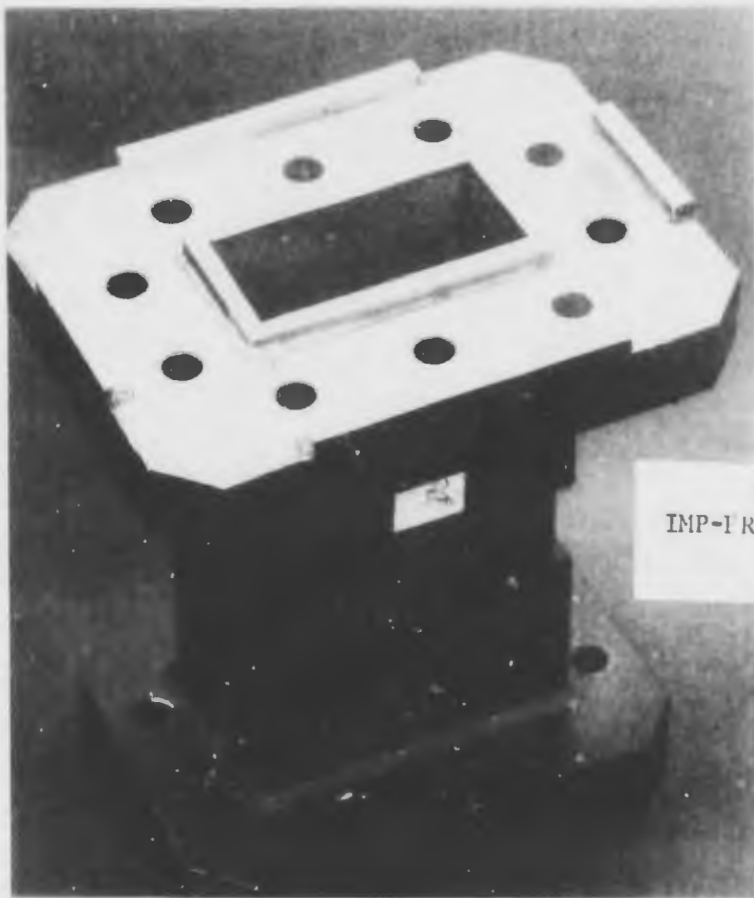


FIGURE 7.5-2  
IMP-FREE COPPER FLANGE

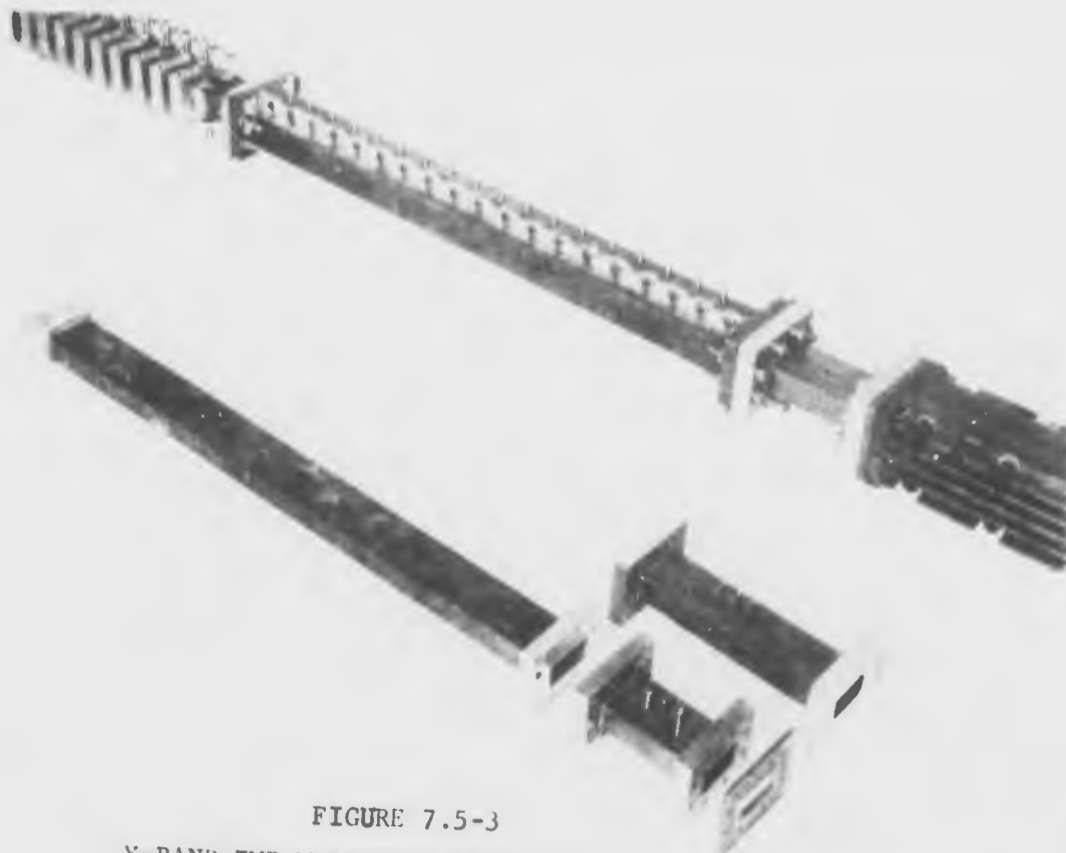


FIGURE 7.5-3  
X-BAND IMP MEASURING TEST SETUP

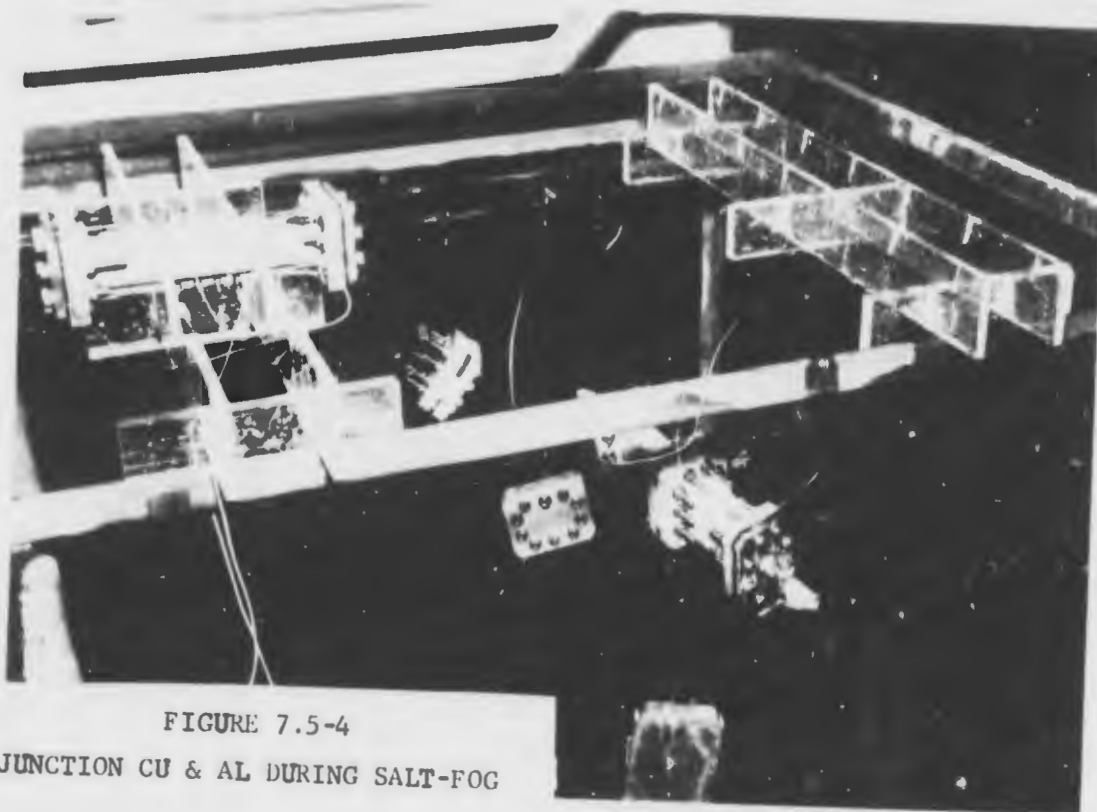


FIGURE 7.5-4  
JUNCTION CU & AL DURING SALT-FOG

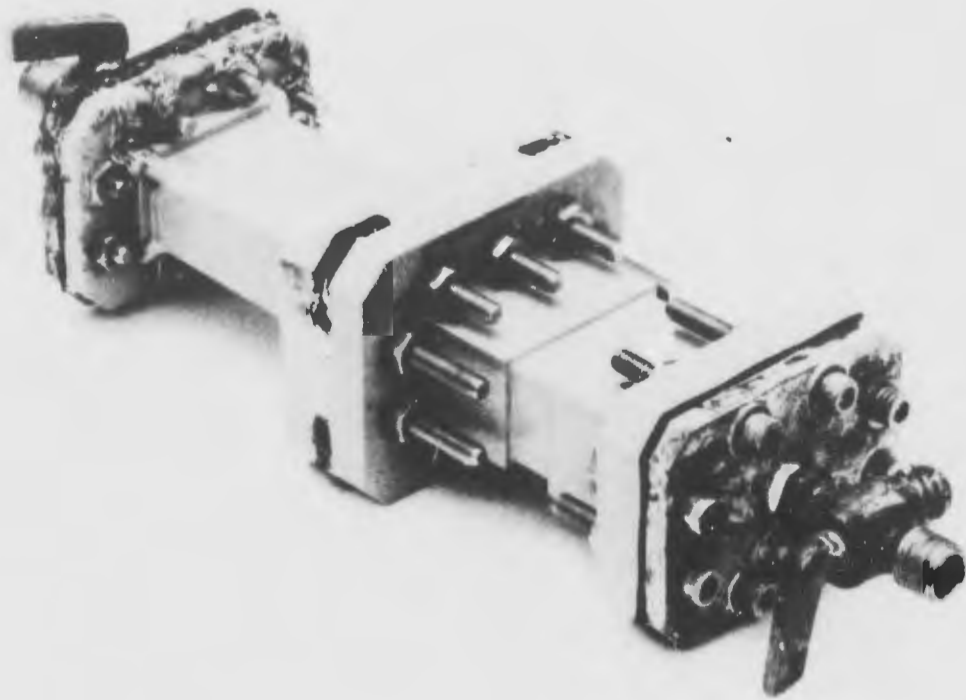


FIGURE 7.5-5  
CU TO AL FLANGE MODEL FROM  
SALT CHAMBER

the unit was removed from the chamber, rinsed with clear water, and dried; then end plates were removed and IMP measurements made. There was no degradation in IMP performance. Figures 7.5-6 and 7.5-7 show the disassembled aluminum and copper flange faces after the salt-fog test. The polished seat surface showed no deterioration of finish. The color appeared to be grayish compared to its initially lapped appearance. After each removal from the chamber, the noise "hiss" of escaping  $N_2$  was strong when the petcock was opened.

During the initial bench IMP testing of the copper to copper and copper to aluminum flanges, it was noted that an initial assembly was immediately IMP-free with bolt torque loads as low as five-inch pounds. As the torque was increased in steps of 5 to 10, 15, 20-inch pounds, there was no IMP generated. When bolts were progressively loosened, there was no IMP until torque load was under 5 inch lbs. A torque of 5-inch pounds on each of the ten screws will produce approximately the following average unit load on the R.F. seat.

In the equation for torque load vs clamping force, if a coefficient of friction of 0.2 is assumed

$$\begin{aligned}
 T &= KF & \text{where } T &= \text{Bolt (on nut) torque inch pounds} \\
 T &= 5" \# & F &= \text{Clamping force of nut/bolt in pounds} \\
 F &= t/.0486 = 102.88\# & K &= \text{Constant depending coefficient of} \\
 & & & \text{friction; thread geometry; metal pairs} \\
 \text{and RF Seat Load is -} & & & \text{and lubrication. } X \text{ is typically =} \\
 & & & .048L \text{ for a \#10-32 thread.} \\
 S_c &= \frac{10F}{\text{Seat Area}} = \\
 & \frac{10 \times 102.88}{.88} \\
 & = 1169 \text{ psi at RF seat}
 \end{aligned}$$

Working back from the 102.88# clamp force per bolt and using  $P = \frac{1}{2}K$ ,  $h_1$ , we can solve for a maximum  $h_1$  by assuming the "valley" just contacting.

---

\* "Bolt Torque Factors", R.H. Lipp, Design News, March 8, 1971



FIGURE 7.5-6  
AL FLANGE AFTER 418 HOURS SALT-FOG



FIGURE 7.5-7  
CU FLANGE AFTER 418 HOURS SALT-FOG

$$H_1 = \frac{P}{4 K_1} = 13.7 \times 10^{-6} \quad K_1 = 1.496 \times 10^8$$

$$\text{or} = 14 \text{ microinches} \quad P = 10 \times 102.88\#$$

This implies that the lapping has produced a surface of this flatness. This is consistent with the polished appearance of the R.F. seat and its polished full area marking when lapped against a dry precision (better than .0001" in 12") lapping plate.

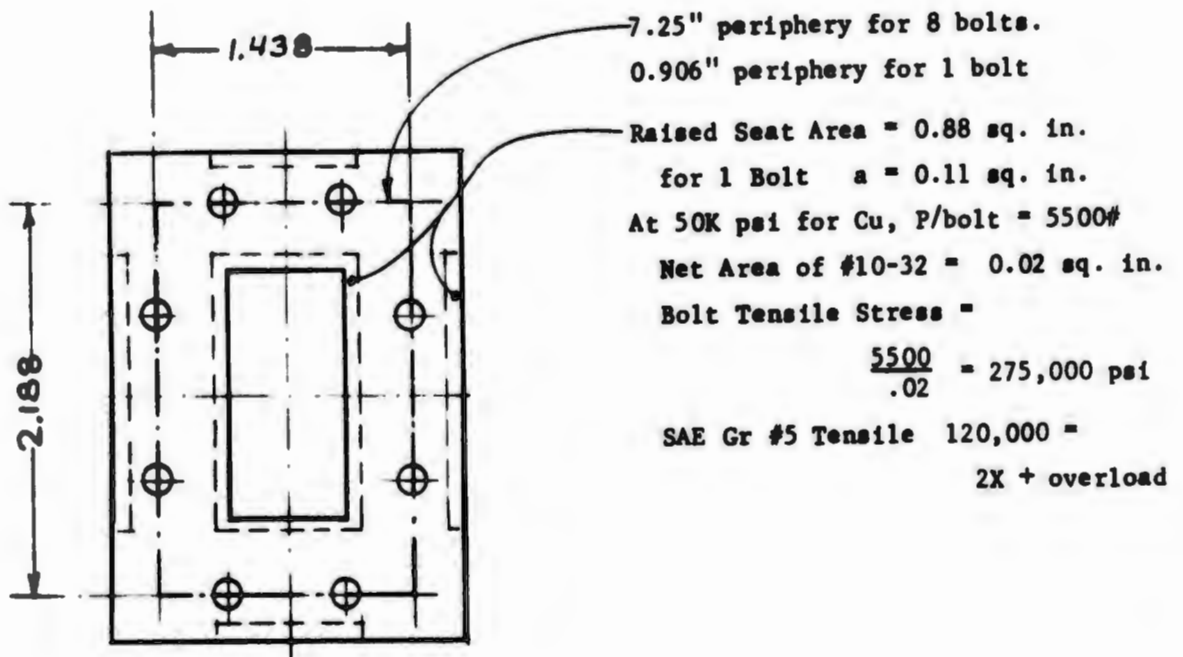
APPENDIX I

MAXIMUM LOADS IN MIL-F-3922/52

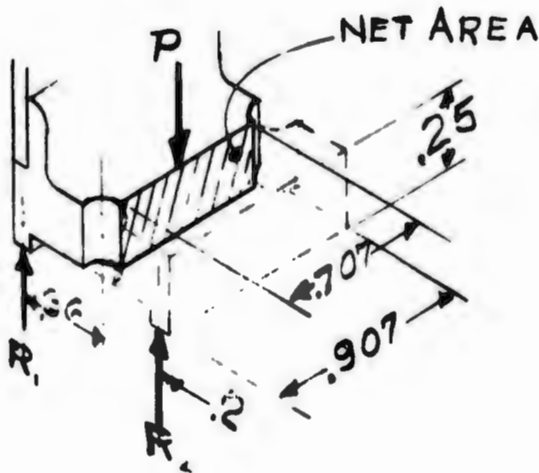
WR-137 Flange - Based on Raised Seat Configuration

Figure 4. Flange Geometry, per MIL F 3922/56

Provides a raised seat area of 0.88 square inches. The flange thickness is inadequate if the maximum seat loading of 50K psi (for Cu) is to be used for equipment safety during normal rough handling after assembly.



APPENDIX I (continued)



With Flange Seat Load at an  
Average Maximum = 50,000 psi  
What is Stress in Flange Thru  
Net Section between Bolts

$$P = \text{Bolt Load Max.} = 5500\#$$

$$R_2 = \frac{.36}{.56} \times 5500 = 3536 \#$$

$$R_1 = \frac{.20}{.56} \times 5500 = 1964 \#$$

$$M_2 = 3536 \times 0.2 = 707" \#$$

$$M_1 = 1964 \times .36 = 707" \#$$

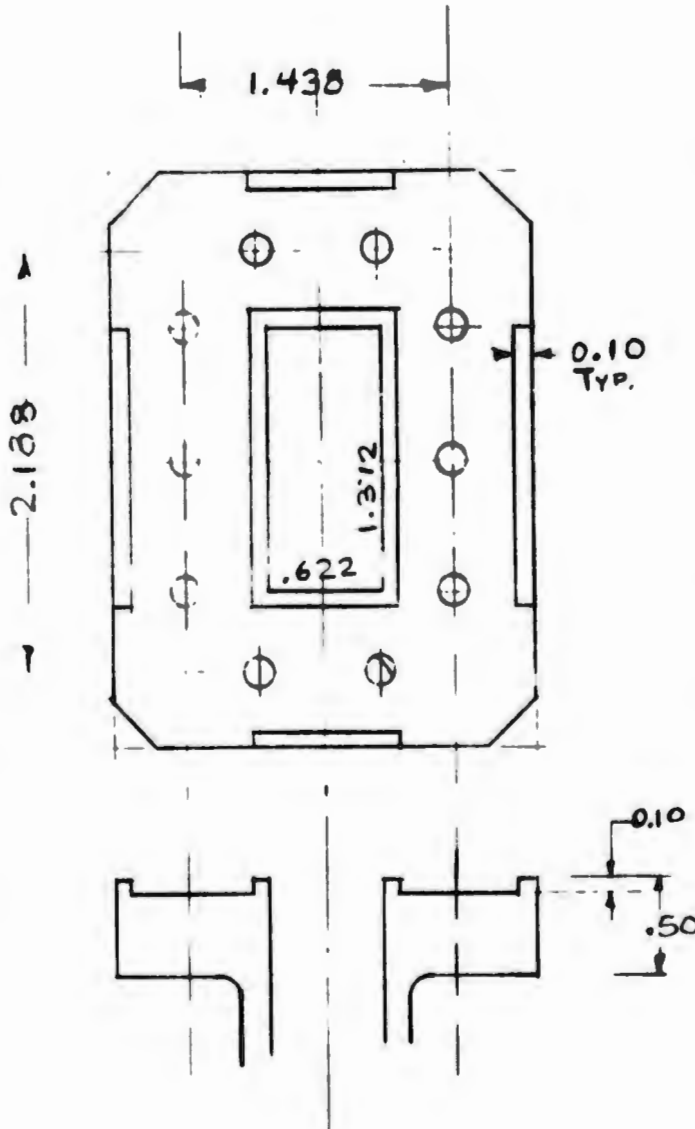
$$S_{\text{net}} = MC/I = 96,000 \text{ K psi} \quad \left\{ \begin{array}{l} I/C = \frac{bh^2}{6} = \frac{.707 \times .25^2}{6} = .00736 \text{ \& C/I} = \\ M = 707 \hspace{15em} 135.8 \end{array} \right.$$

$S_{t(\text{max})}$  for Cu = 50000 K psi &  $\approx 2X$  overload



APPENDIX II

MAXIMUM LOADS IN IMP-FREE FLANGE



Flange Seat Area = 0.88 sq. in.

Hole Periphery

$$2(1.438 + 2.188) = 7.25''$$

$$\text{Periphery per hole} = .725''$$

Using 50K psi for Cu

because it is  $S_y$ ,

the load per bolt is

$$L_B = 50K \times .88 \times 1/10 = 4,400 \#$$

Bolt Tensile Stress is

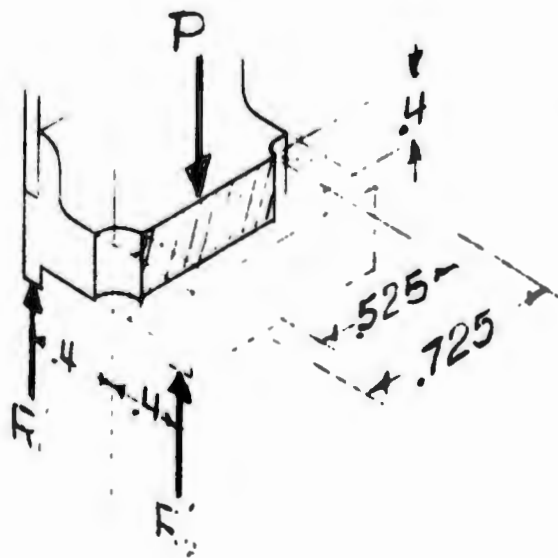
$$S_t = \frac{4400}{0.02} = 220,000 \#/\text{sq. in.}$$

SAE Gr #5 Bolt has

$$S_t = 120,000 \text{ psi}$$

Still too high; indicates more bolts, or less seat, but it may be well to have bolts break if the joint moment is adequate.

APPENDIX II (continued)



Stress in Net Section of Flange

$$P = 4400\#$$

$$R_1' = R_2' = 2200 \#$$

$$M' = R_1' \times .4 = 880'' \#$$

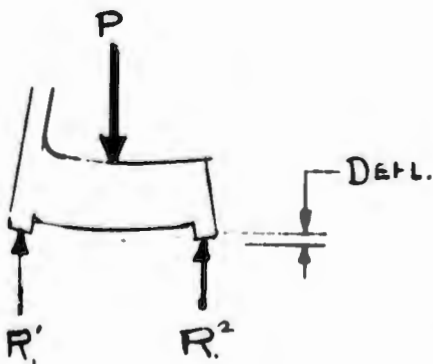
$$C/I = \frac{6}{bh^2} = \frac{6}{.525 \times .4^2} = 71.4$$

$$S_t = MC/I = 880 \times 71.4 = 62,857 \text{ psi}$$

This is a little high for Cu at 50 K psi. It is acceptable for Brass and Hi Strength Cu at 60 K psi.

The bending of flange profile is:

$$\text{Deflection} = \frac{wl^3}{3EI} \quad \text{at 10 K psi Flange seat load}$$



$$\left. \begin{aligned} P &= 1/5 \times 2200 = 440\# \\ &= 0.4; l^3 = .064 \\ E &= 17.3 \times 10^6 \\ I &= \frac{bh^3}{12} = \frac{.525 \times .4^3}{12} = .0028 \end{aligned} \right\}$$

$$= .0002'' \text{ at working load of 10K psi on seat.}$$

No significance, except the .0002 is a reasonable match for .0001 of seat deflection.